University of Minnesota
St. Anthony Falls Hydraulic Laboratory
Minneapolis, Minnesota

Project Report No. 244

COOLING WATER INTAKE MODEL STUDY FOR NSP'S SHERCO UNIT 3 ELECTRIC POWER GENERATING PLANT

by

Heinz G. Stefan,

Richard L. Voigt, Jr., James C. Lennington,

Joseph M. Wetzel, and David W. Bintz

Prepared for

NORTHERN STATES POWER COMPANY
Minneapolis, Minnesota

and

BLACK AND VEATCH
Kansas City, Missouri

Minneapolis, Minnesota
December 1985

TABLE OF CONTENTS

LIST OF FIGURES

LIST OF TABLES

I. INTRODUCTION

Sherco Unit 3 is a coal-fired electric power generation facility under construction for Northern States Power Company (NSP), Minneapolis, Minnesota. It is located near the town of Becker, Minnesota, on the Mississippi River approximately 40 miles northwest of Minneapolis. Upon completion, it will join Sherco Units 1 & 2, which have been on-line since the mid 1970's (Fig. I-1). For condenser cooling, the plant uses a closed cycle cooling water system with forced draft wet cooling towers. To compensate for water losses from evaporation and releases to the Mississippi River, an intake structure with two pumps of 15,000 gpm capacity each is located on the Mississippi River. With the addition of Unit 3, it became necessary to increase the water withdrawal capacity of the system. All three units will share the existing river intake facility. However, two additional pumps will be installed in the intake house (Fig. I-2). To provide the higher flow capacity and to resolve some existing problems with siltation, the existing panel trashracks will be replaced by profile wire, passive, cylindrical screens (Johnson Screens). Two T-shaped units with two screens each (Figs. I-3 & I-4) will be installed as shown in Figure I-5. To keep these screens operational, a sediment backwash-system, a warm water deicing system, and an air-burst screen cleaning system will be installed. Figure I-6 shows the intake structure with some details of the screen installation and the pump sump. To test the operational characteristics of various design alternatives, a 1:6 scale model of the intake was built and used.

The purpose of this report is to document, in conjunction with a video tape, all aspects of the model study.

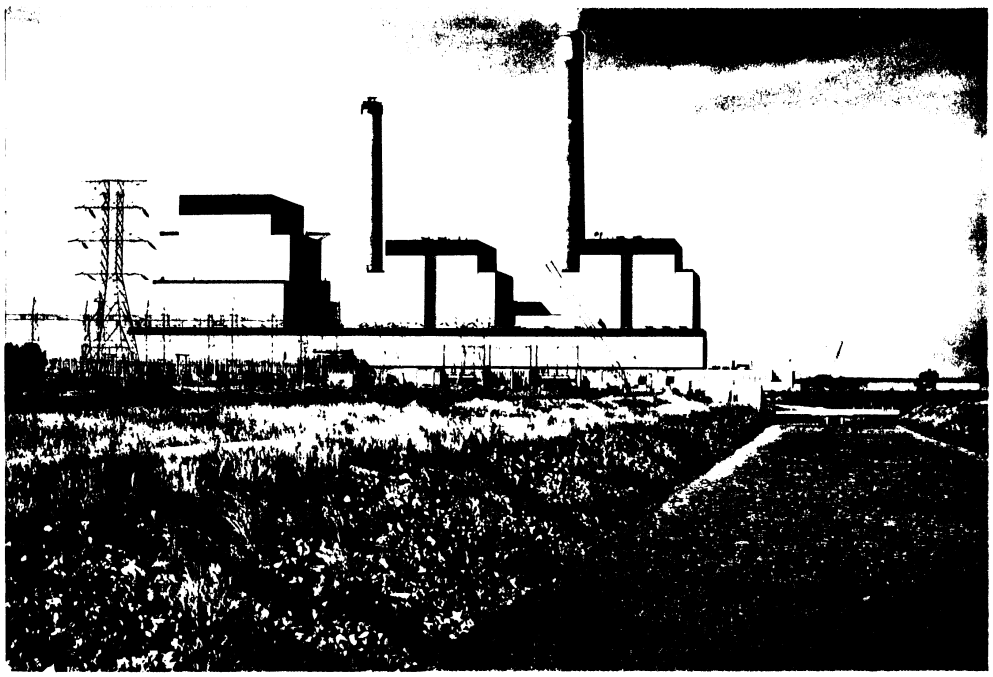

Fig. I-1. NSP's Sherco Power Plant, Units 1, 2, and 3.

Fig. I-2a. NSP Sherco River intake, March, 1985.
View across the river.

Fig. I-2b. NSP Sherco River intake, September, 1985.
View towards river.

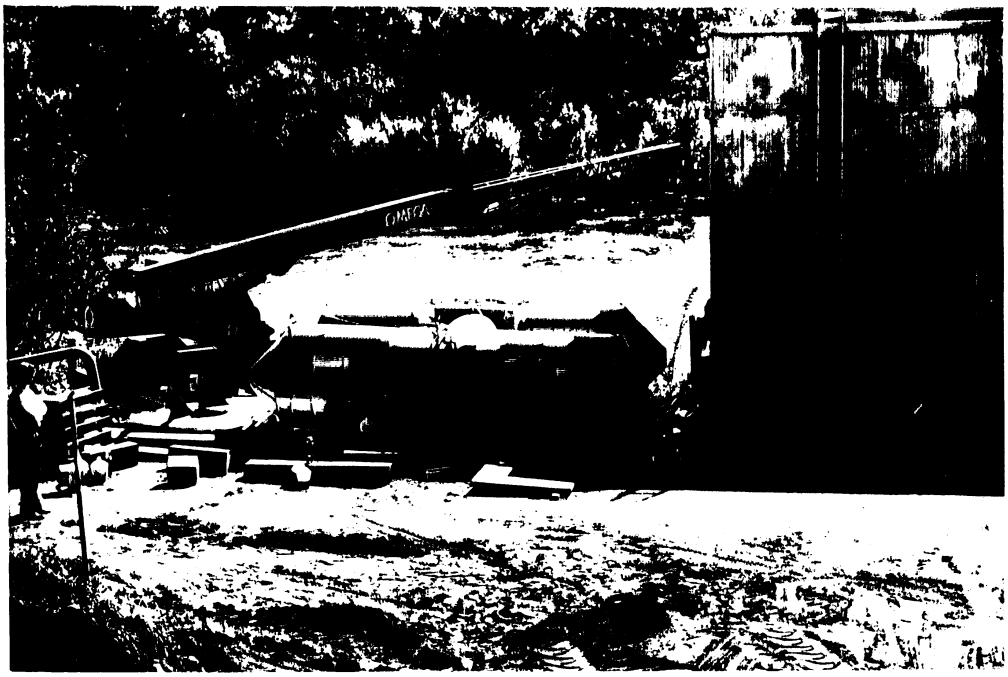

Fig. I-3. Johnson screens on the construction site.

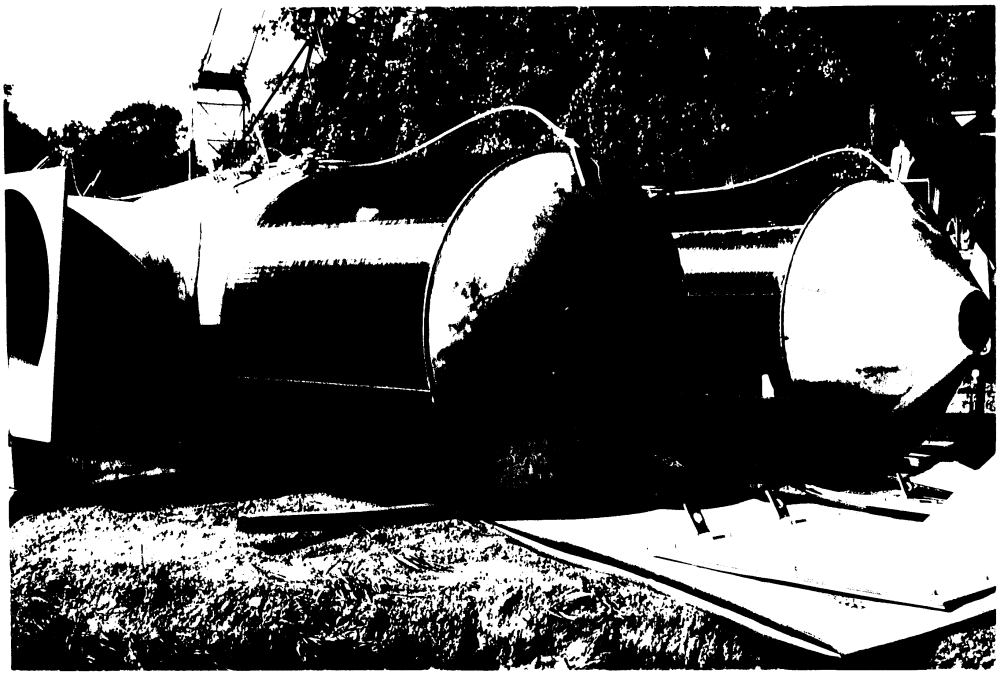

Fig. I-4. Johnson screens assembly.

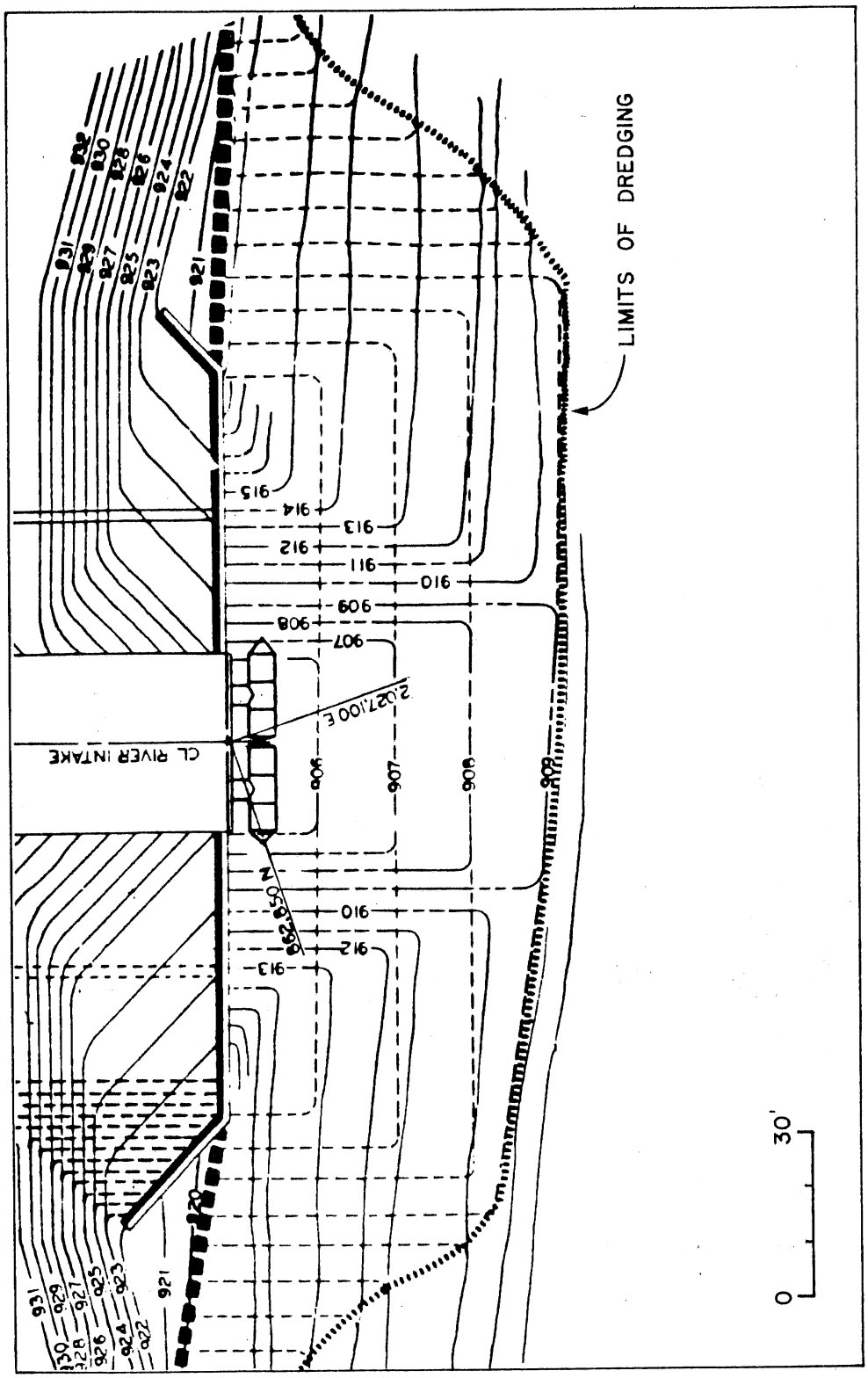

Fig. I-5. Extent of region modeled.

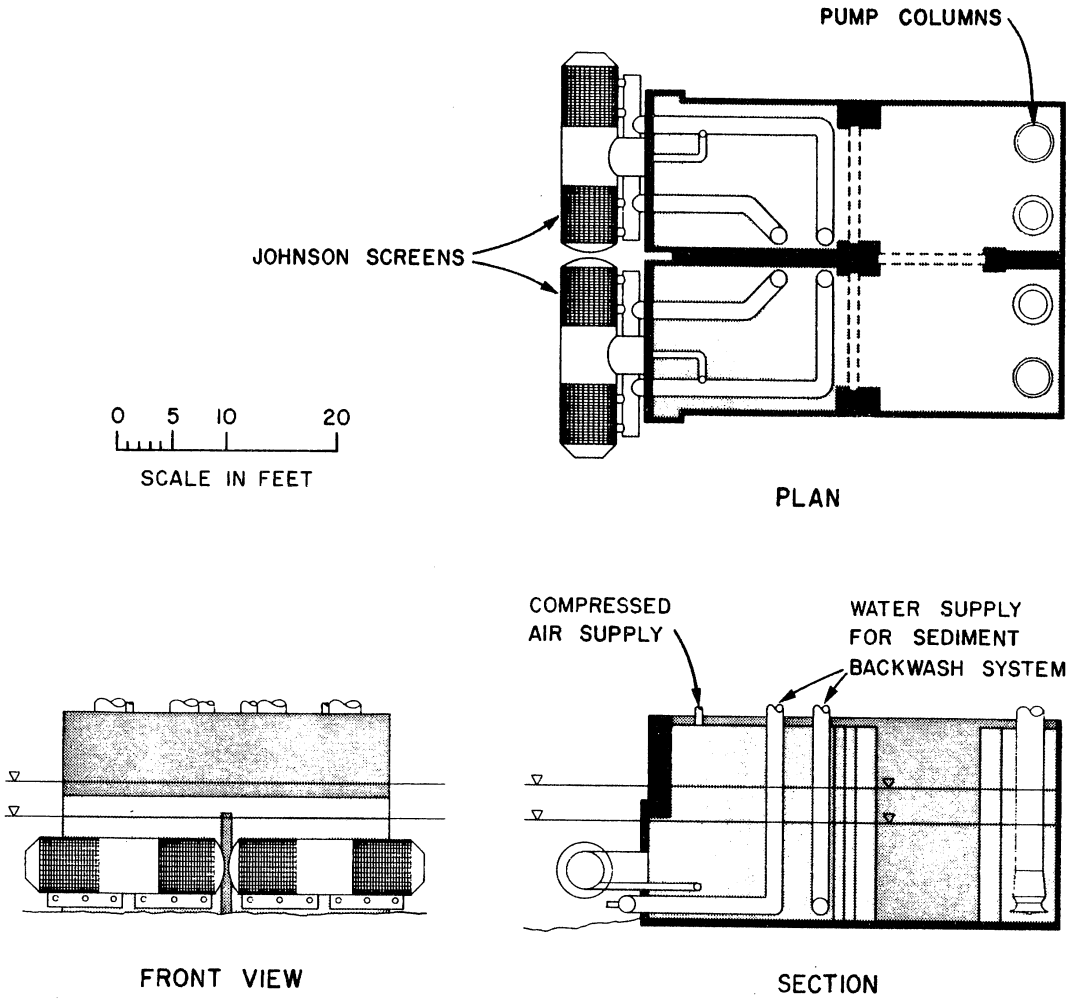

Fig. I-6. River intake structure (power portion).

II. OBJECTIVES

The model study had four basic objectives:

(a) to investigate the effectiveness of a sediment sluicing (backwash) system to be installed underneath the cylindrical screens,

(b) to design and test a warm water diffuser which would, at a total warm water discharge of 3500 gpm, bathe the intake screen in warm water to prevent active frazil ice from clogging the screens,

(c) to demonstrate the effectiveness of the air system in removing debris from the screen surface, and

(d) to test for vortex formation at the pump intakes in the pump sump for all combinations of pump and gate operations.

Documentation included visual observation of the air backwash and measurement of temperature profiles using a multi-thermister probe. The flow patterns in the pump sump were observed by dye tracing and attached yarns. Prerotation in the pump column was measured with a zero-pitch propeller (vortimeter). Pump column velocities were checked for non-uniformity using pitot cylinders connected to chamber mounted pressure transducers.

III. MODEL DESIGN

The model was designed as a 1:6 undistorted scale replica of the intake structure and its vicinity based on drawings provided by Black and Veatch Engineers - Architects, Kansas City, Missouri. Flow parameters were modeled in accordance with Froude scaling relationships. Froude scaling takes into account gravity and inertial forces which predominate in free surface flow. Froude numbers in the model and prototype were identical.

Scaling Ratios:

Length: $L_r = L_m/L_p = 1/6 = 0.167$

Velocity: $V_r = (L_r)^{1/2} = 0.408$

Time: $T_r = (L_r)^{1/2} = 0.408$

Flow Rate: $Q_r = (L_r)^{5/2} = 0.0113$

The model scale was large (1:6) to keep Reynolds numbers sufficiently high. The Reynolds number provides an indication of the degree of turbulence in the flow. It was desirable that the Reynolds numbers be kept above 40,000 in the vicinity of the pump bellmouths to avoid any changes in the flow pattern caused by a reduction in the amount of turbulence. The Reynolds numbers in this region of the model were approximately 85,000. Figure I-5 shows the extent of the region modelled. Figure III-1 gives the size of the model basin. The river topography modelled is also shown in Figure I-5. The screens were designed and manufactured by Johnson Division UOP, New Brighton, Minnesota. The screens were of a two-cylinder, wedge-wire, tee-screen type (Figs. III-1, 2, 3, and 4). All components were scaled 1:6 except the wedge-wires and the spacing between the wedge-wires which were scaled 1:2 because smaller wires were not available. No noticeable effects were found using a similar reduction in scaling ratio in the J. H. Campbell Intake study conducted previously at the St. Anthony Falls Hydraulic Laboratory.

Because of the large size of the model, only approximately 100 feet of the river width could be modelled. This distance was, however, sufficient to provide an accurate representation of the river flow patterns and did not limit model testing capabilities. The maximum withdrawal rate represented only a 15 foot wide streamtube in the river.

Typical river velocities were on the order of 0.5 ft/s prototype (.2 ft/s model) and river stages ranged from 915 to 919 feet above MSL.

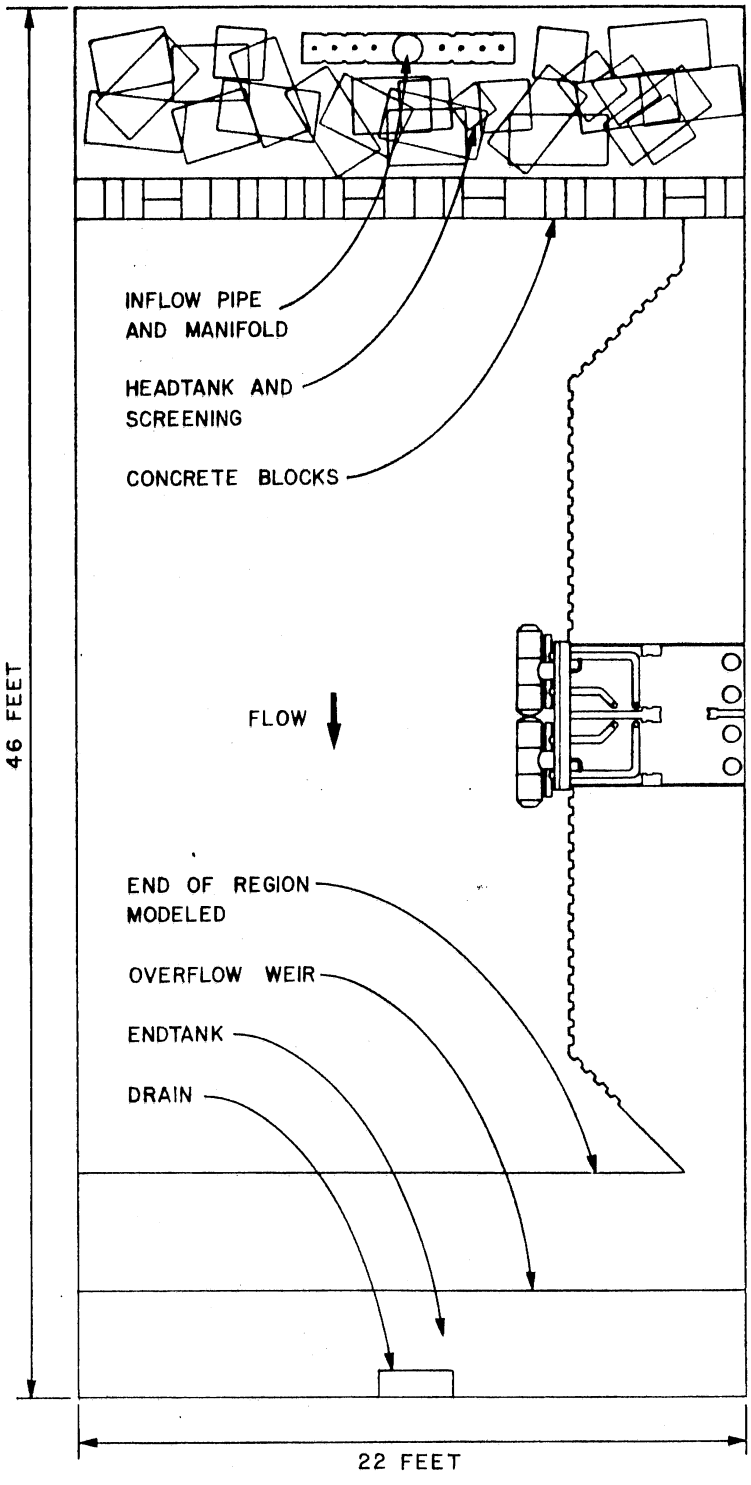

Fig. III-1. Schematic of model basin.

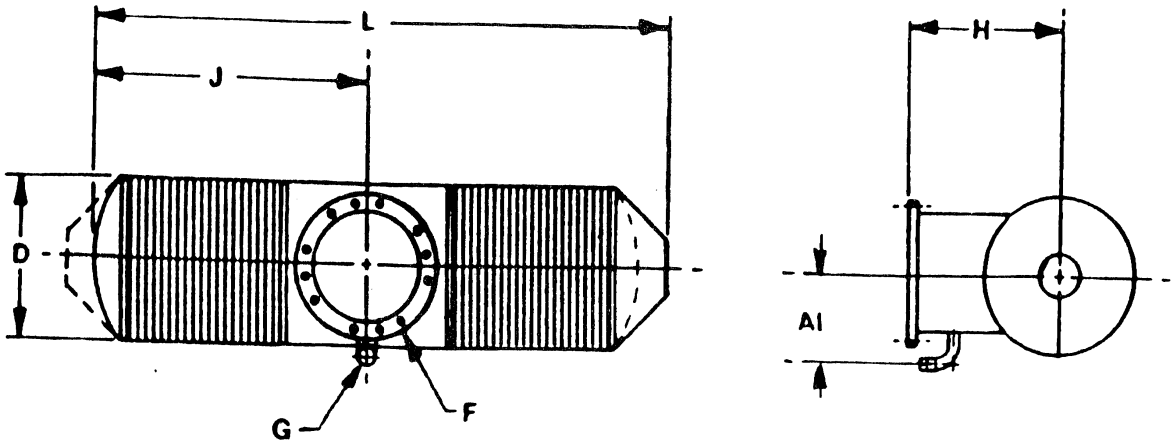

D = 10" NOM A_1 = 7-1/2" Slot Opening: 0.11"

L = 35-1/2" NOM % Open Area: 63

H = 10" Estimated Net Weight: 125 lbs.

J = 16-1/2" Material: 304 Stainless Steel

F: Plate flange to mate with 8" AWWA C-207 Table 1 Class D flange. Pipe diameter is 7".

G: 1: NPT Nipple

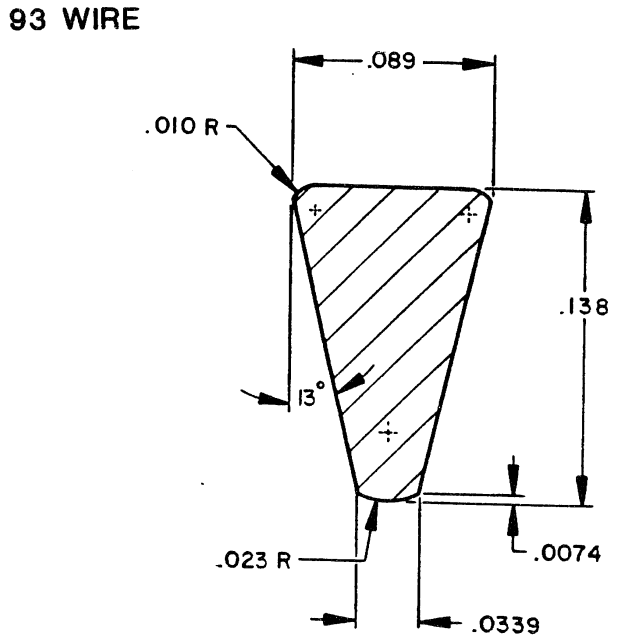

Fig. III-2. Model screen design Johnson Division UOP.

Fig. III-3. Model intake.

Fig. III-4. Model intake from downstream.

IV. MODEL CONSTRUCTION

Construction of the model commenced in January, 1985. Based upon the soundings taken by Gorman, Inc. in October of 1984 and the construction drawing originally used by Black and Veatch, river cross sections were plotted. In the model, these cross sections were 20 inches apart (representing ten foot separations in the prototype). From these plots, shop personnel cut sheet-metal templates, attached these templates to L-shaped bases, and cemented these base-template assemblies to the bottom of the tank. A total of 22 templates were made. The last two templates at the far upstream and downstream end were identical in order to provide a transition from the head tank and to the end tank.

After the templates were installed, concrete block was used to fill between the templates, up to two inches from the top. Tie-rods were placed interconnecting each and every template in order to increase the strength of the model river floor and to reduce the possibility of sag when the concrete pad was poured. A fiberglass cloth was laid atop the blocks to reduce the seepage of fill aggregate and concrete between the blocks and templates. Gravel was poured on the cloth and leveled to a uniform depth of two inches below the crest of the templates. Pea gravel was substituted for sand since repeated cycles of filling and dewatering of the model can cause the sand to seep down and out from below the concrete pad, leaving cavities for the possible collapse of the pad. Finally, the concrete was batched on-site, consisting of Type I Portland Cement, sand, and Zonolite (a lightweight synthetic concrete aggregate) in proportions that would give high tensile strength.

In front of the intake structure a depression 8 feet by 20 feet was left in the fixed riverbed for the placement of sediment. This area was the moveable bed section of the study. The depth of the bed was kept at 8 inches.

The pump sump model represented only that part of the prototype structure below elevation 924 and was made of Plexiglas. This required a longer manufacturing time, but was deemed necessary in order to allow flow observation from several angles. Because of weight and cost restraints, wall thickness was limited to 3/4 inch, making it necessary to limit static head differences on a wall to less than 9 inches. Initially, the pump sump model was built to represent existing conditions. Then, the modifications identical to those planned for the prototype were added. Since the 3/4-inch Plexiglas did not represent the wall thickness of the prototype structure, wood inserts were fabricated for placement at the front (inlet face) of the structure between the Plexiglas and the end of the sheet piling. In this way, geometrical similarity at the face of the structure was properly maintained.

A scaled reproduction of the sheet piling presently located upstream and downstream of the intake structure was an innovative task. Replicas of the individual segments of the piling, with tabs at each end, were produced at the University's Physical Plant Sheet Metal Shop. These segments were delivered in ten foot lengths and then cut in groups down to the desired three foot lengths to be placed in the tank. The cut segments were then spot-welded together at the tabs. At bends and terminations, pieces were pop-riveted or screwed into place. After laying rows of concrete block for the base of the sheet piling, L-shaped brackets were glued to the block and the sheet piling was pop-riveted to these brackets.

The pump intakes were constructed in four sections: bells, bulbs, columns, and siphons. In the model, the pumps were replaced by siphons. The bells were cast plastic resin. A plaster outer mold and a machined Plexiglas inner mold were used. The inner, or male mold, was machined to the exact specification provided by Byron Jackson, Long Beach, California. The outer, or female mold, was simply made by pouring plaster over the male mold coated with a uniform thickness of putty. Upon removal from the molds, the inner faces of the bells were very smooth. The outer surfaces were, of course, quite rough from the exposure to the plaster. The bells were then chucked up in a lathe, wet sanded, and polished to a translucent condition.

The pump bulbs were not perfect reproductions of the Byron Jackson pumps at the prototype structure, but rather easily reproduced shapes that closely approximate the general shapes (see Figure IV-1). Turned out of solid billets of Plexiglas, the external shape of the bulbs resembles two frustrums placed base to base, with the lower frustrum much shorter. Internally, the bulbs have a straight passage downstream of the bell (to provide for measurement of flow conditions) followed by a diffusing section with wall angles of close to 7 degrees to provide better flow conditions and transition to the columns. The downstream ends of the bulbs had outer diameters cut to match the internal diameters of the columns to which they would be attached. These columns were clear sections of Plexiglas stocked by local suppliers with outer diameters of six and five inches, as required to model the two different column diameters in the prototype.

The siphon portion of the pumps was simply the piping that led from the end of the translucent columns, out of the model structure, over the edge of the tank, and down into a laboratory waste channel with an elevation equal to the lower pool level of St. Anthony Falls. Under normal testing conditions, the head provided for the siphon would be on the order of six feet. Calculations showed that the siphons, with pump bulbs and bells attached, should provide in excess of twice the required model flow rate. Flow rate was controlled by a 6-inch gate valve near the water level of the "waste" channel in each siphon.

Upon completion of the construction of each pump bell-bulb-column assembly, the unit was placed in a calibration facility. This facility was specially constructed above the Laboratory's weighing tanks. A pressure tap was inserted in the pump bulb midway along the straight section of the bulb. Flow was pulled through the bell-bulb-column assembly by a siphon, and a differential manometer measured pressure differences between the static head

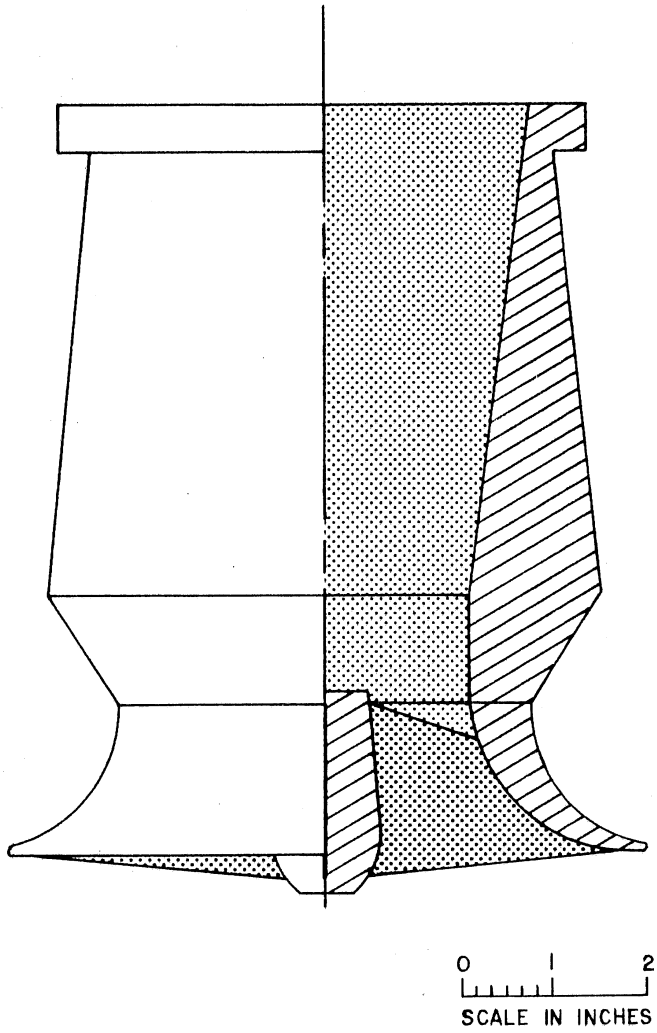

Fig. IV-1. Model pump bell.

in the bulb and a constant head tank. Flow conditions in the facility were kept as close as possible to those in the model structure, and each pump assembly was calibrated individually. Upon completion of calibration, each unit was placed in the model structure.

Model screens were manufactured by Johnson Division, UOP. A physical ice protection system consisting of piles and beams was modeled around the screens (Fig. IV-2). This structure was designed by Black and Veatch. Its purpose is to protect the screens from drift ice and ice jams in the Mississippi River. Utilizing PVC pipe to represent the pilings and wood for the horizontal square beams, the structure was put in place by mounting dowels in the bottom of the pilings and drilling holes in the riverbed to accept the dowels. In this manner, the ice protection system could be removed for ease of modification. In addition, a warm water deicing line for protection from frazil ice was brought through the sheet pile wall and attached to the nearest pile of the ice barrier for stability. The deicing line was made of 3-inch PVC pipe and discharged warm water through several orifices. In the prototype, the warm water is supplied by an 18-inch diameter line directly from the powerplant. In the model study, city water was heated in a heat exchanger connected to the Laboratory's boiler (steam supply).

A sediment backwash system consisting of four manifolds placed underneath the screens was installed in the model and tested. Details are given in Section VII.

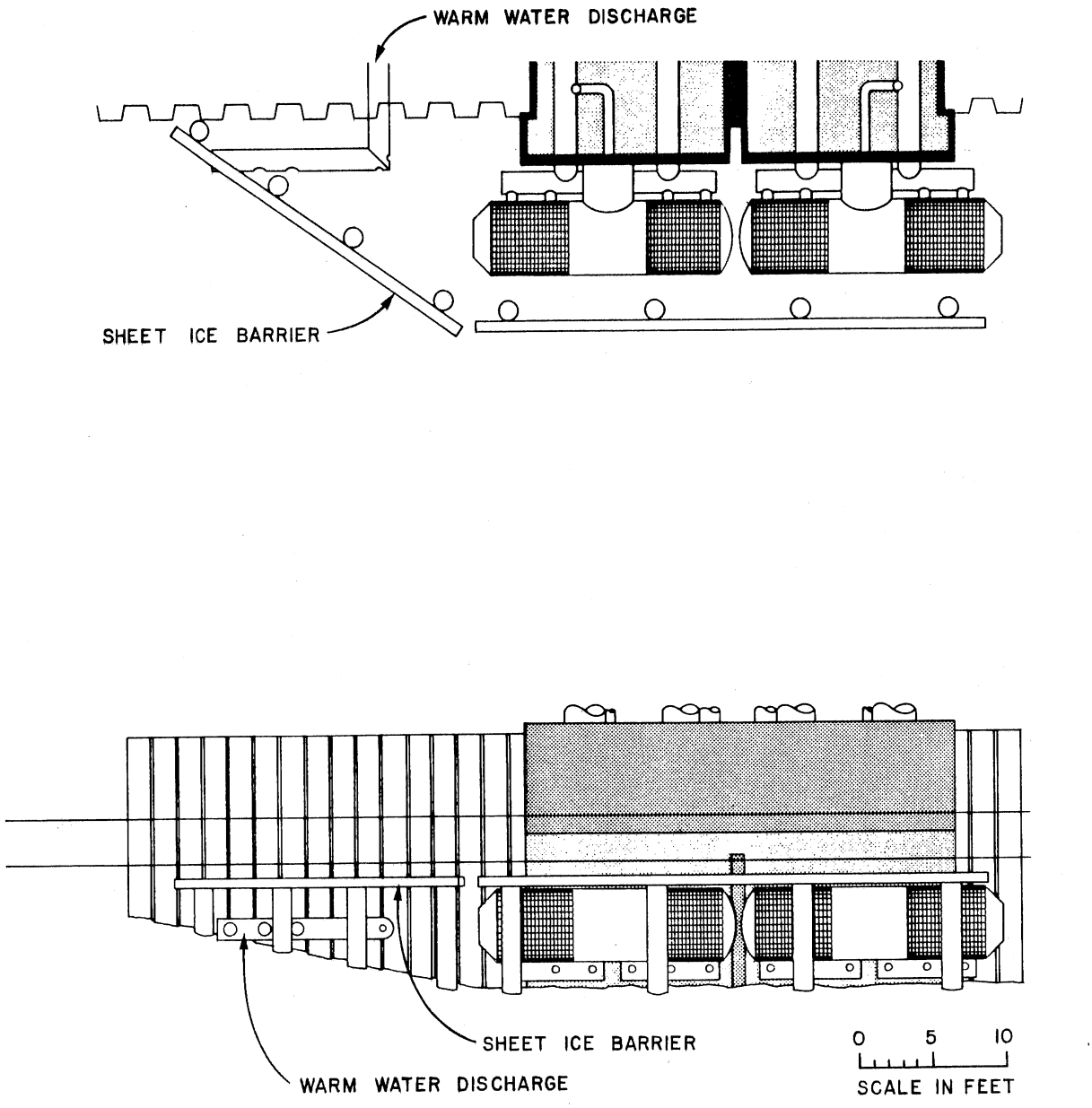

Fig. IV-2. Ice protection system.

V. MODEL CALIBRATION

All flows of water into and out of the model were measured. The orifice and other meters used for this purpose were calibrated in the Laboratory's weighing facility. The following flow metering devices were calibrated:

(a) The four siphons representing the pump withdrawal,

(b) The orifices in the sediment backwash system,

(c) The orifice in the warm water (deicing) flow,

(d) The orifice in the riverwater supply to the model.

In addition, it was necessary to reproduce a realistic river velocity distribution in front of the intake structure. This met with some difficulty because of the large width (approximately 16 feet from the face of the intake structure to the opposite laboratory tank wall), and the short length of the experimental tank. Providing a velocity distribution representative of that river in such a short distance required substantial effort. Many combinations of flow controlling devices were used. The most satisfactory flow distribution system was developed using a large amount of screening around the inflow manifold in the headbox, and a wall made of perforated concrete blocks. By tightly packing the screening and staggering the openings in two rows of blocks, it became possible to accurately simulate the river flow. The downstream control consisted of a variable height weir which correctly proportioned the amount of overflow from each streamtube of the river.

VI. FRAZIL ICE PROTECTION, WARM WATER DISCHARGE

The term frazil ice refers to minute waterborne ice particles formed in supercooled turbulent water [Williams, 1959]. Concern was expressed at the outset of the model study over the sensitivity of the intake screens to plugging by frazil ice particles. This portion of the report deals with the solution of this problem by a warm water discharge. The objective was to find a suitable warm water discharge configuration. The purpose of the discharge was to raise, by several degrees, the temperature of the river water flowing into the intake screens and thus melt any frazil ice particles which might clog those screens. The warm water discharge manifold was to be adapted to a 18-inch pipe located twenty-four feet upstream of the centerline of the intake building. Discharge of warm water into cold water leads to density stratification, and modeling of stratified flows requires dynamic similarity. This is satisfied by using identical densimetric Froude numbers in the model and prototype.

$$Fr'_m = Fr'_p \qquad \text{where} \qquad Fr' = \frac{V}{\left(\frac{\Delta\rho}{\rho} gh\right)^{1/2}}$$

where V = flow velocity, g = acceleration of gravity, h = flow depth, ρ = water density and $\Delta\rho$ = density differential between warm and cold water.

The warm water to be discharged in the prototype will be at a temperature of approximately 85° F while the ambient river water temperature will be at or near 32° F. The ambient temperature of the river water available in the model ranged from 64° to 67° F. This necessitated a warm water discharge temperature of approximately 90° F to satisfy the densimetric Froude requirement. Figure VI-1 demonstrates the variance of water density with temperature.

Temperature profiles were measured with evenly spaced thermistors attached to a rod which was then placed vertically in the flow with the first probe placed just beneath the surface. The probes were evenly spaced three inches apart in the model. This produced temperature readings to a depth of 10.5 feet in increments of 1.5 feet in the prototype. The temperature profiles were measured in three cross-sections normal to the river flow: 1 foot (prototype) upstream of the upstream screen, 1 foot downstream of the downstream screen, and between the two screens.

The warm water discharge manifold consisted of an 18-inch pipe. A jet velocity of 10.0 feet per second in the prototype was selected. Five different manifold configurations of the warm water discharge were constructed

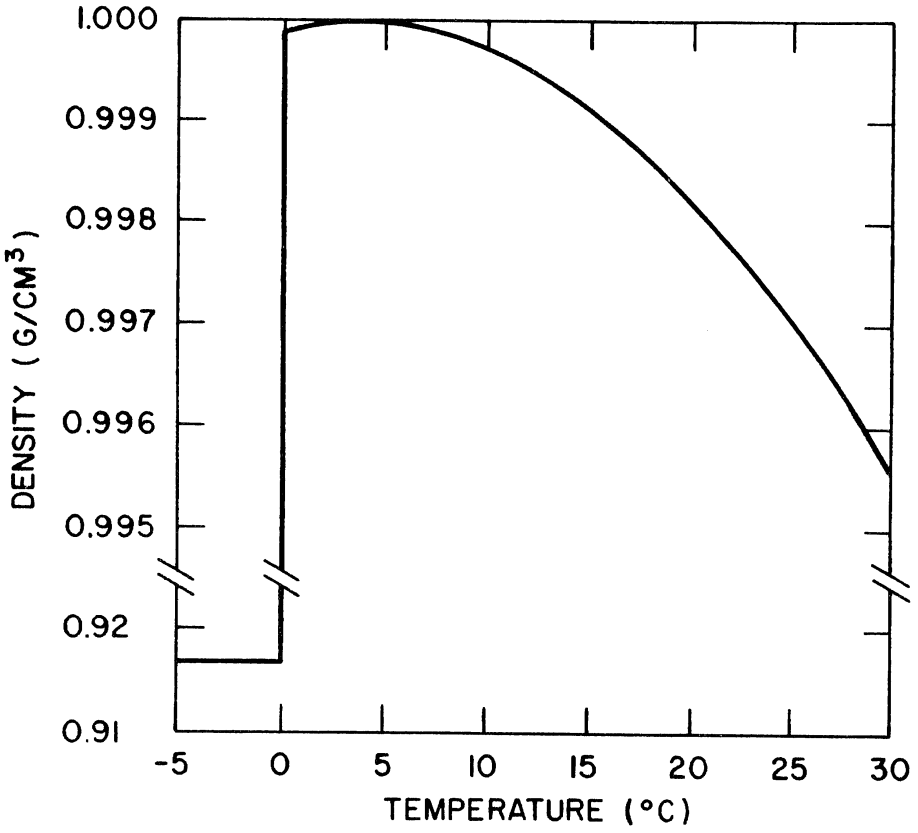

Fig. VI-1. Effect of temperature on density of water.

and tested until a fully satisfactory design was found. The first configuration (Figure VI-2) consisted of a straight piece of pipe 10.5 feet long with three 10.5 inch holes bored into its upstream face along with a 3 inch hole bored into the downstream face next to where the pipe emerges from the sheetpiling. The holes faced upstream with the intent to better disperse the warm water while the small downstream facing hole was expected to "fill in" the area immediately adjacent to the sheet-piling. With dye injected into the hot water stream, it was noticed that most of the hot water spread alongside the sheet-piling and not enough was reaching the front (river side) of the intake screens.

The second configuration tested used the same pipe as the first design but the jet closest to the sheet-piling and the adjacent downstream jet were both sealed. In addition, an additional jet was placed in the flanged end of the pipe (Figure VI-3). This caused most of the warmed water to be injected too far out into the stream away from the intake screens.

The next three configurations tested used a pipe with a 90° upstream bend 22.5 inches after its exit from the sheet-piling (Figures VI-4, 5, and 6). The pipe runs upstream along the sheet-piling for a distance of 12 feet. The first of these three configurations had four 10.5 inch jets placed in the pipe adjacent to the river flow and a smaller 3.0 inch jet located on the downstream side of the 90° elbow. Dye injection showed that this third configuration was a vast improvement over the previous two, and temperature profiles were therefore measured in three cross-sections shown in Fig. VI-7. Isotherms are plotted in Figs. VI-8, 9). In Figure VI-9, one notes the intrusion of water only 0.2°F warmer than the ambient river water. It was decided that this was not sufficient.

The fourth configuration had the furthest downstream jets sealed (Fig. VI-5). This design was an improvement but had a small pocket of ambient temperature water present alongside the wall of the intake structure. For this reason it was decided that a larger downstream jet be installed for configuration five (Fig. IV-6). The temperature profiles for this configuration under different flow conditions were measured and are shown in Figures VI-10, 11, and 12. The water entering the intake screens is usually 1.0°F and at least 0.5°F warmer than the ambient river water. This configuration's performance met the design objectives and was accepted as the final design (Fig. VI-13). In response to concerns of the Minnesota Pollution Control Agency, downstream temperatures were obtained at the end of the model reach for the final design. The maximum temperature rise recorded approximately 90 ft downstream of the intake centerline was 1.0°F 25 ft from the bank. At a distance of 50 ft fromt he bank, the temperature increase was 0.5° F.

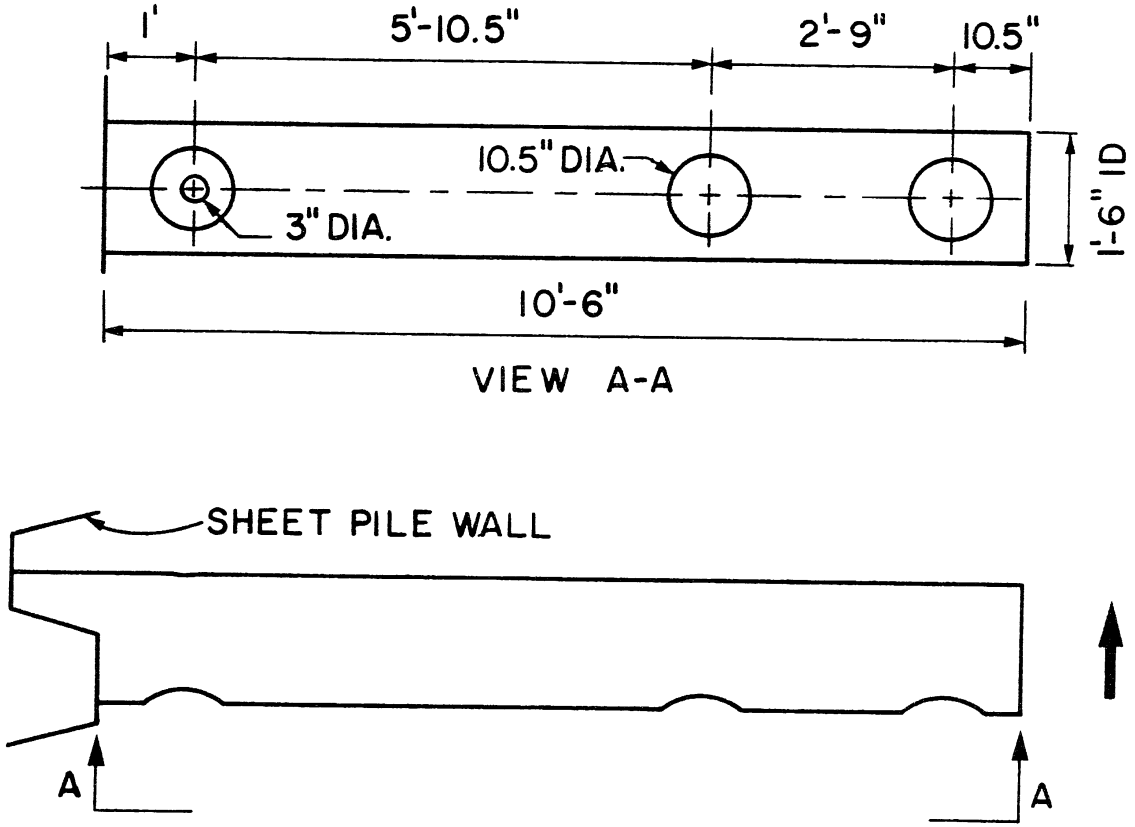

WARM WATER DISCHARGE DIFFUSER DESIGN NO. 1

Figure VI-2

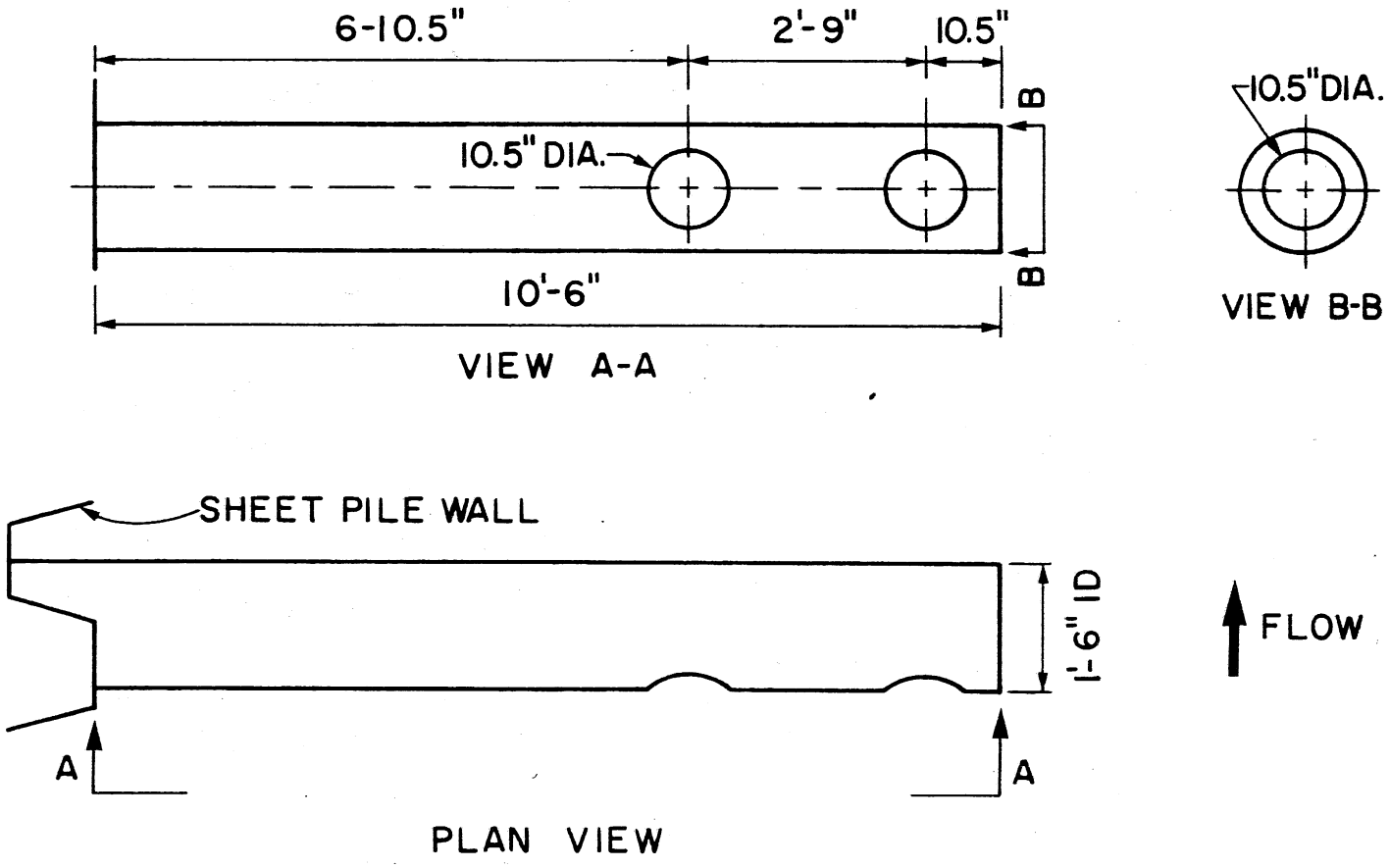

WARM WATER DISCHARGE DIFFUSER DESIGN NO.2

Figure VI-3

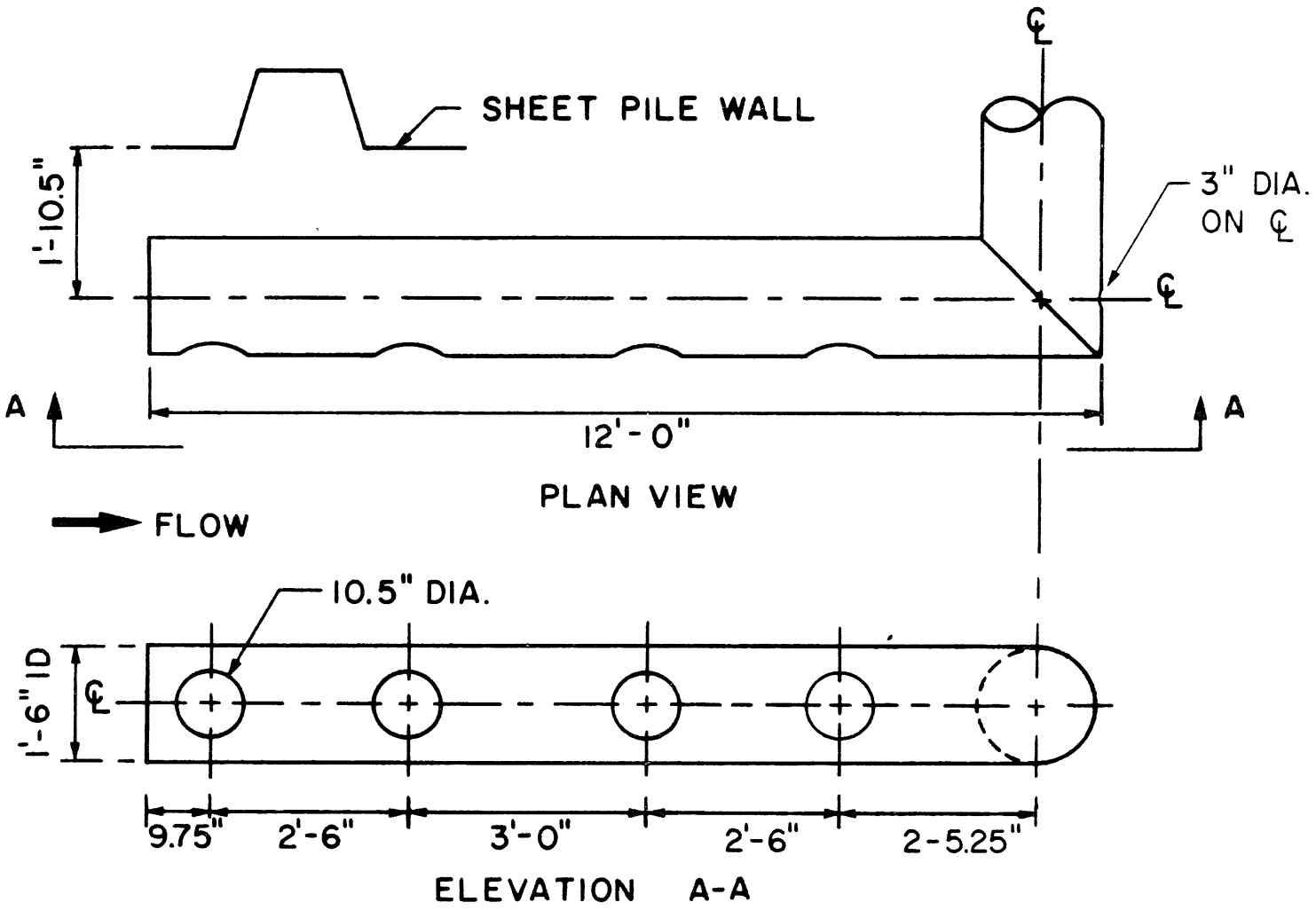

WARM WATER DISCHARGE DIFFUSER DESIGN NO. 3

Figure VI-4

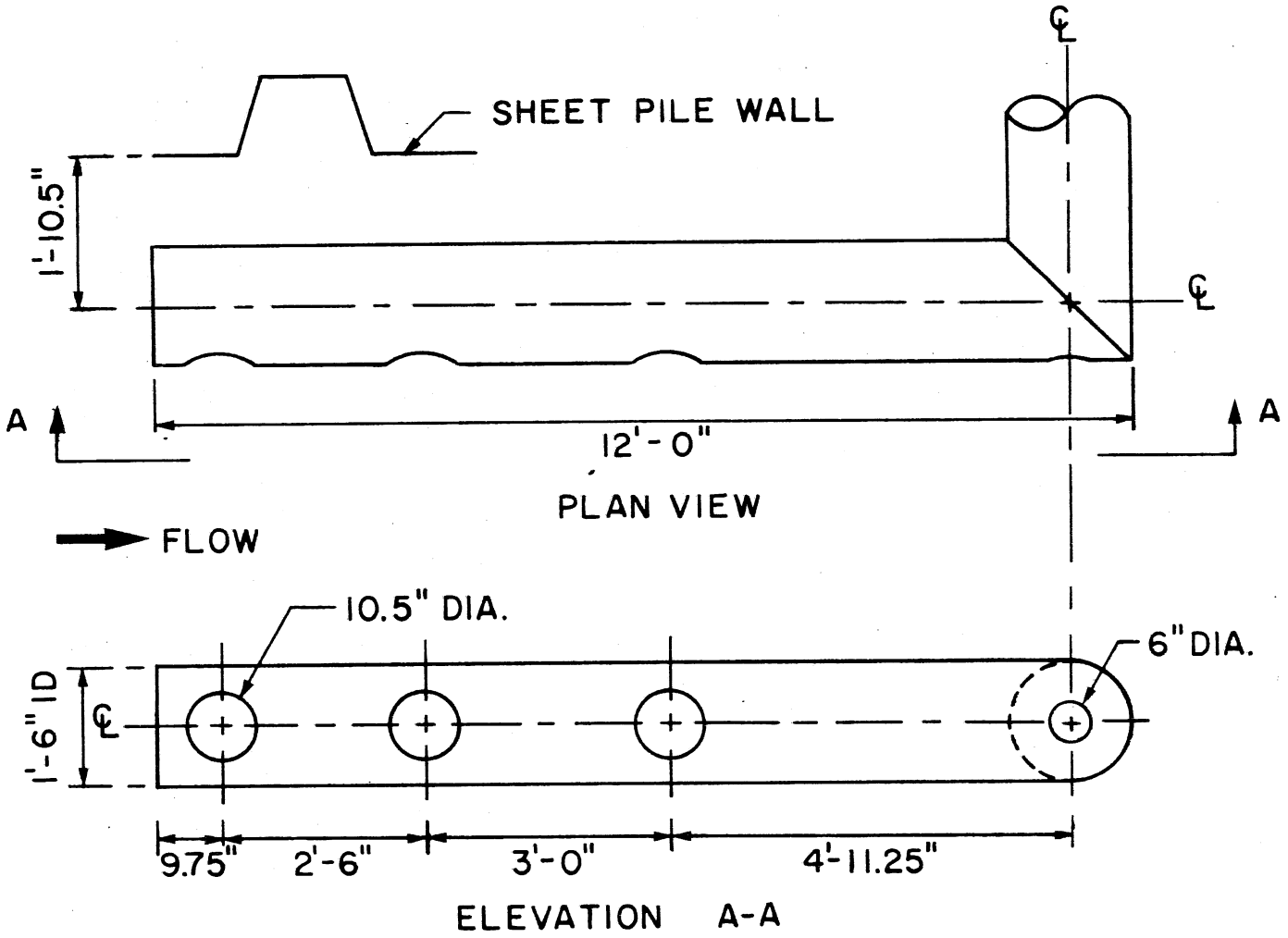

WARM WATER DISCHARGE DIFFUSER DESIGN NO.4

Figure VI-5

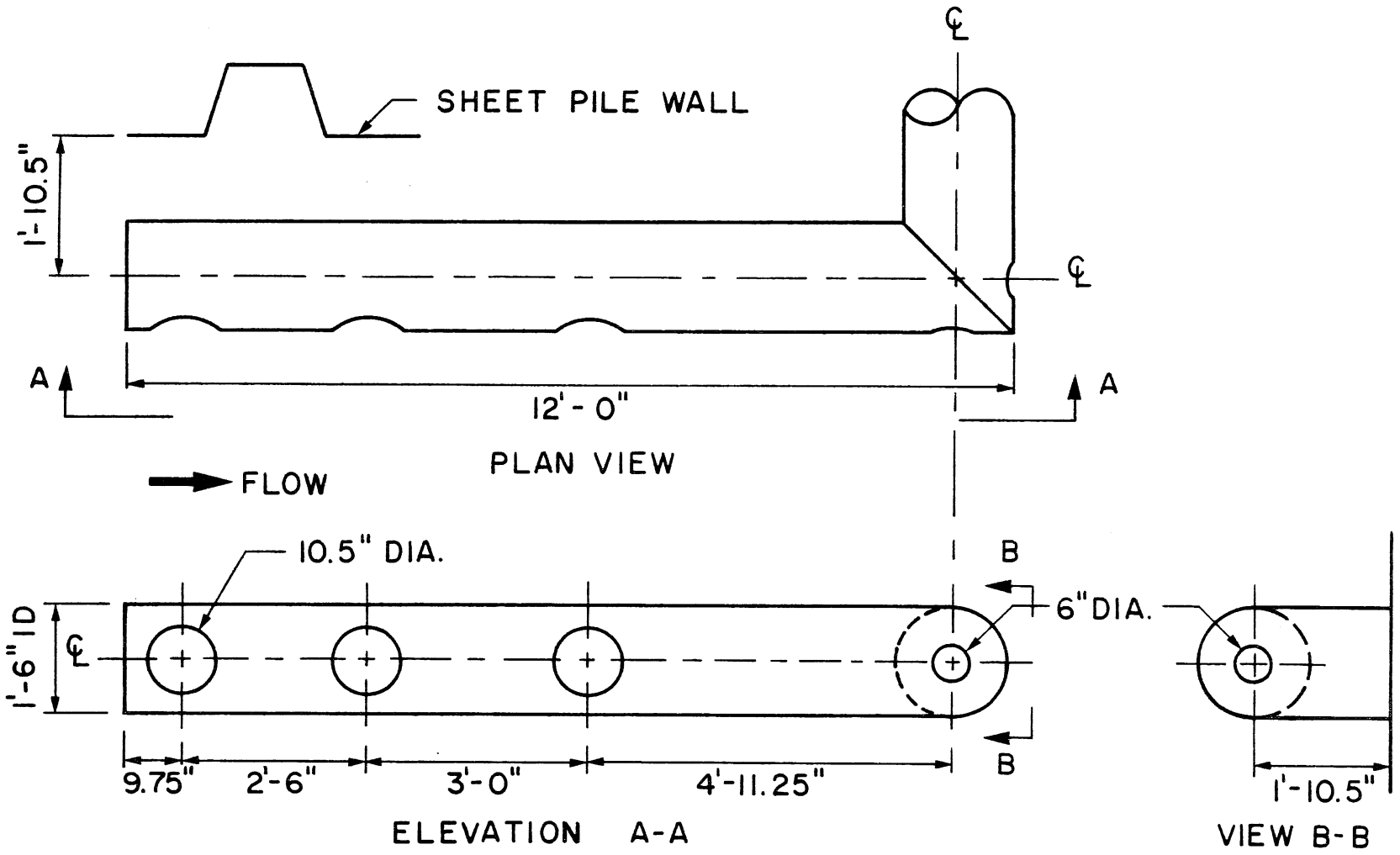

WARM WATER DISCHARGE DIFFUSER DESIGN NO.5

(Accepted warm water discharge diffuser design.)

Figure VI-6

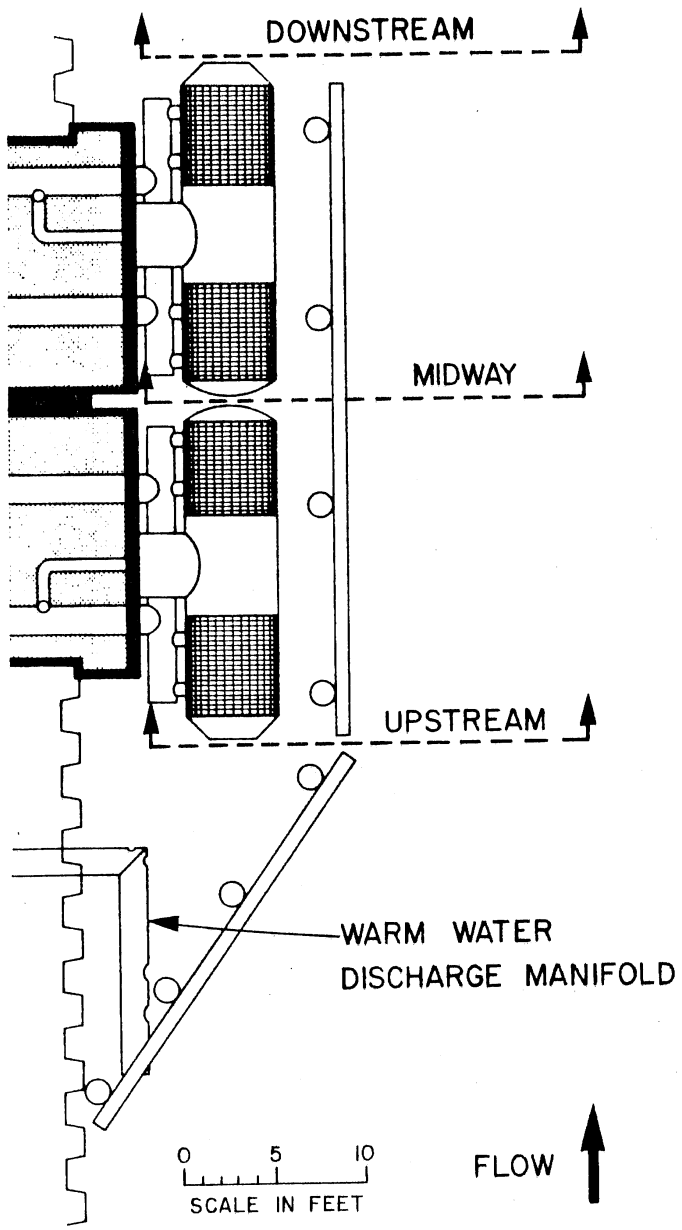

Fig. VI-7. Location of cross sections in which water temperatures were measured.

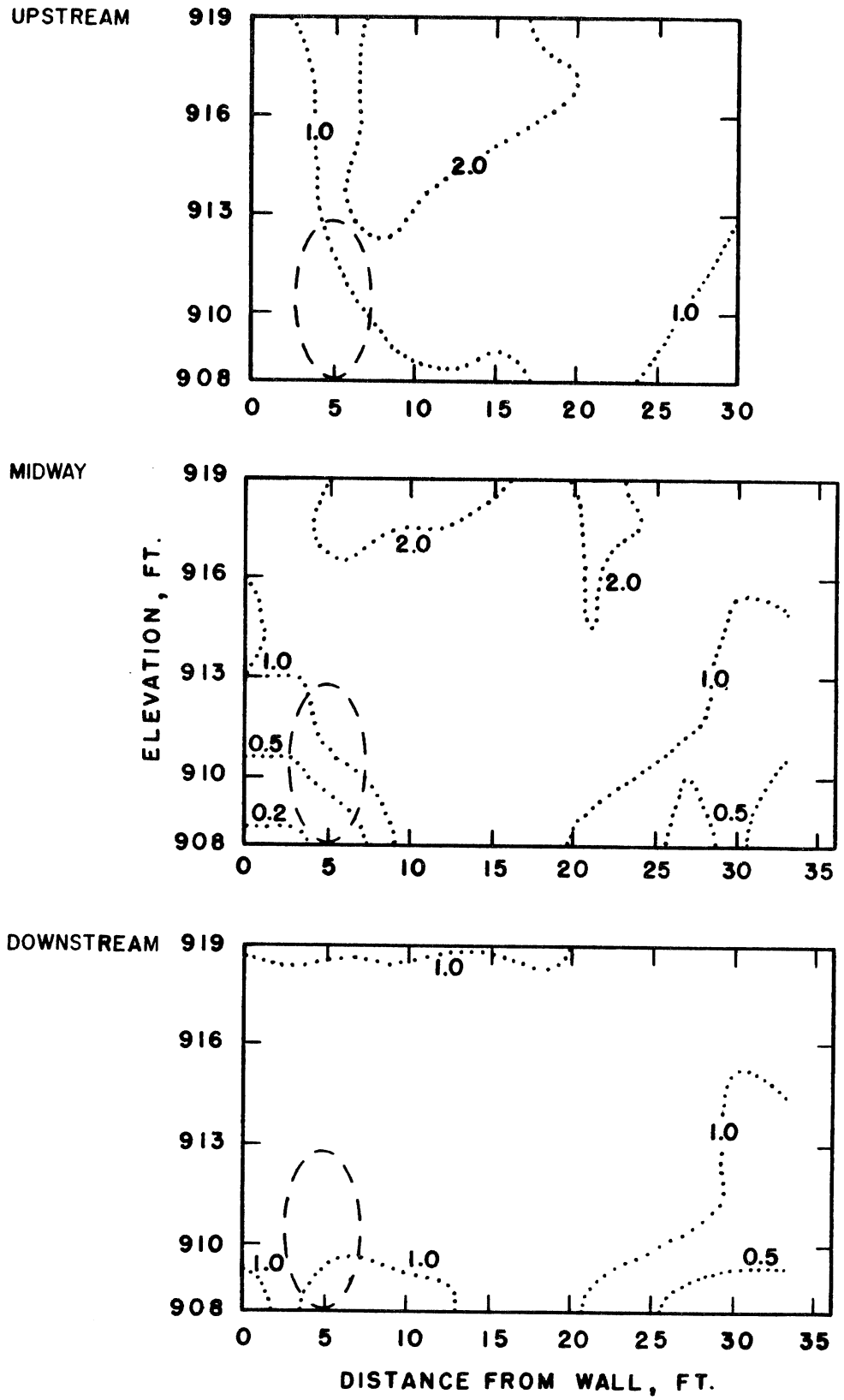

Fig. VI-8. Winter isotherms (^{o}C) in cross sections perpendicular to screen axis. Diffuser Design No. 3. Withdrawl rate 10,000 gpm.

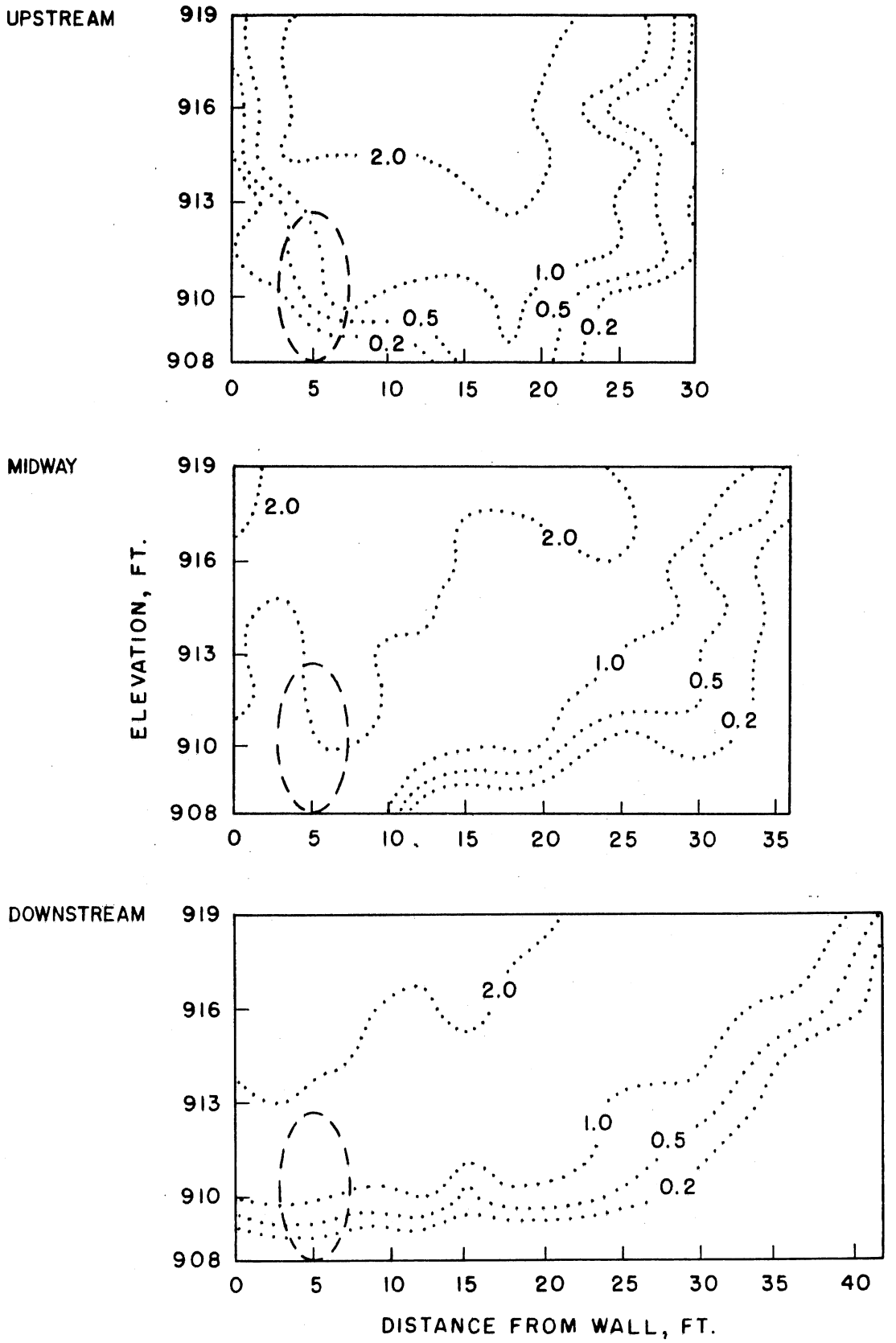

Fig. VI-9. Winter isotherms (^{o}C) in cross sections perpendicular to screen axis. Diffuser Design No. 3. Withdrawal rate 20,000 gpm.

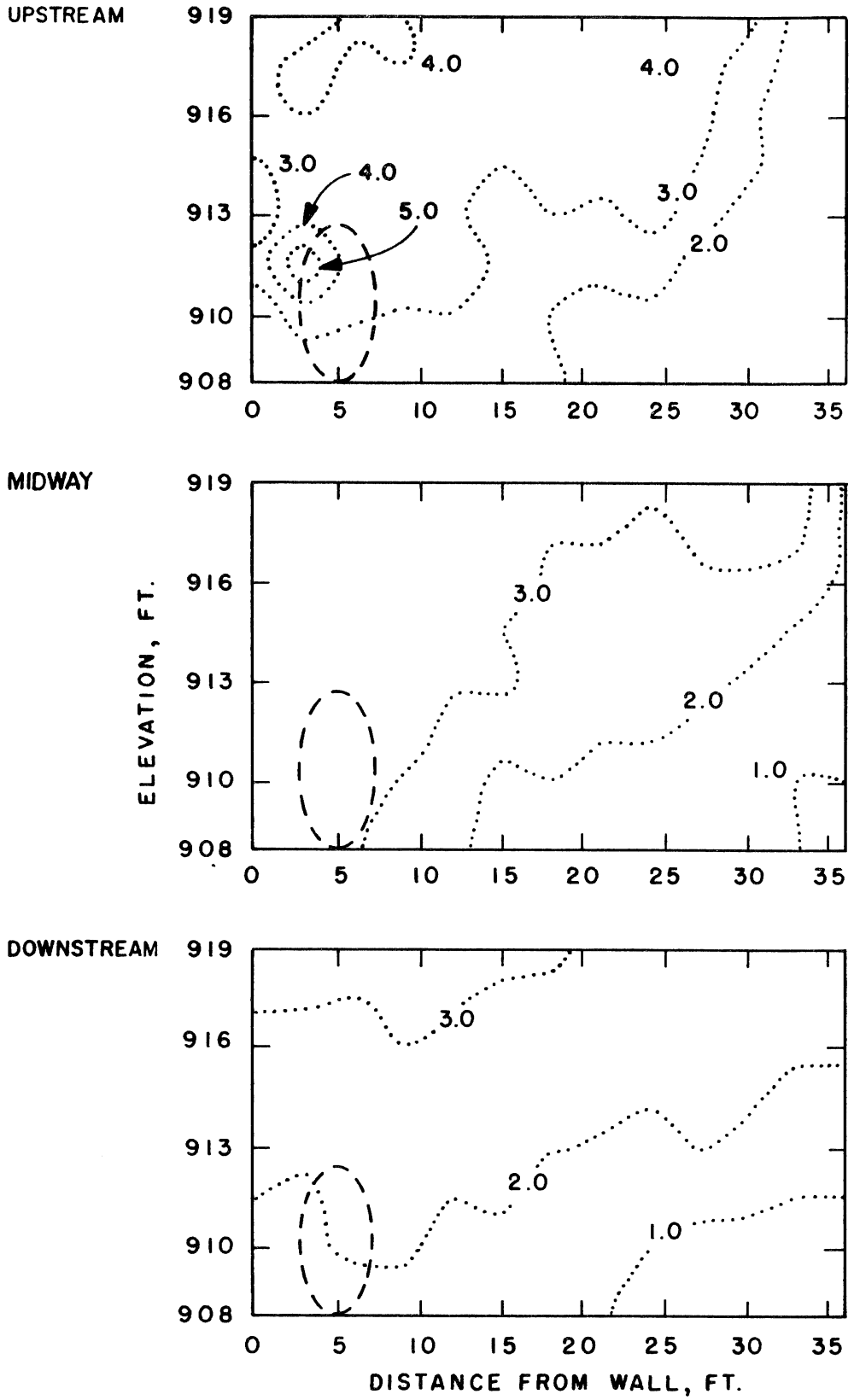

Fig. VI-10. Winter isotherms (^{o}C) in cross sections perpendicular to screen axis. Diffuser Design No. 5. Withdrawal rate 10,000 gpm.

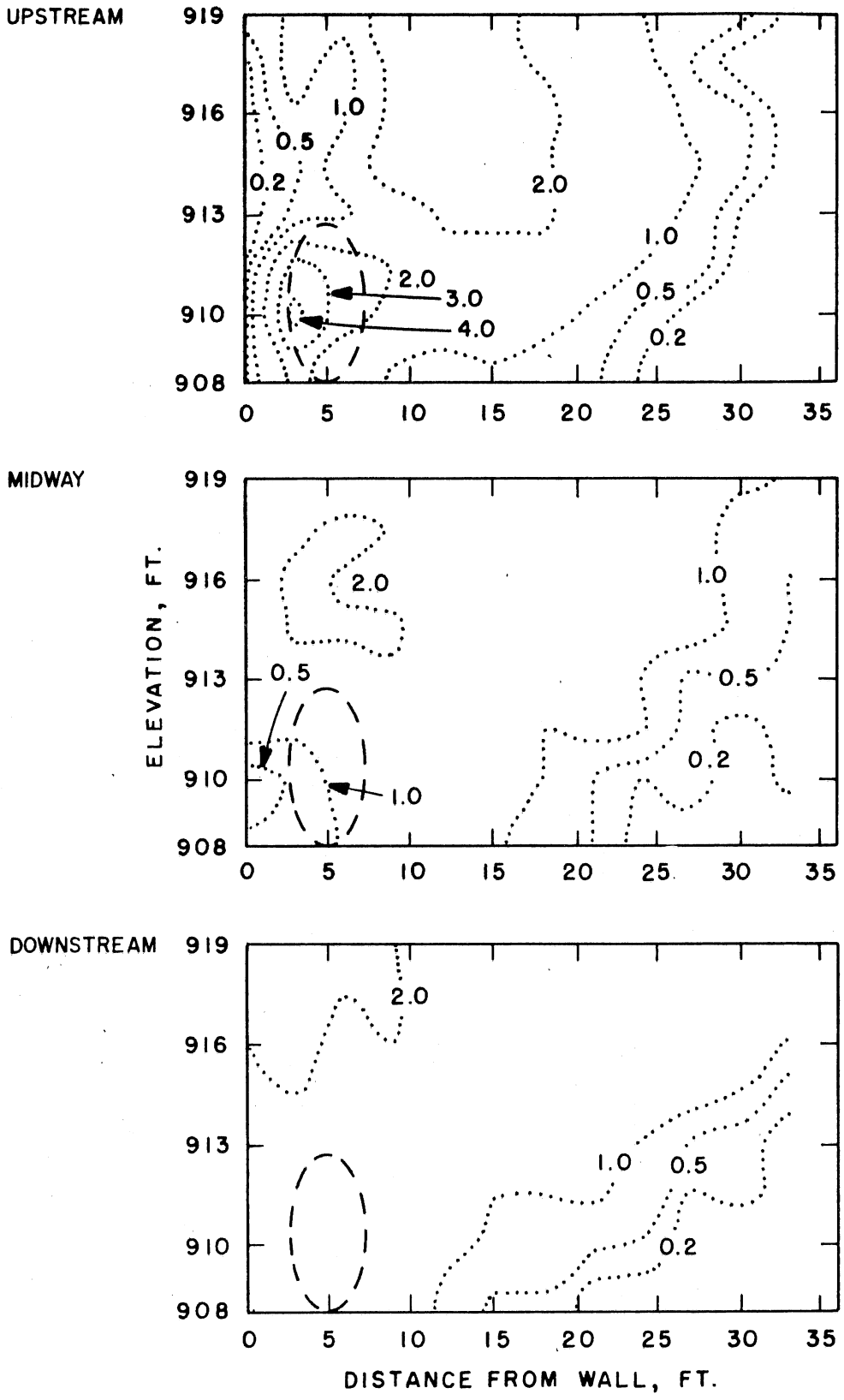

Fig. VI-11. Winter isotherms (^{o}C) in three cross sections perpendicular to screen axis. Diffuser Design No. 5. Withdrawl rate 20,000 gpm.

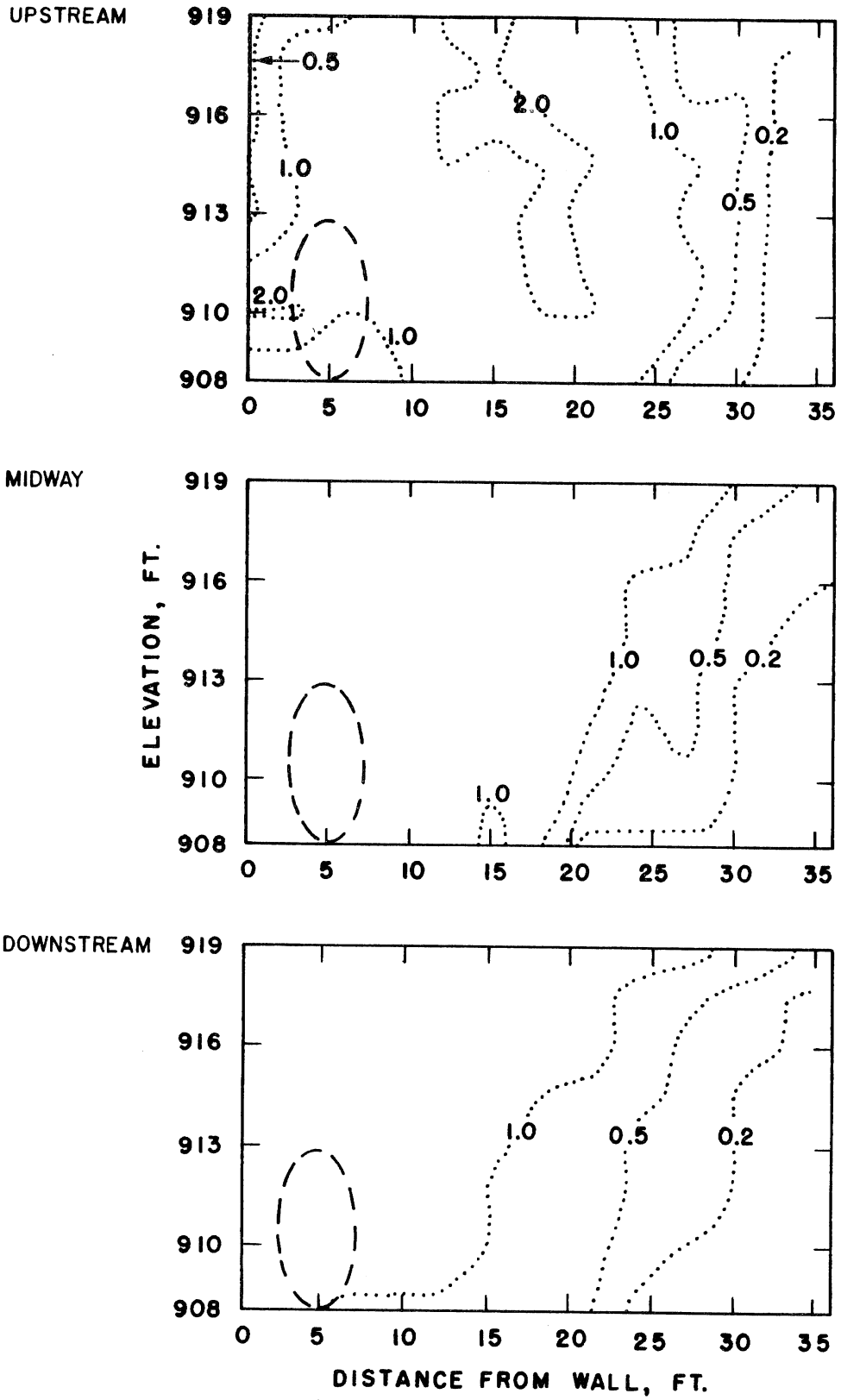

Fig. VI-12. Winter isotherms (^{o}C) in cross sections perpendicular to screen axis. Design No. 5. Withdrawl rate 30,000 gpm.

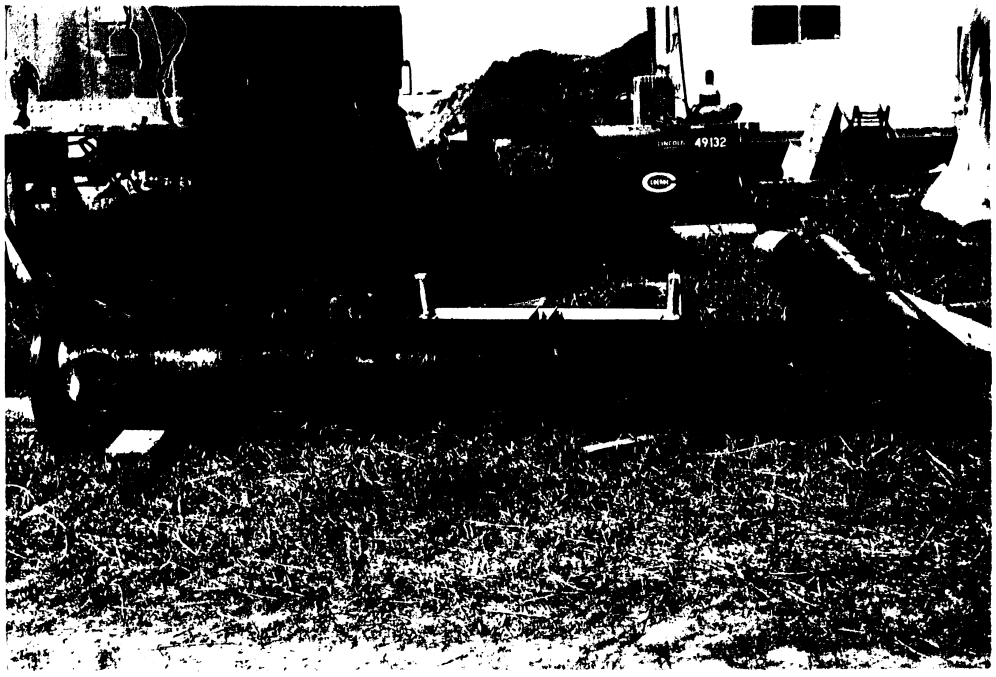

Fig. VI-13. Warm water discharge diffuser at construction site.

VII. SEDIMENT BACKWASH (SILT SLUICING)

Because of possible sediment buildup around the intake screens, testing of a backwash system design was included in the model study. The backwash system would be used to periodically "jet" away the sediment build-up around the intake screens while avoiding any undermining of the structure. The backwash design tested in the model study consisted of four individually operated manifolds, each with three jets. The manifolds and jets were located just beneath the intake screens (Fig. VII-1). Each manifold is 1.5 feet in diameter and 6.75 feet long and discharges up to 15,000 gpm through three horizontal pipe stubs 0.5 feet in diameter and 1.0 feet long. Maximum horizontal discharge velocity is 57 ft/s (prototype). The axis of the manifolds is 3 feet below the screen axis and the end of the discharge stubs is 2 feet from the screen axis towards the face of the intake structure. The direction of the backwash jets is normal to the river flow and parallel to the river bottom. Each manifold is fed by an 18-inch pipe running from a junction with the intake water piping system thus avoiding the necessity of separate pumps for this purpose.

In a Froude model dealing with sediment movement, the important parameter is not particle diameter but fall velocity of the sediment particles. To ensure Froude similarity, the fall velocity of the sediment particles must be scaled the same as flow velocity. The ratio of the particle fall velocities in the model and prototype, respectively, must equal the square root of the length ratio. It was found that sand derived from local St. Peter Sandstone fit the fall velocity requirements of the model (Appendix A). The sand was placed in the model to an elevation equal to 908 feet in the prototype which is tangent to the bottom of the intake screens. Immediately in front of and around the screens the sand was piled and heaped so as to simulate an extreme, unfavorable condition.

In the first test of the design, all of the four manifolds were operated at their design flow rate of 15,000 gpm consecutively from downstream to upstream for a period of 1.5 minutes each. Because of the Froude scaling of the model time, a 1.5 minute model test represents three minutes and forty seconds in the prototype. During this short time period, the backwash formed a scour hole in front of each manifold. The experiment progressed from downstream to upstream and as a result the downstream scour holes were to a degree filled in by sediment scoured from the upstream holes. It was noted during the test that a plume of waterborne sand was carried out into the river channel by the force of the water jets and deflected downstream by the current (Fig. VII-2).

After the model was drained it was observed that a mound of sand had formed approximately 30 feet out from the manifolds. This mound presents little or no detrimental effect to the operation of the intake. The hole

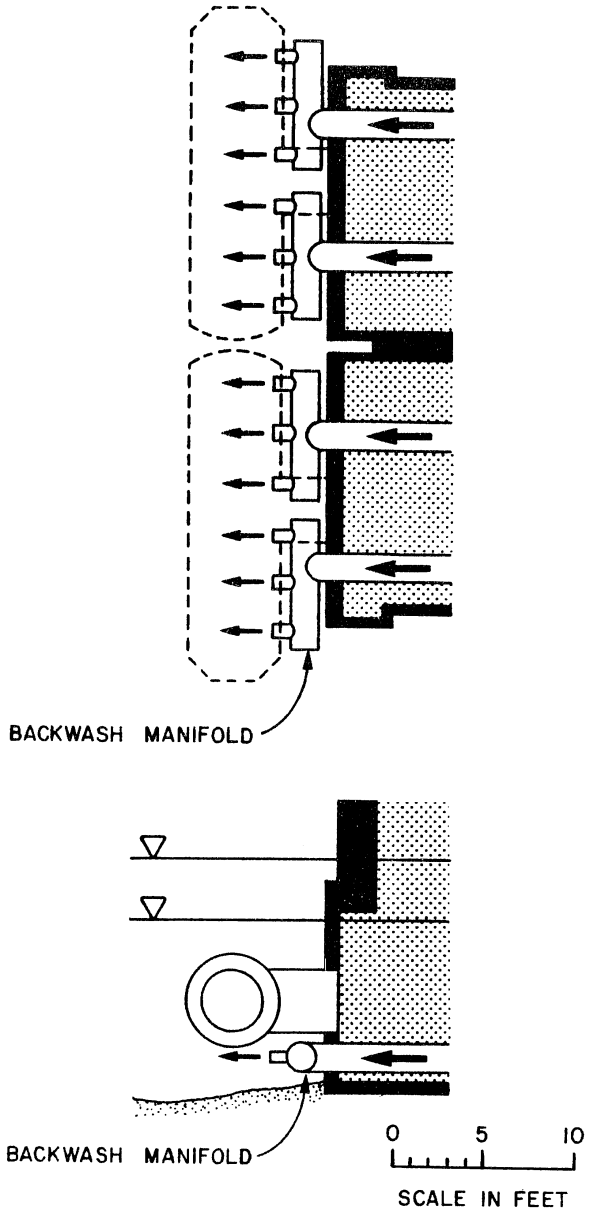

Fig. VII-1. Sediment backwash system.

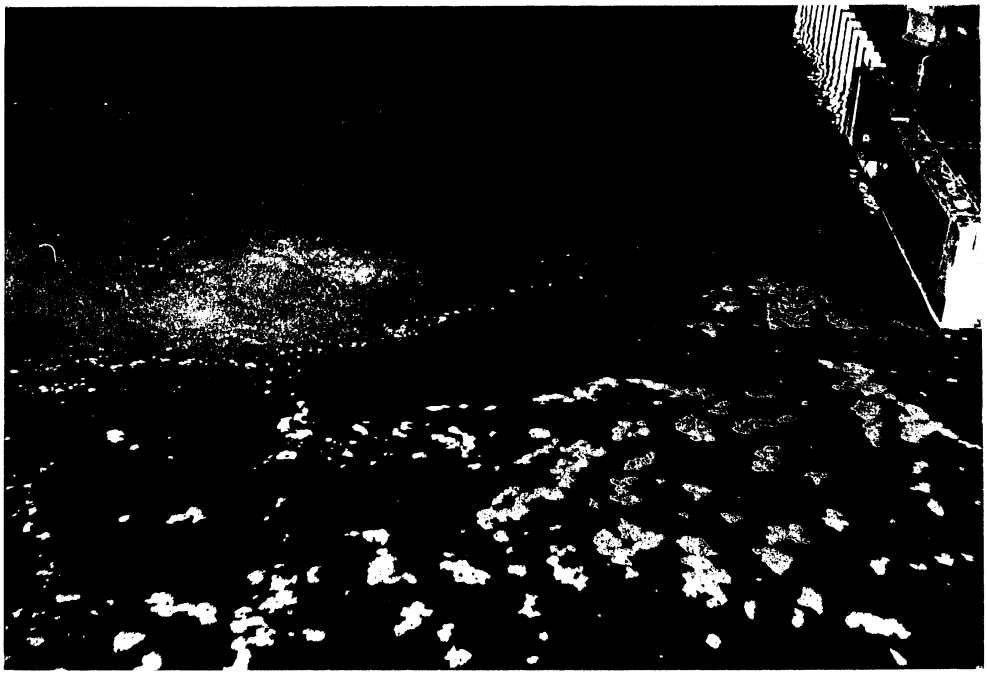

Fig. VII-2. View of model river downstream with sediment backwash in operation. Foam in foreground is residue from air in pipeline

scoured by the water jets reached a maximum depth of 5 feet at a point 4.5 feet from the front of the screens (Fig. VII-3). The bottom of the scour hole depth corresponds to an elevation of 903.0 feet above sea level.

The experiment was also run with one manifold discharging at 15,000 gpm for a period of ten minutes in the model (25 minutes in the prototype) (Fig. VII-4). The maximum scour depth reached was six feet (elevation 902 feet above sea level). The center of the scour hole formed was about 10.5 feet (prototype) in front of the screens.

The experiment was run for 2 hours model (5 hours prototype) time (Fig. VII-5). The scour hole did not reach a much greater depth but rather moved further out into the stream. The area of maximum depth extended from 12 to 19.5 feet from the screens. After examining the results of these first three tests it was concluded that the backwash system was performing too vigorously resulting in excessive scour. The flow rate was reduced to 7500 gpm and several additional tests were conducted.

For the first of these tests, the manifolds were operated in pairs, with the downstream two operated first. The manifolds were each run at a flow rate of 7500 gpm for a period of approximately 4 minutes prototype time. The maximum depth reached during the test was 3.5 feet (elevation of 904.5 feet above MSL). This is considerably less scour than that produced at the higher flow rate. The areal extent of the scour hole was also significantly reduced, as can be seen in Fig. VII-6. The experiment was then conducted at the same flow rate of 7500 gpm for a model period of 2.0 hours. Observing the plume during the test, it was noted that little suspended sediment was carried by the jets after 1 hour and 15 minutes model time (3 hours prototype time). The maximum depth reached during the test was 4.5 feet (elevation of 903.5 feet above sea level). It can be seen in Figure VII-7 that the scour hole is less extensive with most of the scour occurring just in front of the screens. It is apparent from the cross section shown in Figure VII-8 that the slope of the scour hole does not change much with time, but the location and depth of maximum scour change significantly.

The performance of the sediment backwash system at 7500 gpm backwash flow was considered acceptable and testing was halted. The effectiveness of the sediment backwash system and the appearance of the final scour hole are shown in Fig. VII-9.

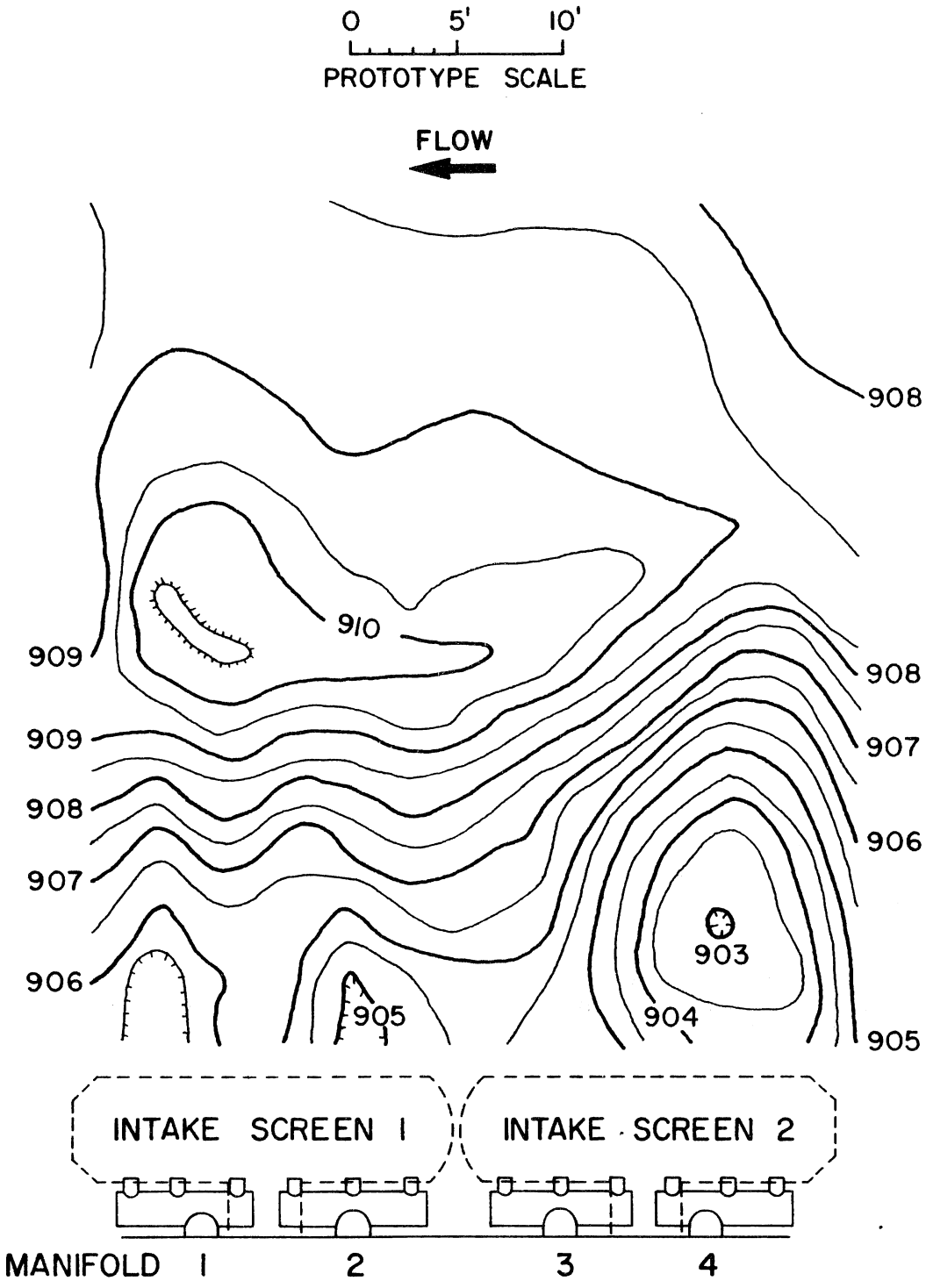

Fig. VII-3. Sediment backwash scour hole pattern (values are for prototype unless otherwise stated.)

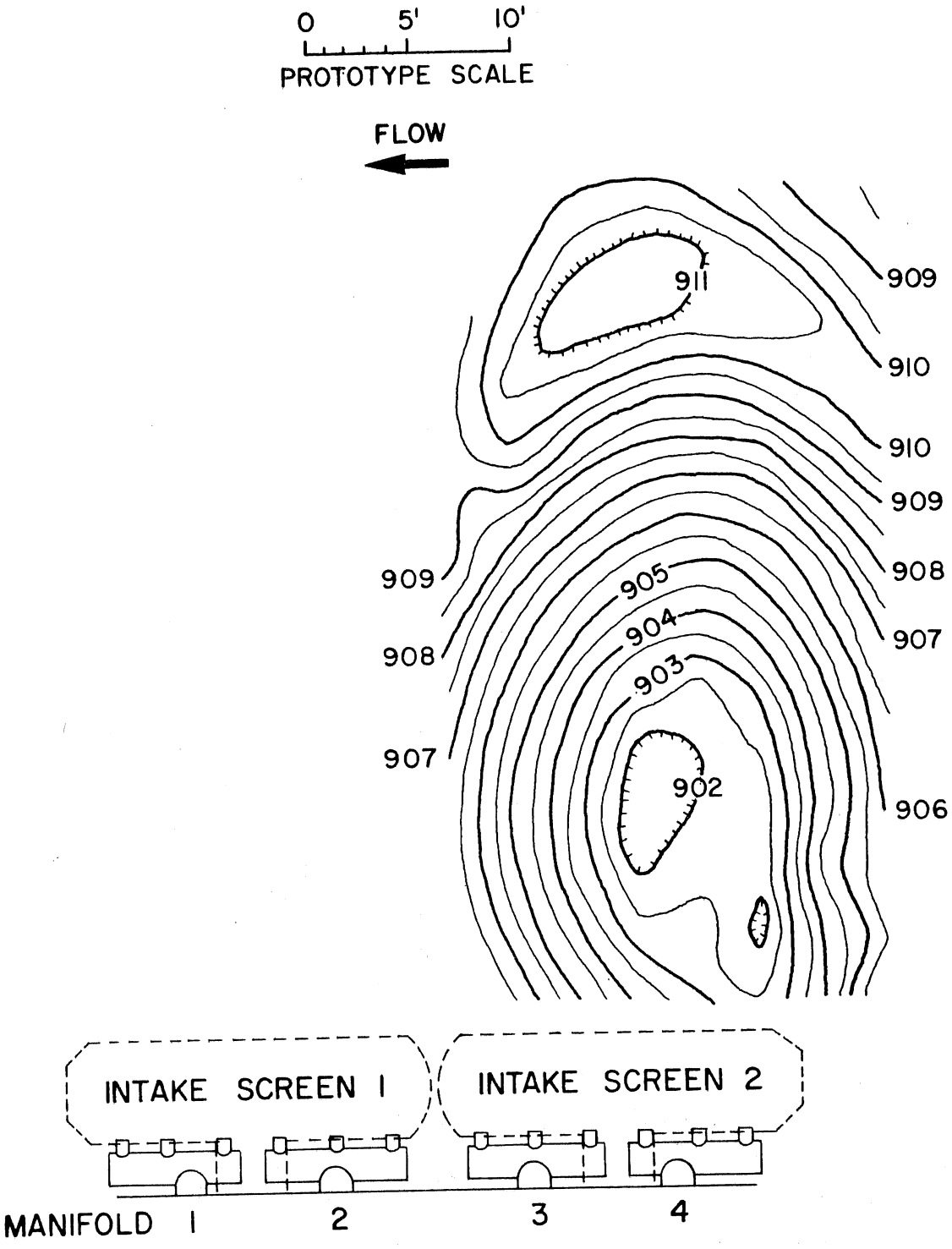

Fig. VII-4. Sediment backwash scour hole pattern (values are for prototype unless otherwise stated.)

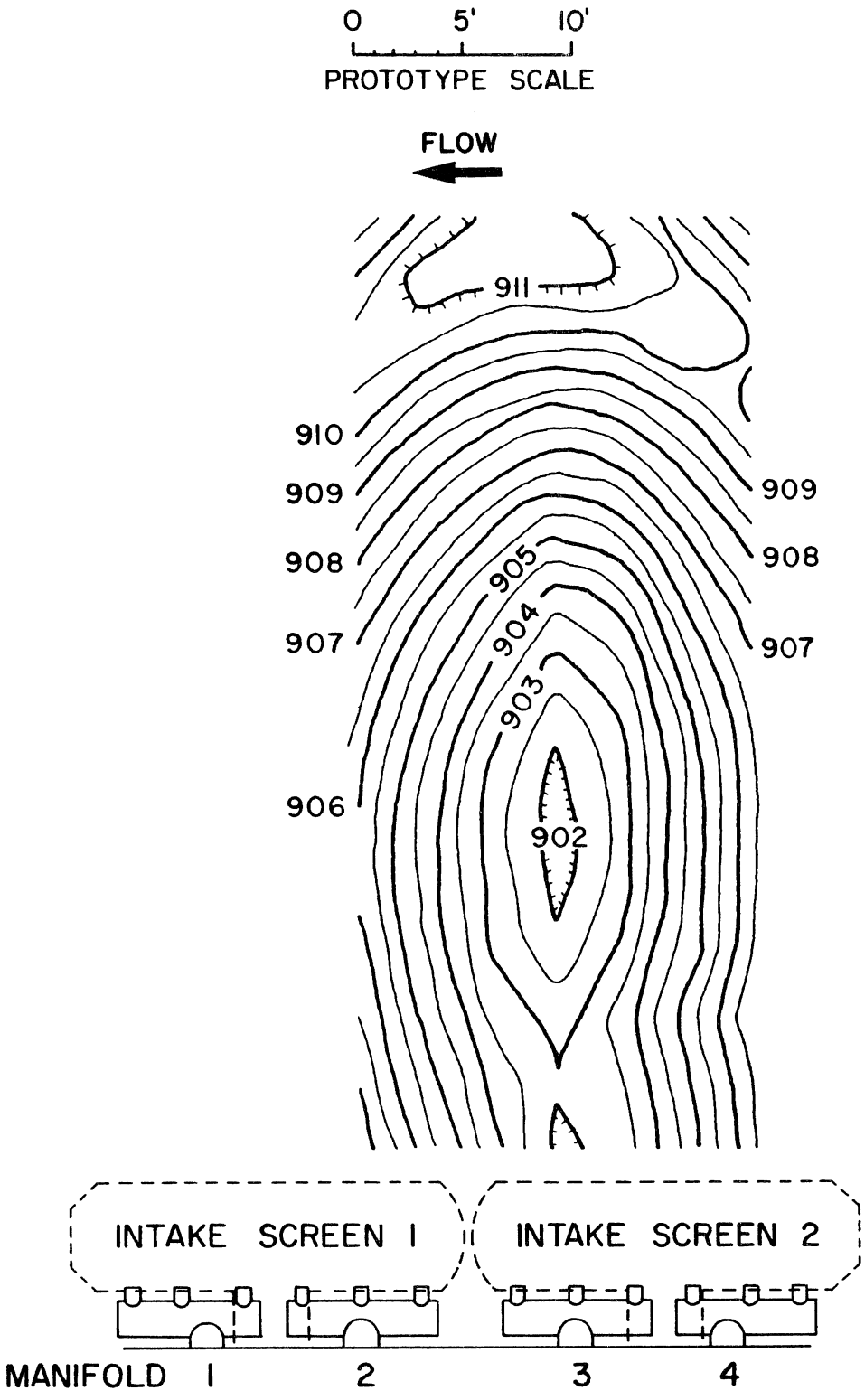

Fig. VII-5. Sediment backwash scour hole pattern (values are for prototype unless otherwise stated.)

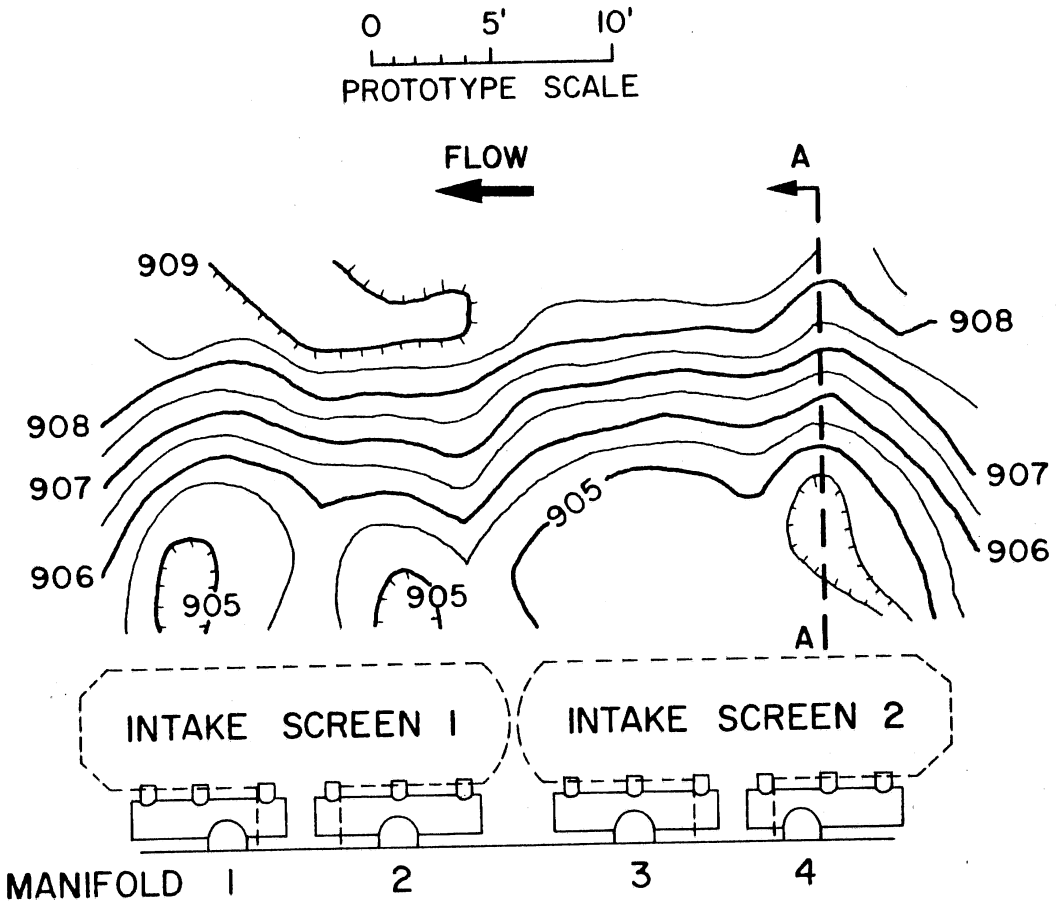

Fig. VII-6. Sediment backwash scour hole pattern (values are for prototype unless otherwise stated.)

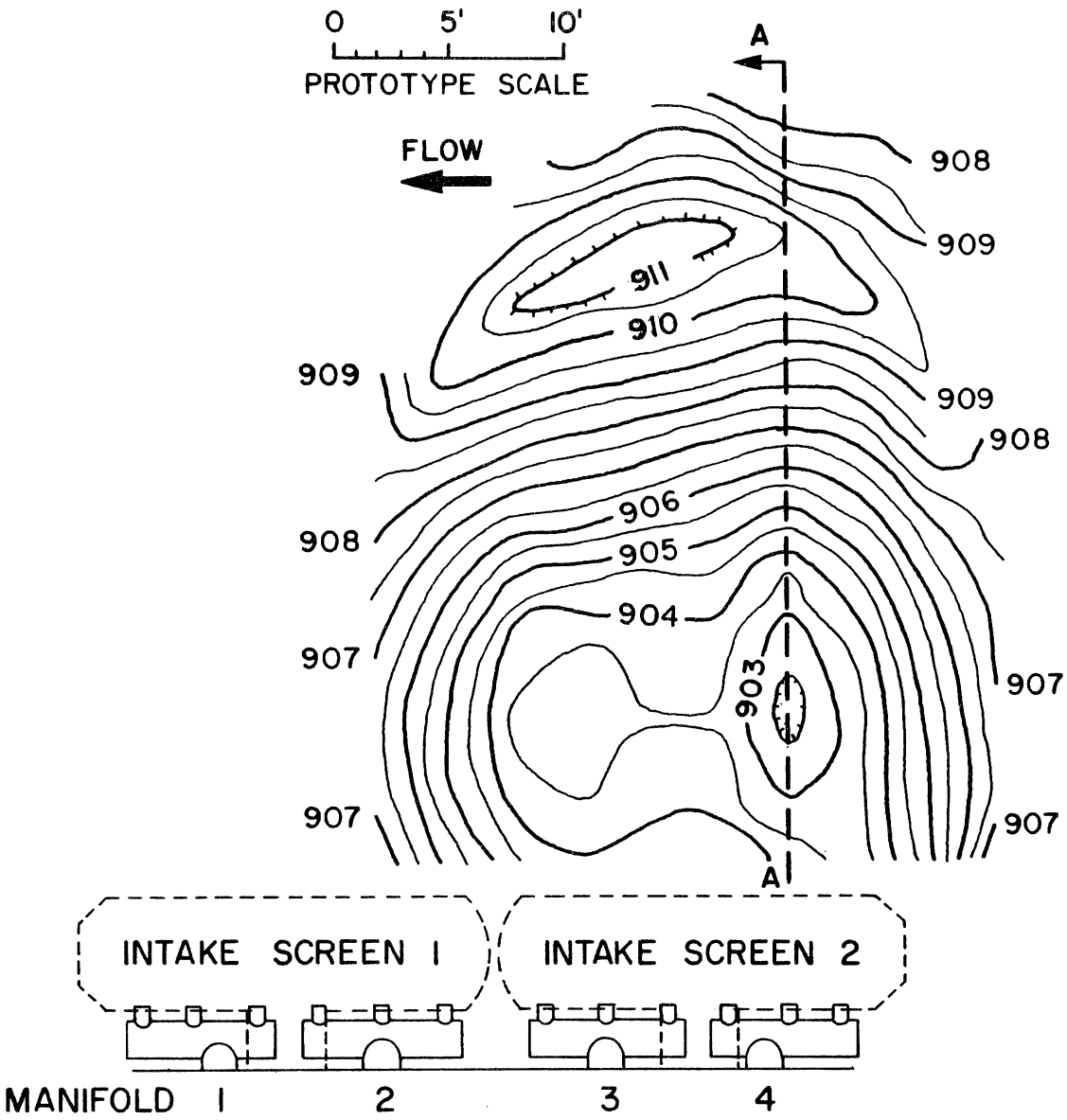

Fig. VII-7. Sediment backwash scour hole pattern (values are for prototype unless otherwise stated.)

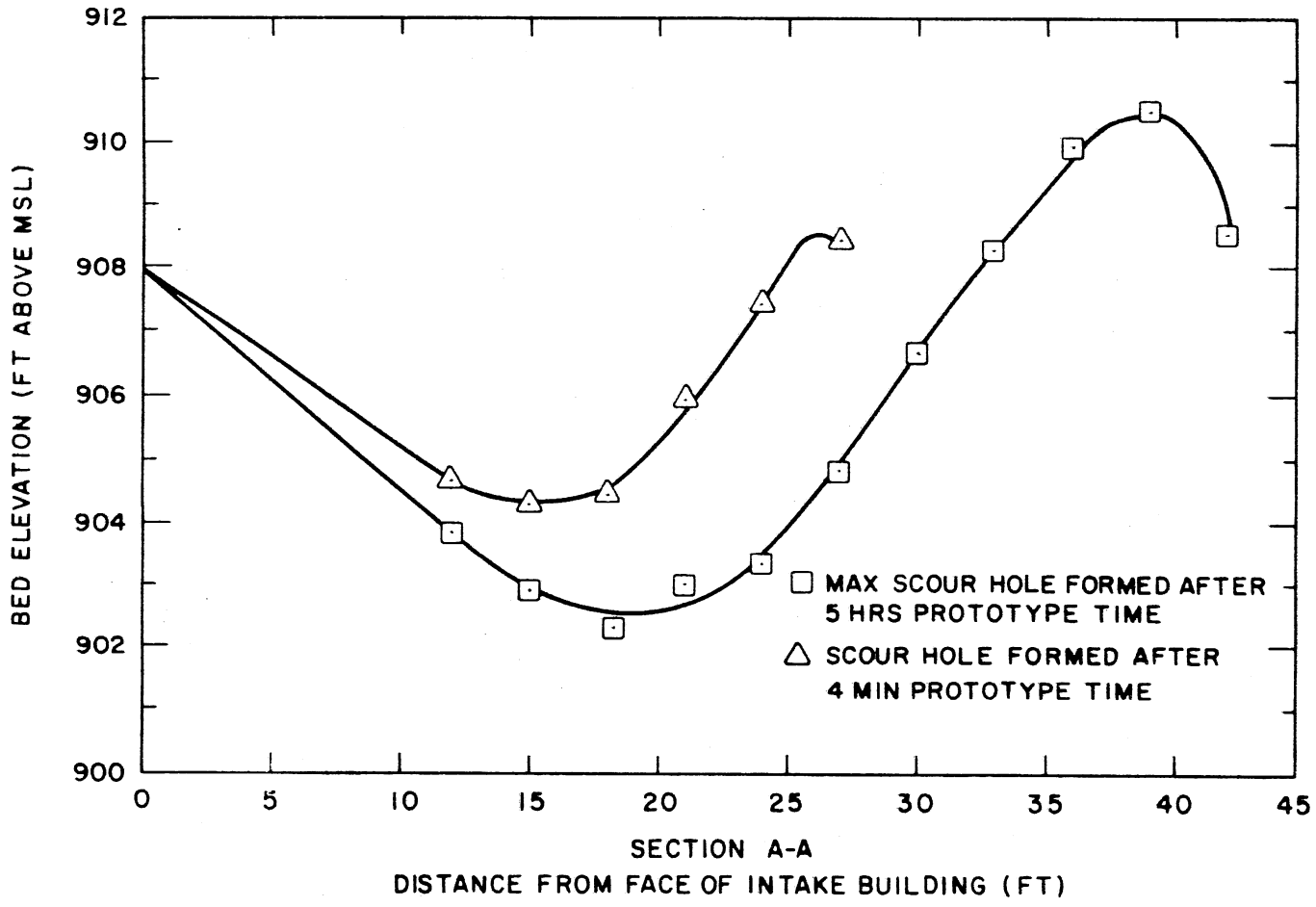

Fig. VII-8. Cross section A-A of scour holes shown in Figs. VII-6 and VII-7 .

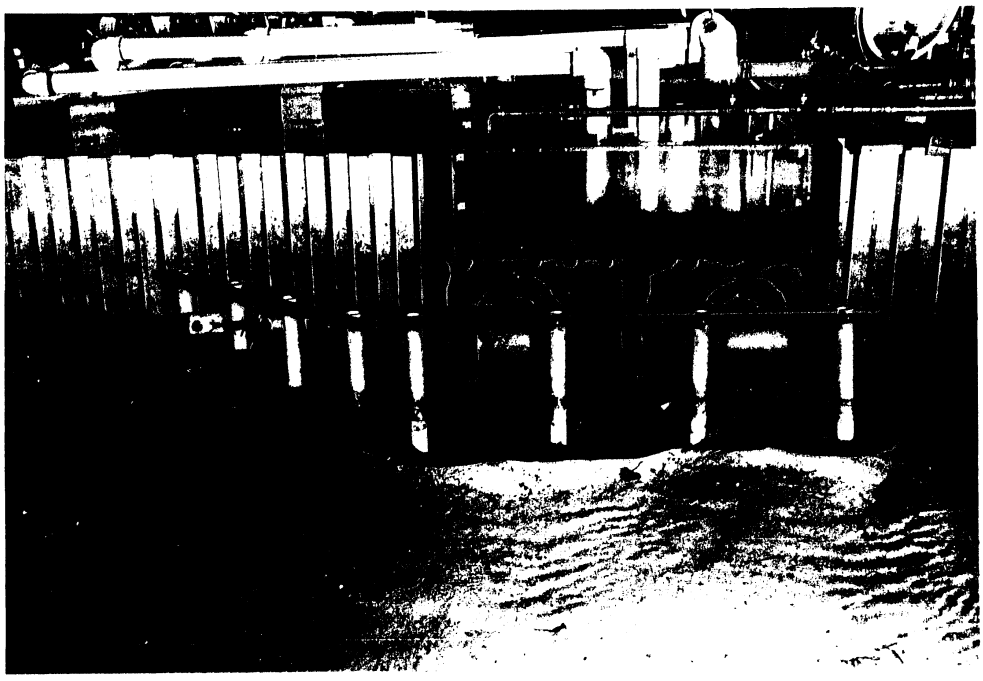

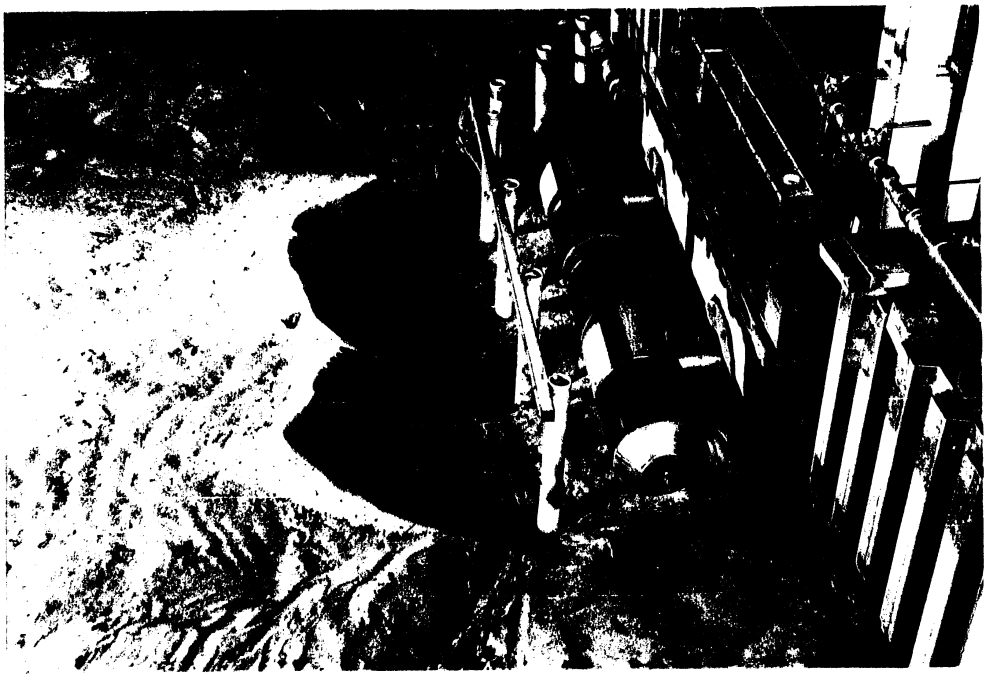

Fig. VII-9. Scour hole after sequential sluicing with 7,500 gpm per manifold for 4 minutes (prototype).

VIII. AIR BACKWASH

The purpose of the air system is to restore a clean screen surface by "blasting" away debris accumulated on the surface by a burst of compressed air released inside the screens. A compressed air supply system consisting of a tank with 130 ft^3 capacity, a small compressor, and a piping system leading to and into the screens, is therefore part of the intake screen system. Air is released inside the screens from a manifold with multiple orifices as designed by Johnson Division, UOP; operational tank pressure is 80 to 100 psi. The air volume released is about three times the screen volume at ambient water pressure.

The design of the air system in the model proved challenging because ambient atmospheric pressure could not be scaled and was the same in prototype and model. Therefore, geometrical similarity for the air flow system was not used. Instead, the air flow model was designed to satisfy the following three criteria: (a) Air pressure in the tank was scaled by the geometrical scale ratio (1:6). The model was operated at 16.7 psi initial tank pressure. (b) Tank volume was scaled such that the ratio of air/volume released to screen volume was the same in model and prototype. The value was about 3. (c) Duration of the air release was scaled according to Froude's law. Model times had to be $\sqrt{6}$ shorter than prototype times. This was achieved by designing the model air tank and pipe system such that initial air flow velocities were all scaled $1:\sqrt{6}$ (Appendix B).

The model air tank and piping system is shown in Figure VIII-1, and in the prototype in Figure VIII-2.

The air blowout system was designed by Johnson Division UOP and tested at the Laboratory. Blowout operation was observed and accepted by personnel from NSP and Black and Veatch.

Blowout experiments were conducted with and without leaf cover on the screen surfaces. Typically, an experiment would last from 2 to 3 seconds in the model, that is, air bubbles would stop to appear on the water surface after that time. Photographs of the water surface at the beginning and at the peak of the airburst are shown in Figures VIII-3 and VIII-4. Leaves were placed on the screen surface by hand. Reducing the initial prototype air tank pressure from 100 psi to 60 psi had no noticeable effect on debris cleaning efficiency.

At typical pressure and typical riverflow, it appeared that approximately 15% of the leaves on the screen at the time of the blowout operation would return to the screen surface when the withdrawal rate was 15,000 gpm per screen.

All air experiments were conducted with one or two water pumps operating, that is, water withdrawal from the pump sump continued during the blowout. To observe possible air ingestion, water flows up to 30,000 gpm per screen were tested. At all water withdrawal flows, only a small amount of air was pulled into the sump from the screens. All of it was released through the water surface before the water reached the pumps (Fig. VIII-5). There is no danger that air is ingested by the pumps from the blowout.

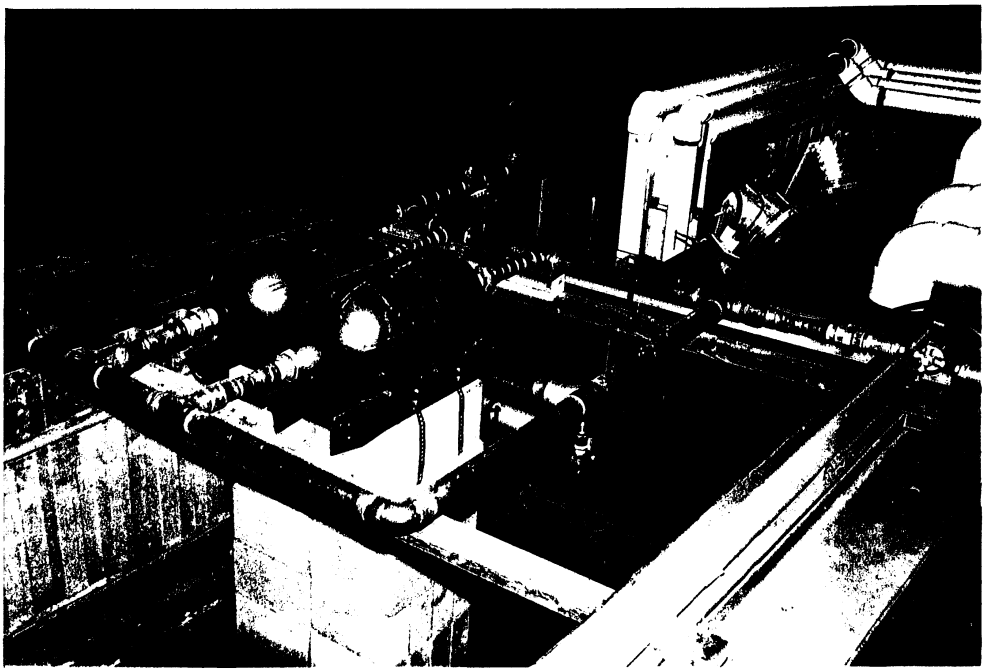

Fig. VIII-1. Model tank and piping system.

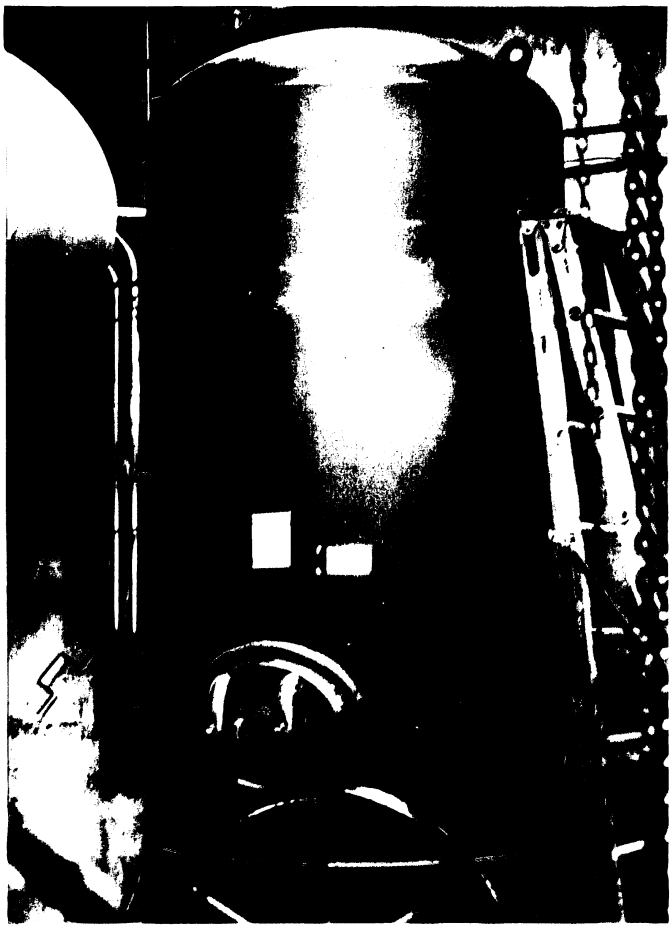

Fig. VIII-2. Prototype air tank.

Fig. VIII-3. Water surface at beginning of air blowout.

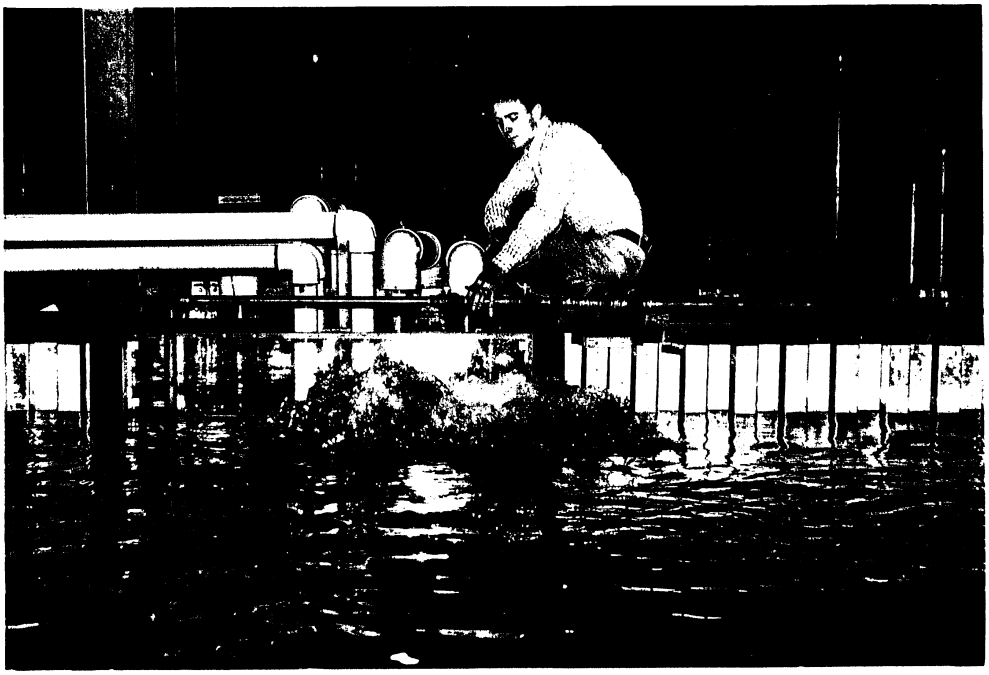

Fig. VIII-4. Water surface at "peak" of air blowout.

Fig. VIII-5. Air from blowout surfacing in pump sump. Withdrawal rate of 30,000 gpm through screen being cleaned.

IX. FLOW PATTERNS IN PUMP SUMP

With the addition of two new pumps to the pump sump, it was necessary to examine flow patterns for any detrimental effects on pump operation. Of concern was the formation of submerged vortices adjacent to the pump bellmouths. Nonuniformity of flow in the pump columns also was measured. Since the pump sump consists of two bays which are symmetrical with regard to the center wall (Fig. IX-1), testing was done in only one half of the sump.

Flow patterns into the bellmouth and pump columns were documented using several techniques:

(a) Dye tracing showed general flow patterns, presence and intensity of vortices.

(b) Yarn angle relative to a radius provided information on the angular direction of the flow entering the pump bellmouth.

(c) A vortimeter (a zero-pitched propeller) located near the probable impeller placement allowed measurement of bulk rotation in the pump column.

(d) Horizontal pitot cylinders placed in the intake column and connected to chamber mounted pressure transducers were used for velocity measurements to check the uniformity of flow distribution in the four quadrants of the pump column (Fig. IX-2).

Through dye tracing, it was possible to find the origin of any detrimental vortex activity. Pathlines of dye were readily observable and effects of structural modifications in the pump sump could be observed.

Yarn angle in terms of degrees deviation from radial flow indicates whether or not the flow entering the bellmouth has much or little angular momentum. The yarn was placed on pins one half the height of the distance between the bellmouth and the sump floor. Yarns were 1.5" long. They were located at the outer perimeter of the bellmouth and at an angular spacing of 60°. The largest acceptable deviation was 30° from radial.

The principal device used for documentation of the swirl in the pump intake was a vortimeter (swirlmeter). The design of such a vortimeter is described by Lee and Durgin [1980]. While dye tracing permitted good observation of general inflow and submerged vortex activity, the vortimeter permitted quantifying the overall flow circulation in the pump intake. It was required that the average prerotation angle be less than 3°, and the maximum instantaneous value during a 30 second (prototype) sampling period be less than 6°. The prerotation angle was defined as the arctangent of the ratio of the tangential velocity divided by the axial velocity of the water in the pump

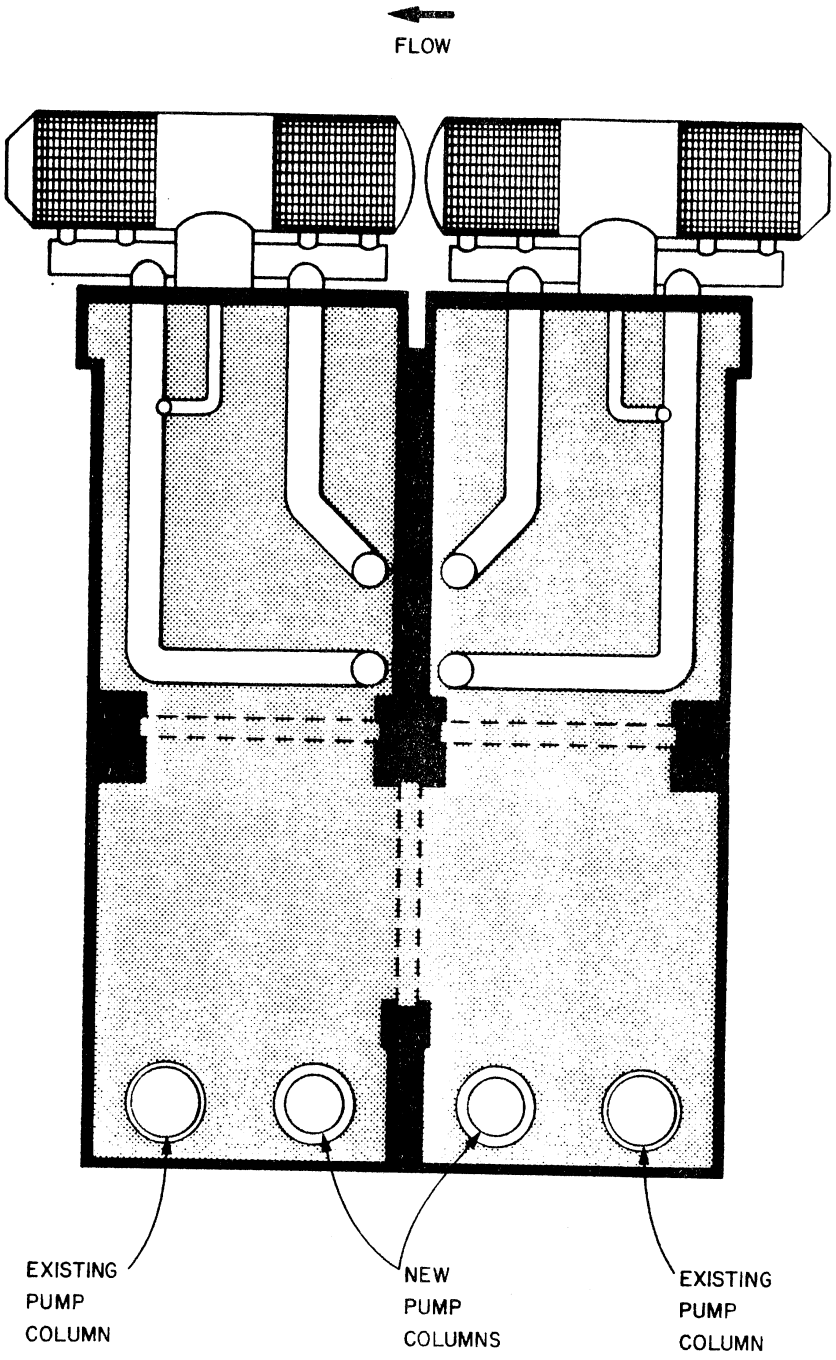

Fig. IX-1. Model pump sump region.

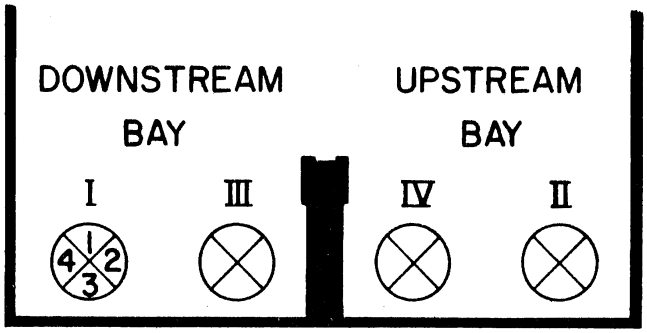

I,II - OUTBOARD PUMPS
III,IV - INBOARD PUMPS

1-FRONT QUADRANT
2-RIGHT QUADRANT
3-BACK QUADRANT
4-LEFT QUADRANT

Fig. IX-2. Pump sump terminology.

column. Using these values equivalent rotational rates for the vortimeter were obtained. These values were 40 and 81 rpm for average and maximum permissible rotation, respectively.

Using all of the above methods, particularly dye tracing and vortimeter rotation, 24 possible combinations of pump and gate operations were tested. The results are given in Table IX-1 in terms of vortimeter rotation rates and vortex activity. The worst case conditions are easily identified. These conditions were associated with high cross-flow velocities into the pump sump bay, which in turn were produced by adverse gate settings. Increased crossflow leads to more angular momentum.

Strong swirls occurred on the floor and under the bellmouth and on the backwall directly behind the intake columns under the most adverse flow conditions. Although the swirls were unable to develop into dyecore type vortices (see definition in Appendix C), it was desirable to reduce their activity. Wedge shaped bodies were placed underneath the pump columns to reduce vortex activity, as shown schematically in Figure IX-3. The wedges assist the flow along the pump sump floor to turn upwards into the bellmouths. The crestline of the wedges provides a well-defined location for flow separation. The wedges tested varied in total height, total length, and convergence angle of the sides (Fig. IX-4). In addition to the wedges, a submerged wall was sometimes placed in front of the bellmouths. The wall had the same orientation as the wedges and was typically 1.25 feet high and 4 feet long. Table IX-2 shows the effectiveness of the various structural modifications tested. All testing was done under worst case conditions. Worst flow condition is configuration No. 10 in Table IX-1. It has a strong cross-flow component because all water is withdrawn through one screen assembly and sent to the diagonally opposed pumps.

Twelve combinations of wedge heights, wedge location, and submerged wall were tested as specified in Figure IX-5. Design 1, with minimal geometrical interference, was found to suppress vortex formation underneath the bellmouth intake effectively. The wedge was the smallest tested, but it was large enough to provide the effect required. Steeper and higher wedges have the potential to form their own separated flow regions when flow combinations other than the worst case are tested. The 30° side angle reduced swirl not only underneath the bellmouth intake, but also behind the bellmouth where strong wall swirls occurred under certain conditions. The 30° slope also provided adequate wedge height for construction. A large apex angle reduces the size of the separation zone on the downstream side of the wedge during strong crossflow. This was an important factor in minimizing the amount of swirl along the back wall.

It was observed during testing that under some flow conditions surface vortices would develop. As seen in Table IX-1, under the most severe flow conditions dye core type surface vortices were quite prevalent. Several remedial structures consisting of I-beams were tested. They were placed in regions of high surface shear. The beams were very effective in eliminating the dye core vortices in regions of high crossflow. However, the I-beams were found to be ineffective in secondary flow regions and occasional dyecore formation was still noted.

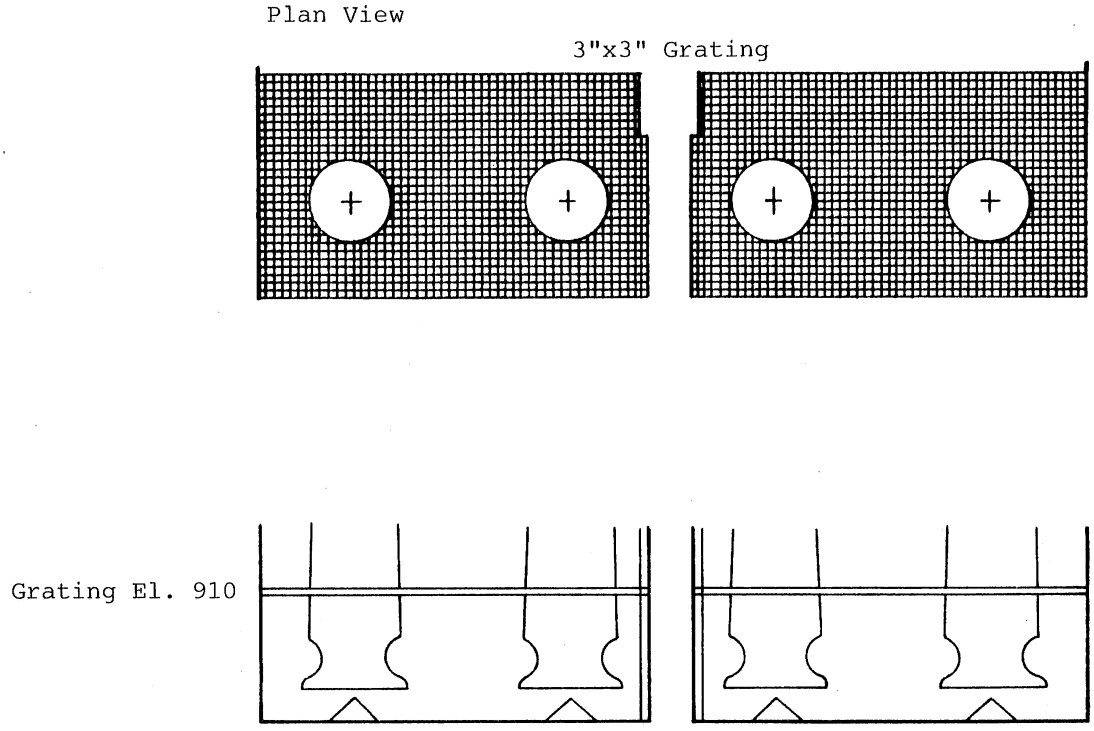

Fig. IX-3. Accepted surface vortex prevention measures. (Not to scale.)

TABLE IX-1. Summary of Initial Design Testing.

Initial Design Testing — Water Surface Stage 915.0 AMSL

CONFIGURATION	GATE			PUMPS OPERATING				VORTEX ACTIVITY			VORTIMETER ROTATION RATE	
	DS[1]	US[2]	SW[3]	1	3	4	2	Surface	Submerged: Wall	Submerged: Floor	Average RPM 5 min Prototype	Maximum RPM 30 sec Prototype
1 Q_4=15,000*	UP	UP	UP			X		Dye core 21% inboard front left	moderate swirl	moderate swirl	less than 1	2.5
2 Q_2=15,000*	UP	UP	UP				X	none	moderate swirl	weak to moderately weak swirl	less than 1	less than 2
3 Q_4=Q_2=15,000*	UP	UP	UP			X	X	dye core 11% inboard front left	(4) weak to moderate swirl (2) weak to moderate swirl	(4) moderately strong to strong swirl (2) weak to moderately strong swirl	(4) 6.5 (2) 2.5	(4) 9 (2) 8
4 Q_1=Q_4=15,000*	UP	UP	UP	X		X		none	weak to moderate swirl	inconsistent weak to moderate swirl	less than 1	less than 2
5 Q_3=Q_4=15,000*	UP	UP	UP		X	X		none	weak to moderate swirl	inconsistent weak swirl	less than 1	less than 2
6 Q_1=Q_2=15,000	UP	UP	UP	X			X	none	moderately weak to moderate swirl	weak swirl	less than 1	less than 2
7 Q_3=Q_2=15,000*	UP	UP	UP		X		X	none	moderate swirl	weak swirl	1	2
8 Q_4=15,000*	UP	DOWN	UP			X		dye core 25% front left	inconsistent weak to moderate swirl	moderate swirl	3.5	7.5
9 Q_2=15,000*	UP	DOWN	UP				X	minimal	moderate consistent swirl	moderate inconsistent swirl	2.0	5.0
10 Q_4=Q_2=15,000*	UP	DOWN	UP			X	X	dye core 12% air bubbles pulled down inboard front left	(4) weak to moderate swirl (2) moderate swirl	(4) strong swirl (2) strong swirl	(4) 26.75 (2) 6.0	(4) 30 (2) 16
11 Q_1=Q_4=15,000*	UP	DOWN	UP	X		X		small short-lived dimples shed from center pier +30%	weak to weakly moderate swirl	moderate swirl	3.75	8.75
12 Q_3=Q_4=15,000*	UP	DOWN	UP		X	X		some short-lived dimples shed from center pier +30%	inconsistent weak to moderate swirl	moderate to moderately strong swirl	2.0	5.0

[1]Downstream
[2]Upstream
[3]Splitter Wall

*15,000 gpm prototype

TABLE IX-1. (Cont.)

Initial Design Testing — Water Surface Stage 915.0 AMSL

CONFIGURATION	GATE			PUMPS OPERATING				VORTEX ACTIVITY			VORTIMETER ROTATION RATE	
	DS[1]	US[2]	SW[3]	1	3	4	2	Surface	Submerged: Wall	Submerged: Floor	Average RPM 5 min Prototype	Maximum RPM 30 sec Prototype
13 $Q_1=Q_2=15,000$*	UP	DOWN	UP	X			X	some short-lived dimples	moderate swirl	moderately strong swirl	2.3	6.7
14 $Q_3=Q_2=15,000$*	UP	DOWN	UP		X		X	short-lived dimples approximately 10%	inconsistent weak to moderate swirl	strong swirl	15	18.1
15 $Q_4=15,000$*	DOWN	UP	UP			X		none	moderately weak to moderate swirl	moderate swirl	less than 1	less than 2
16 $Q_2=15,000$*	DOWN	UP	UP				X	none	weak to moderate swirl	weak swirl	less than 1	less than 2
17 $Q_4=Q_2=15,000$*	DOWN	UP	UP			X	X	none	(4) weak to moderate swirl (2) moderately strong to strong swirl	(4) strong swirl (2) strong swirl	(4) 6.5 (2) 7	(4) 11 (2) 10
18 $Q_1=Q_4=15,000$*	DOWN	UP	UP	X		X		20% dimple generalized circulation in back right corner	moderately strong swirl	moderate swirl	3.25	9
19 $Q_3=Q_4=15,000$*	DOWN	UP	UP		X	X		none	moderately strong swirl	moderate to moderately weak swirl	2.25	5
20 $Q_1=Q_2=15,000$*	DOWN	UP	UP	X			X	loose dye core approximately 5% outboard back right	moderately strong to strong swirl	moderate to strong swirl	3	5
21 $Q_3=Q_2=15,000$*	DOWN	UP	UP		X		X	none	moderate to strong swirl	moderate to strong swirl	5	10
22 $Q_4=15,000$*	UP	UP	DOWN			X		dye core approximately 3% inboard back left	moderately weak to moderate swirl	moderately weak to moderately strong swirl	less than 1	3
23 $Q_2=15,000$*	UP	UP	DOWN				X	none	moderate to strong swirl	weak to moderate swirl	less than 1	less than 2
24 $Q_4=Q_2=15,000$*	UP	UP	DOWN			X	X	dye core 4% inboard back left to back center	(4) moderate swirl (2) moderate to strong swirl	(4) strong swirl (2) strong swirl	(4) 8 (2) 5	(4) 12 (2) 7

[1]Downstream
[2]Upstream
[3]Splitter Wall

*15,000 gpm prototype

TABLE IX-2. Summary of Submerged Circulation Inhibitor Testing.

Submerged Circulation Inhibitor Testing — Water Surface Stage 915.0 AMSL — Q = 15,000 gpm per pump in operation

CONFIGURATION	GATE			PUMPS OPERATING				VORTEX ACTIVITY			VORTIMETER ROTATION RATE	
	DS[1]	US[2]	SW[3]	1	3	4	2	Surface	Submerged Wall	Submerged Floor	Average RPM 5 min Prototype	Maximum RPM 30 sec Prototype
Circulation Inhibitor Design 1	UP	DOWN	UP			X	X		reduced in strength, position fixed	overall circulation under bellmouth reduced, may increase in back quadrant	(4) 15.5 (2) 3.6	(4) 21 (2) 8
Circulation Inhibitor Design 2	UP	DOWN	UP			X	X	forces more flow to left side of intake, little noticed shedding from wall		inboard (4) moderate to strong floor swirl, outboard (2) weak to moderately strong swirl on floor	(4) 13 (2) 4.7	(4) 22.5 (2) 10
Circulation Inhibitor Design 3	UP	DOWN	UP			X	X				(4) 9.8 (2) 7	(4) 10 (2) 13
Circulation Inhibitor Design 4	UP	DOWN	UP			X	X	reduces overall circulation further than design 1, more local vorticity in back quadrant			(4) 1 (2) 3	(4) 4 (2) 10
Circulation Inhibitor Design 5	UP	DOWN	UP			X	X	inconsistent rotational direction		more general circulation, less concentrated in back	(4) 5.75 (2) 2.3	(4) 10 (2) 7
Circulation Inhibitor Design 6	UP	DOWN	UP			X	X			inboard: some rotation in back quadrant, may have uneven flow distribution outboard: floor swirl moderate	(4) 2.6 (2) 1.8	(4) 8.0 (2) 5.0
Circulation Inhibitor Design 7	UP	DOWN	UP			X	X		circulation reduced along wall	strong swirl on wedge in back quadrant	(4) 0.9 (2) 4.5	(4) 2.5 (2) 12.0

[1]Downstream
[2]Upstream
[3]Splitter Wall

TABLE IX-2. (Cont.)

Submerged Circulation Inhibitor Testing — Water Surface Stage 915.0 AMSL — Q = 15,000 gpm per pump in operation

CONFIGURATION	GATE			PUMPS OPERATING				VORTEX ACTIVITY			VORTIMETER ROTATION RATE	
									Submerged		Average RPM 5 min Prototype	Maximum RPM 30 sec Prototype
	DS[1]	US[2]	SW[3]	1	3	4	2	Surface	Wall	Floor		
Circulation Inhibitor Design 8	UP	DOWN	UP			X	X			inboard: weak to weakly moderate swirl in back quadrant outboard: moderate to strong bottom swirl	(4) 1.0 (2) 1.8	(4) 2.5 (2) 5
Circulation Inhibitor Design 9	UP	DOWN	UP			X	X		inboard: moderate to strong back-wall swirl, outboard: weak to weakly moderate back wall swirl	inboard: moderate floor swirl general and back quadrant, outboard: weak floor swirl	(4) 0.6 (2) 1.3	(4) 5 (2) 7
Circulation Inhibitor Design 10	UP	DOWN	UP			X	X		inboard: strong back wall swirl, outboard: weak variable back wall swirl	inboard: weak floor (general) swirl, strong back quadrant swirl, outboard: weak to non-existent floor swirl	(4) 0.4 (2) 0.8	(4) less than 2 (2) 5
Circulation Inhibitor Design 11	UP	DOWN	UP			X	X			inboard: moderate back quadrant swirl, some circulation behind front edge, little in back	(4) 0.1 (2) 0.9	(4) less than 2 (2) 2.4
Circulation Inhibitor Design 12	UP	DOWN	UP			X	X	dead zone in line with wedge		inboard: moderate back quadrant swirl, some circulation behind front edge outboard: small amount of circulation behind front edge, little in back	(4) 0.5 (2) 0.7	(4) 3.75 (2) 3.3

[1]Downstream
[2]Upstream
[3]Splitter Wall

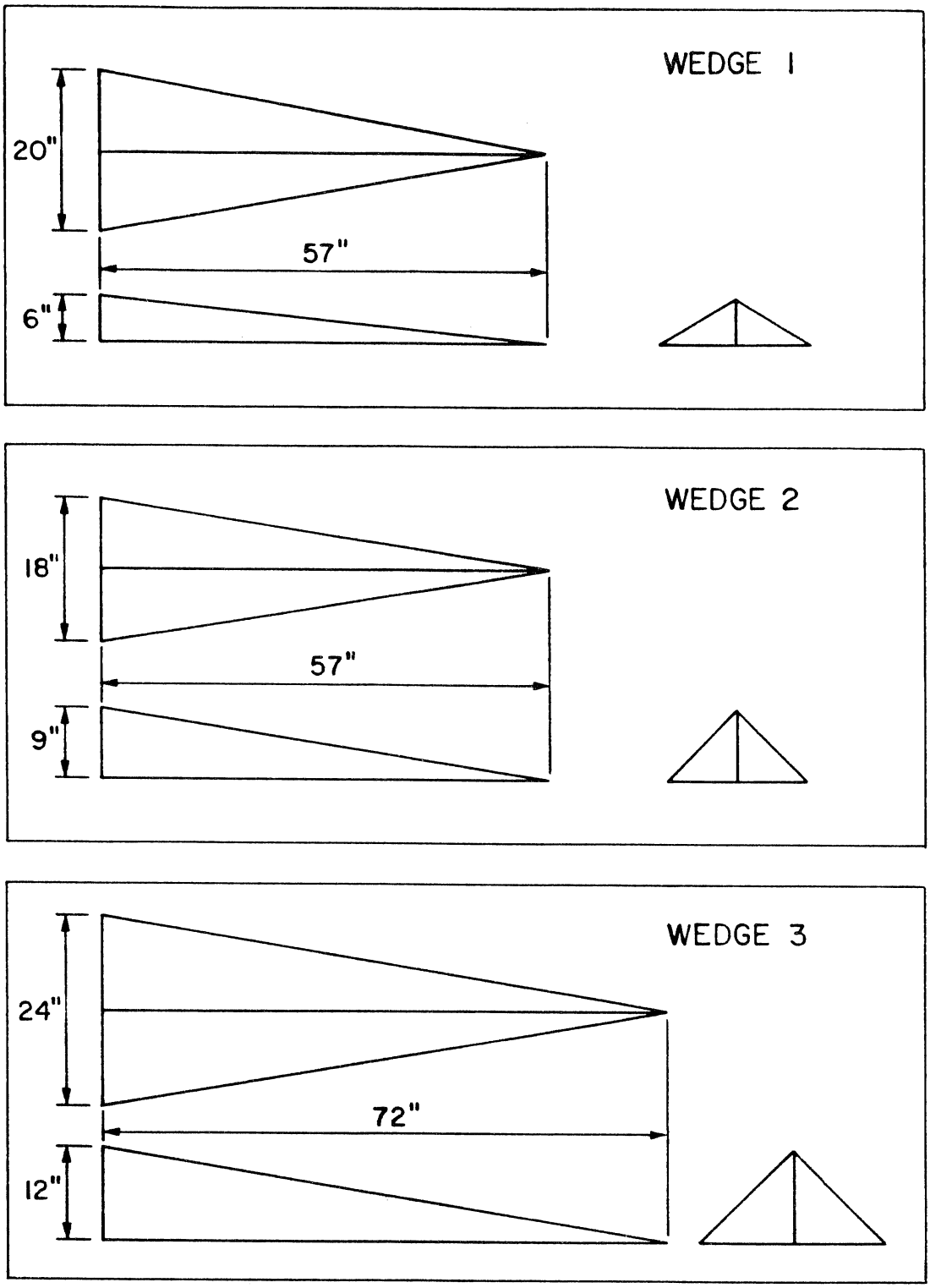

Fig. IX-4. Wedge designs tested.

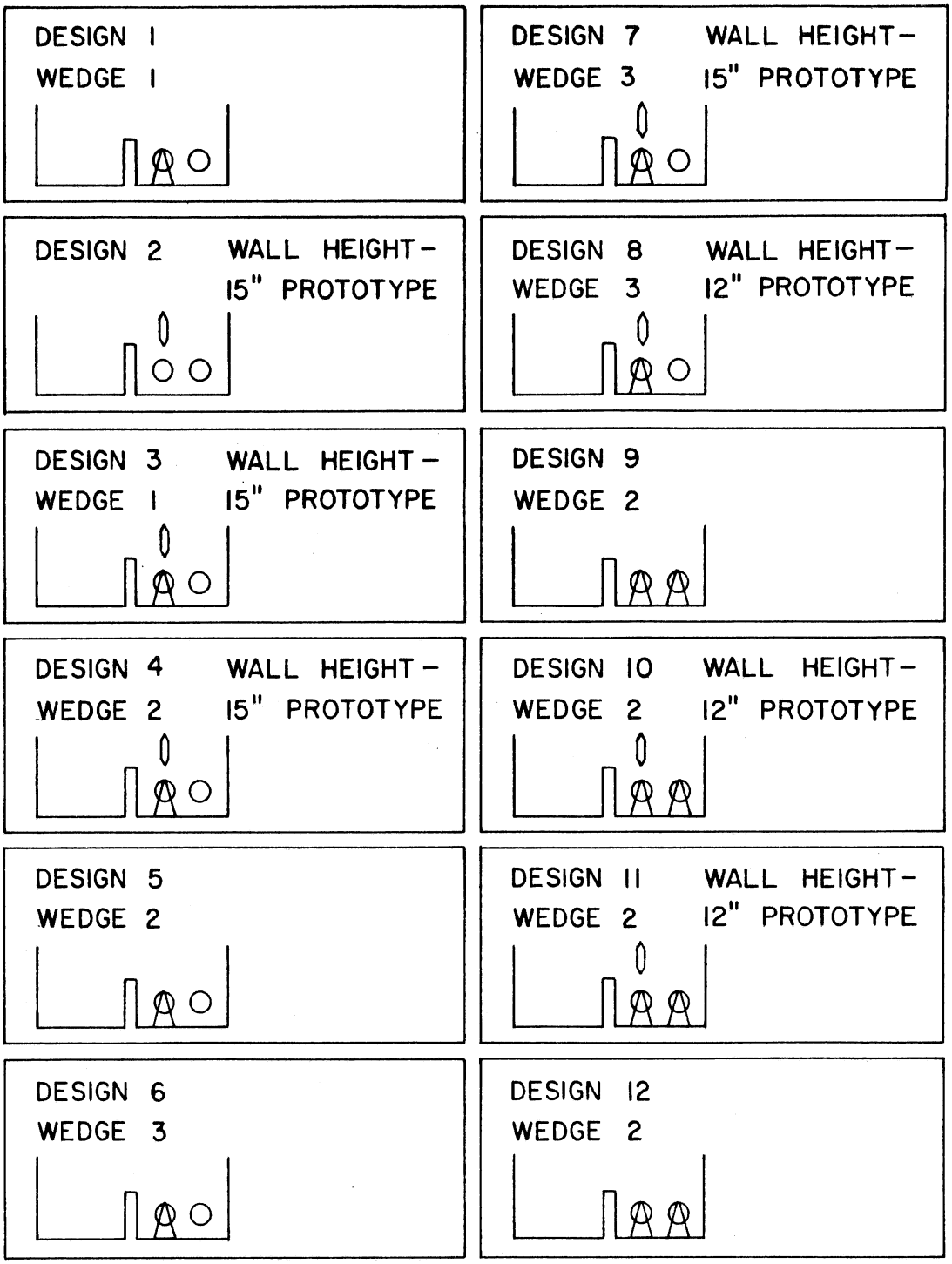

Fig. IX-5. Submerged circulation reduction designs tested.

Reasoning that a tighter grid size may be more effective than the loose grid formed by the I-beams, horizontal grating was tested. Grating can be submerged to nearly any level. This was advantageous because the water surface elevation at the site, and therefore in the pump sump, has a large seasonal fluctuation. The grating used had dimensions of 3x3 inches for the openings and was 2 inches thick. In the model (1:6 scale), this matched the dimensions of grids used on fluorescent light diffusers. With the agreement of Black and Veatch, the grating was installed horizontally at elevation 910 feet above MSL, 4 feet above the floor of the pump sump (Fig. IX-3). This provides adequate submergence without any detrimental effect on the inflow to the bellmouths. During testing, the grating prevented any surface vortex activity from reaching the bellmouths.

After completion of the design modifications within the sump pump, all 24 possible flow conditions within the sump pump were documented (Table IX-3). This was similar to the initial testing program summarized in Table IX-1.

Dye was used to observe the general flow patterns of the final design. Dye was also necessary to detect surface and subsurface vorticity in the flow. Yarn angles were recorded and are shown in Figure IX-6 for the worst case and for a typical operational condition. Prerotation in the pump columns was measured with the vortimeters. The values of prerotation obtained, along with the dye tracing observations are shown in Table IX-3.

To further quantify pump intake conditions, axial pump throat velocities were measured in each of four quadrants of pump columns 2 and 4 for all operating conditions. The measurements were made using Pitot cylinders connected to chamber mounted pressure transducers. The stagnation pressure hole was located at the centroid of each quadrant. The lines connecting the Pitot tube and the transducers were of copper and carefully purged of air before each experiment. A sampling rate of 3.3 measurements per second in the prototype (8 measurements per second in the model) was chosen. A total of 1440 data points was obtained for each location during a 7.4 minute prototype (3 minute model time) testing period. A flush mounted static pressure hole was also connected to a transducer to provide the static pressure values necessary for velocity calculations. All measurements were made in the throat of the pump column.

The 1440 instantaneous velocity data in each quadrant were reduced to the following values:

(1) time average velocity $\overline{V}_i$, where i = 1 to 4 designates the quadrant.

(2) standard deviation of velocity σ_i , relative to the time average $\overline{V}_i$.

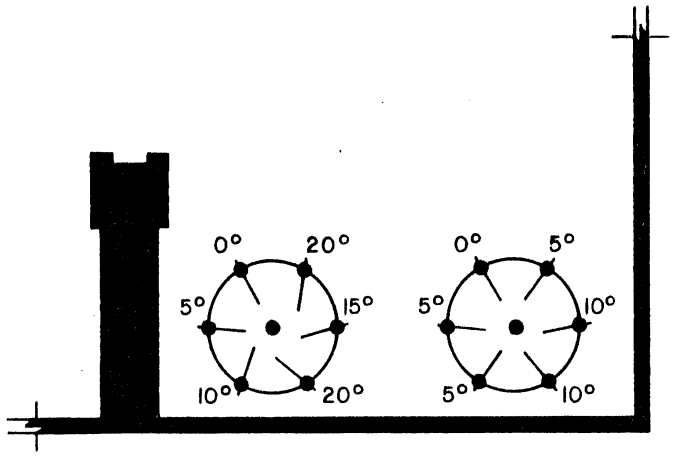

WORST CASE OPERATION
$Q_2 = Q_4 = 15000$ GPM
UPSTREAM GATE DOWN

CONFIGURATION NO. 10
WATER SURFACE EL. 915

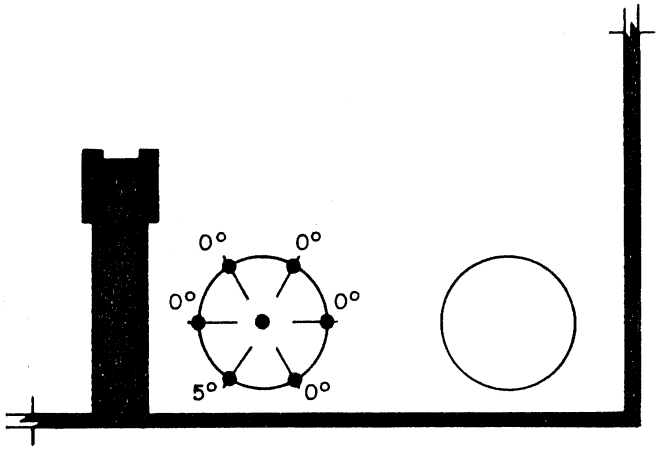

TYPICAL OPERATIONAL CONDITION
$Q_4 = 15000$ GPM
ALL GATES UP

CONFIGURATION NO. 1
WATER SURFACE EL. 919

Fig. IX-6. Yarn angles below bellmouth perimeter.

TABLE IX-3. Summary of Final Design Documentation.

Final Design Documentation — Water Surface Stage 915.0 AMSL — Q = 15,000 gpm per pump in operation

CONFIGURATION	GATE			PUMPS OPERATING				VORTEX ACTIVITY			VORTIMETER ROTATION RATE	
	DS[1]	US[2]	SW[3]	1	3	4	2	Surface	Submerged: Wall	Submerged: Floor	Average RPM 5 min Prototype	Maximum RPM 30 sec Prototype
1	UP	UP	UP			X		swirls front left 80% dye core back left approximately 10%, broken up by grate	weak swirl	none to weak swirl	less than 1	less than 2
2	UP	UP	UP				X	slight swirl back right	none to weak swirl	none to weak swirl	less than 1	less than 2
3	UP	UP	UP			X	X	(4) swirl shed from center wall 60% (2) dimple back left 15%	(4) weak to moderate swirl (2) moderate swirl	(4) moderate swirl (2) moderate swirl	(4) 1.4 (2) 4.1	(4) 5.0 (2) 10.0
4	UP	UP	UP	X		X		some swirls shed from center wall	weak to moderately weak swirl	none to weak swirl	1	2
5	UP	UP	UP		X	X		surface swirls shed from center wall only	none to moderate swirl	none to weak swirl	3	6
6	UP	UP	UP	X			X	dimple approximately 40% back right, occasional dye core broken up by grate	weak to moderate swirl	not to weak swirl	1	3.3
7	UP	UP	UP		X		X	dimples back right to center right approximately 10%	weak to moderate swirl	weak swirl	less than 1	less than 2
8	UP	DOWN	UP			X		swirls shed off of center wall	weak to moderate swirl	none to moderately weak swirl	1	2
9	UP	DOWN	UP				X	none	moderate swirl	moderate swirl	7.0	12
10	UP	DOWN	UP			X	X	(4) swirls shed from center wall 80% (2) nothing seen	(4) strong swirl (2) moderately strong swirl	(4) strong swirl (2) moderately strong swirl	(4) 8.5 (2) 7.0	(4) 16 (2) 18.0
11	UP	DOWN	UP	X		X		none	moderate to strong swirl	moderate swirl	14.5	18
12	UP	DOWN	UP		X	X		none	moderate to strong swirl	moderate swirl	16	22

[1]Downstream
[2]Upstream
[3]Splitter Wall

TABLE IX-3. (Cont.)

Final Design Documentation — Water Surface Stage 915.0 AMSL — Q = 15,000 gpm per pump in operation

CONFIGURATION	GATE			PUMPS OPERATING				VORTEX ACTIVITY			VORTIMETER ROTATION RATE	
	DS[1]	US[2]	SW[3]	1	3	4	2	Surface	Submerged Wall	Submerged Floor	Average RPM 5 min Prototype	Maximum RPM 30 sec Prototype
13	UP	DOWN	UP	X			X	none	weak to moderate swirl	weak to moderately weak swirl	2.5	5.0
14	UP	DOWN	UP		X		X	none	moderate swirl	none to weak swirl	less than 1	less than 2
15	DOWN	UP	UP			X		none	weak swirl	none to weak swirl	less than 1	less than 2
16	DOWN	UP	UP				X	slight swirl back right, strong swirl back left, rotation is slowed by grate	weak swirl	none to weak swirl	less than 1	less than 2
17	DOWN	UP	UP			X	X	(4) none (2) none	(4) none to moderate swirl (2) weak to moderately weak swirl	(4) none to moderately swirl (2) weak swirl	(4) 4.0 (2) 12.0	(4) 7.5 (2) 22.0
18	DOWN	UP	UP	X		X		none	weak swirl	none to moderately weak swirl	5.0	9.0
19	DOWN	UP	UP		X	X		none	weak to moderate swirl	none to moderately weak swirl	6.25	12
20	DOWN	UP	UP	X			X	none	moderate swirl	none to moderate swirl	6	16
21	DOWN	UP	UP		X		X	dimples back right 25%	weak to moderate swirl	none to weak swirl	8	15
22	UP	UP	DOWN			X		general swirl back left, slowed by grate	weak swirl	none to moderately weak swirl	less than 1	less than 2
23	UP	UP	DOWN				X	moderate swirl back left, rotation slowed by grate	weak swirl	none to weak swirl	less than 1	less than 2
24	UP	UP	DOWN			X	X	(4) none (2) none	(4) none to moderate swirl (2) weak swirl	(4) none to moderately weak to weak swirl (2) none to weak swirl	(4) 8.5 (2) 7.5	(4) 15.0 (2) 17.0

[1]Downstream
[2]Upstream
[3]Splitter Wall

(3) the longterm spatial distribution ratios $\overline{V}_i/\overline{V}$, where $\overline{V} = Q/A$ is the column average of the velocity $= 1/4 \sum_1^4 \overline{V}_i$.

(4) the longterm spatial non-uniformity ratio $\overline{V}_i/\overline{V}_{max}$, where $\overline{V}_{max}$ is the largest of the time averaged $\overline{V}_i$ values in the four quadrants.

(5) the minimum instantaneous velocity ratio MIVR $= \underset{1}{\overset{1440}{MIN}} [V_i/V_{max}]$, where V_{max} is the largest of the velocities in the four quadrants at every instant. The minimum ratio is selected from the 1440 measurements.

(6) the minimum sliding average velocity MOSAVR $= \underset{1}{\overset{1440}{MIN}} [V_{isave}/V_{savemax}]$ where the subscript save refers to an eight value sliding average.

Numerical values of the above six parameters are given in Tables IX-4 and IX-5. A one-minute graphical sample of the data is given in Appendix D.

The time averages $\overline{V}_i$ need no particular explanation. The standard deviations σ_i in pump column 4 are on the order of 3 to 6 percent of the time averages. In pump column 2 they are higher. The higher values may be affected by vibrations of the pump columns. The spatial distribution ratios $\overline{V}_i/\overline{V}$ are within .93 to 1.04 and all $\overline{V}_i/\overline{V}_{imax}$ values within .90 to 1.0, indicating good spatial uniformity of the flow field in the columns. Instantaneous MIVR-values indicate large variations, not necessarily representative only of velocity fluctuations, and not necessarily calculated. MOSAVR values are not within the range 0.9 to 1.0 for all operating conditions, indicating that velocities will differ by more than 10 percent between quadrants for short time periods. The total range of MOSAVR is from 0.69 to .97.

On the basis of all flow observations, velocity measurements and yarn angle observations, the 24 possible operating conditions investigated have been divided into three categories:

TABLE IX-4a. Throat Velocities in Pump Columns 2 and 4 at Normal Operating Conditions (Design Flow).

OPERATING CONFIGURATION NO.*	PUMP COLUMN NO.	QUADRANT NO.	Velocity	
			7.4-MIN. AVERAGE (ft/s)	STANDARD DEVIATION (ft/s)
1	4	1	17.8	0.73
		2	18.0	0.74
		3	17.0	0.91
		4	18.4	0.84
3	4	1	20.0	0.89
		2	20.6	0.89
		3	19.6	1.07
		4	20.1	1.00
4	4	1	17.9	0.60
		2	18.2	0.61
		3	16.7	0.69
		4	18.2	0.77
5	4	1	17.3	0.67
		2	17.6	0.66
		3	16.2	0.74
		4	17.7	0.77
8	4	1	17.7	0.68
		2	18.0	0.68
		3	17.2	0.79
		4	18.1	0.77
10	4	1	19.8	0.95
		2	20.3	0.91
		3	19.1	1.10
		4	20.1	1.01
11	4	1	18.3	0.69
		2	18.7	0.67
		3	17.2	0.76
		4	18.6	0.80
12	4	1	17.2	0.94
		2	17.5	0.89
		3	15.8	1.03
		4	17.4	1.10
15	4	1	17.9	0.70
		2	17.9	0.74
		3	16.9	0.90
		4	18.4	0.76

*From Table IX-2.

TABLE IX-4a. (Cont.)

OPERATING CONFIGURATION NO.*	PUMP COLUMN NO.	QUADRANT NO.	Velocity	
			7.4-MIN. AVERAGE (ft/s)	STANDARD DEVIATION (ft/s)
17	4	1	19.7	0.84
		2	19.9	0.83
		3	19.5	0.95
		4	19.7	0.92
18	4	1	19.0	0.67
		2	19.2	0.73
		3	17.6	0.90
		4	19.5	0.76
19	4	1	17.4	0.65
		2	17.4	0.69
		3	16.1	0.81
		4	17.8	0.76
22	4	1	18.0	0.69
		2	18.0	0.73
		3	16.9	0.85
		4	18.3	0.74
24	4	1	19.7	0.82
		2	20.1	0.83
		3	19.7	0.94
		4	19.7	0.90
2	2	1	20.1	2.61
		2	20.4	1.82
		3	19.4	2.30
		4	19.9	2.05
3	2	1	22.1	3.39
		2	22.4	1.70
		3	22.0	2.04
		4	22.0	1.88
6	2	1	21.4	2.64
		2	21.6	1.81
		3	21.3	1.92
		4	21.8	1.83
7	2	1	20.5	2.92
		2	20.9	2.00
		3	19.8	2.50
		4	20.1	2.30

TABLE IX-4a. (Cont.)

OPERATING CONFIGURATION NO.*	PUMP COLUMN NO.	QUADRANT NO.	Velocity	
			7.4-MIN. AVERAGE (ft/s)	STANDARD DEVIATION (ft/s)
9	2	1	22.0	2.77
		2	22.5	1.52
		3	21.4	2.53
		4	22.0	1.78
10	2	1	21.6	3.24
		2	22.4	1.59
		3	21.2	2.08
		4	21.5	1.73
13	2	1	21.2	2.90
		2	21.4	1.78
		3	20.4	2.13
		4	21.7	1.69
14	2	1	20.3	2.64
		2	20.8	1.57
		3	19.0	3.04
		4	20.2	1.66
16	2	1	20.5	2.75
		2	20.7	1.85
		3	19.6	2.31
		4	20.2	2.09
17	2	1	21.3	3.19
		2	21.4	1.69
		3	21.4	2.04
		4	21.6	1.78
20	2	1	20.6	2.67
		2	20.7	1.77
		3	20.6	1.96
		4	20.9	1.85
21	2	1	20.2	2.61
		2	20.8	1.75
		3	19.4	2.31
		4	20.2	1.91
23	2	1	20.8	2.70
		2	21.1	1.86
		3	20.2	2.32
		4	20.5	2.06
24	2	1	20.9	2.68
		2	21.0	1.79
		3	21.1	1.92
		4	21.2	1.90

*From Table IX-2.

TABLE IX-4b. Throat Velocities in Pump Columns 2 and 4 at Selected Operating Conditions with 1.5 Times Design Flow.

OPERATING CONFIGURATION NO.*	PUMP COLUMN NO.	QUADRANT NO.	Velocity	
			7.4-MIN. AVERAGE (ft/s)	STANDARD DEVIATION (ft/s)
10	4	1	22.5	2.61
		2	23.7	2.03
		3	24.2	1.45
		4	23.8	1.89
11	4	1	22.7	1.60
		2	22.9	1.67
		3	22.7	1.60
		4	22.6	1.81
12	4	1	22.6	1.46
		2	23.3	1.62
		3	22.9	1.35
		4	22.6	1.73
17	4	1	22.5	1.58
		2	22.6	2.01
		3	22.4	1.66
		4	22.3	1.90
24	4	1	21.8	1.71
		2	22.0	2.11
		3	21.5	1.66
		4	21.8	2.03
7	2	1	28.1	2.37
		2	27.8	1.23
		3	28.1	1.95
		4	27.8	1.14
10	2	1	26.3	2.42
		2	27.4	1.23
		3	25.7	2.11
		4	25.9	1.32
17	2	1	25.7	2.26
		2	26.0	1.42
		3	25.2	1.95
		4	25.5	1.25
24	2	1	25.8	2.34
		2	26.1	1.41
		3	25.4	2.00
		4	25.7	1.24

*From Table IX-2.

Table IX-5a. Throat Velocity Ratios in Pump Columns 2 and 4 at Normal Operating Conditions (Design Flow).

OPERATING CONFIGURATION NO.*	PUMP COLUMN NO.	QUADRANT NO.	$\overline{V}_i/\overline{V}$	$\overline{V}_i/\overline{V}_{MAX}$	MIVR	MOSAVR
1	4	1	.999	.968	0.848	0.920
		2	1.01	.979	0.871	0.934
		3	.957	.927	0.792	0.879
		4	1.03	1.000	0.905	0.967
3	4	1	.996	.971	0.832	0.944
		2	1.03	1.00	0.879	0.978
		3	.976	.951	0.817	0.914
		4	1.00	.976	0.825	0.907
4	4	1	1.01	.984	0.860	0.926
		2	1.02	1.00	0.896	0.935
		3	.941	.918	0.811	0.874
		4	1.02	1.00	0.886	0.947
5	4	1	1.00	.977	0.838	0.918
		2	1.02	.994	0.889	0.946
		3	.942	.915	0.810	0.873
		4	1.03	1.00	0.873	0.960
8	4	1	.997	.978	0.865	0.935
		2	1.01	.994	0.906	0.956
		3	.969	.950	0.828	0.892
		4	1.02	1.00	0.877	0.958
10	4	1	.999	.975	0.756	0.923
		2	1.02	1.00	0.759	0.946
		3	.963	.941	0.523	0.870
		4	1.01	.990	0.826	0.924
11	4	1	1.00	.979	0.845	0.923
		2	1.03	1.00	0.887	0.964
		3	.945	.920	0.792	0.874
		4	1.02	.995	0.855	0.937
12	4	1	1.01	.983	0.486	0.868
		2	1.03	1.00	0.609	0.918
		3	.931	.903	*****	0.810
		4	1.02	.994	0.393	0.871
15	4	1	1.01	.973	0.873	0.940
		2	1.01	.973	0.884	0.938
		3	.951	.918	0.658	0.883
		4	1.04	1.00	0.809	0.979

*From TABLE IX-2

TABLE IX-5a. (Cont.)

OPERATING CONFIGURATION NO.*	PUMP COLUMN NO.	QUADRANT NO.	$\overline{V}_i/\overline{V}$	$\overline{V}_i/\overline{V}_{MAX}$	MIVR	MOSAVR
17	4	1	1.00	.990	0.895	0.940
		2	1.01	1.00	0.916	0.968
		3	.990	.980	0.888	0.937
		4	1.00	.990	0.888	0.943
18	4	1	1.01	.974	0.868	0.934
		2	1.02	.985	0.881	0.918
		3	.935	.902	0.739	0.813
		4	1.04	1.00	0.916	0.972
19	4	1	1.01	.978	0.867	0.927
		2	1.01	.978	0.858	0.914
		3	.937	.904	0.725	0.835
		4	1.04	1.00	0.849	0.946
22	4	1	1.01	.984	0.859	0.939
		2	1.01	.984	0.888	0.944
		3	.949	.923	0.767	0.885
		4	1.03	1.00	0.882	0.966
24	4	1	.995	.980	0.893	0.953
		2	1.01	1.00	0.910	0.972
		3	.995	.980	0.895	0.949
		4	.995	.980	0.879	0.946
2	2	1	1.01	.985	0.544	0.855
		2	1.02	1.00	0.801	0.907
		3	.972	.951	0.507	0.847
		4	.997	.975	0.714	0.893
3	2	1	.999	.987	0.249	0.808
		2	1.01	1.00	0.688	0.862
		3	.994	.982	0.609	0.820
		4	.994	.982	0.660	0.847
6	2	1	.994	.982	0.525	0.847
		2	1.00	.991	0.730	0.886
		3	.990	.977	0.721	0.869
		4	1.01	1.00	0.759	0.904
7	2	1	1.01	.981	*****	0.836
		2	1.03	1.00	0.686	0.908
		3	.974	.947	0.579	0.798
		4	.989	.962	0.650	0.892

*From TABLE IX-2

TABLE IX-5a. (Cont.)

OPERATING CONFIGURATION NO.*	PUMP COLUMN NO.	QUADRANT NO.	$\overline{V}_i/\overline{V}$	$\overline{V}_i/\overline{V}_{MAX}$	MIVR	MOSAVR
9	2	1	1.00	.978	0.358	0.837
		2	1.02	1.00	0.756	0.915
		3	.974	.951	0.492	0.845
		4	1.00	.978	0.704	0.898
10	2	1	.996	.964	0.469	0.751
		2	1.03	1.00	0.728	0.887
		3	.978	.946	0.644	0.827
		4	.992	.960	0.700	0.837
13	2	1	1.00	.977	0.421	0.807
		2	1.01	.986	0.694	0.875
		3	.963	.940	0.569	0.790
		4	1.02	1.00	0.730	0.895
14	2	1	1.01	.976	0.0955	0.793
		2	1.04	1.00	0.670	0.860
		3	.946	.913	*****	0.738
		4	1.01	.971	0.638	0.858
16	2	1	1.01	.990	0.375	0.819
		2	1.02	1.00	0.785	0.917
		3	.968	.947	0.551	0.830
		4	.998	.976	0.656	0.881
17	2	1	.994	.986	0.336	0.786
		2	.999	.991	0.719	0.863
		3	.999	.991	0.656	0.791
		4	1.01	1.00	0.641	0.866
20	2	1	.995	.986	0.450	0.817
		2	1.00	.990	0.733	0.899
		3	.995	.986	0.652	0.877
		4	1.01	1.00	0.705	0.892
21	2	1	1.00	.971	0.530	0.832
		2	1.03	1.00	0.708	0.923
		3	.963	.933	0.460	0.822
		4	1.00	.971	0.556	0.876
23	2	1	1.01	.986	0.608	0.854
		2	1.02	1.00	0.743	0.910
		3	.978	.957	0.580	0.834
		4	.992	.972	0.712	0.865
24	2	1	.993	.986	0.338	0.781
		2	.998	.990	0.689	0.832
		3	1.00	.995	0.659	0.829
		4	1.01	1.00	0.712	0.857

*From TABLE IX-2

TABLE IX-5b. Throat Velocity Ratios in Pump Columns 2 and 4 at Selected Operating conditions with 1.5 Times Design Flow.

OPERATING CONFIGURATION NO.*	PUMP COLUMN NO.	QUADRANT NO.	$\overline{V}_i/\overline{V}$	$\overline{V}_i/\overline{V}_{MAX}$	MIVR	MOSAVR
10	4	1	.955	.930	*****	0.687
		2	1.01	.979	0.580	0.852
		3	1.03	1.00	0.744	0.842
		4	1.01	.983	0.638	0.867
11	4	1	.999	.961	0.845	0.934
		2	1.01	1.00	0.862	0.955
		3	.999	.961	0.873	0.946
		4	.994	.987	0.821	0.904
12	4	1	.989	.970	0.761	0.875
		2	1.02	1.00	0.783	0.942
		3	1.00	.983	0.809	0.925
		4	.989	.970	0.667	0.863
17	4	1	1.00	.996	0.747	0.908
		2	1.01	1.00	0.686	0.885
		3	.998	.991	0.687	0.840
		4	.993	.987	0.656	0.875
24	4	1	1.00	.991	0.723	0.830
		2	1.01	1.00	0.543	0.860
		3	.987	.977	0.765	0.890
		4	1.00	.991	0.672	0.876
7	2	1	1.00	1.00	0.623	0.879
		2	.995	.989	0.773	0.906
		3	1.00	1.00	0.698	0.880
		4	.995	.989	0.797	0.911
10	2	1	.999	.960	0.569	0.821
		2	1.04	1.00	0.826	0.940
		3	.976	.938	0.599	0.800
		4	.984	.945	0.740	0.864
17	2	1	1.00	.988	0.557	0.847
		2	1.02	1.00	0.772	0.912
		3	.984	.969	0.631	0.804
		4	.996	.981	0.794	0.888
24	2	1	1.00	.988	0.565	0.869
		2	1.01	1.00	0.767	0.909
		3	.986	.973	0.556	0.712
		4	.998	.985	0.767	0.905

*From TABLE IX-2

TABLE IX-6. Classification of Possible Operating Conditions. (Configuration numbers refer to TABLE IX-7.)

Recommended	Acceptable	Avoid
2, 13, 15, 16, 20, 23, 26, 28, 29, 35, 39, 42, 45,	1, 3, 4, 5, 6, 7, 8, 9, 14, 18, 19, 21, 22, 24, 25, 27, 30, 31, 32, 34, 36, 37, 38, 40, 41, 43, 44, 46,	10, 11, 12, 19, 21, 33

All flow observations were made in the number 2 and number 4 pump columns (Fig. IX-2). Conditions which occur in the number 1 and number 3 pump columns can be classified similarily because of the symmetry of the pump sump.

TABLE IX-7. Summary of Possible Operating Conditions.

CONFIGURATION	GATE			PUMPS OPERATING			
	Down-stream	Up-stream	Splitter wall	1	3	4	2
1	UP	UP	UP			X	
2	UP	UP	UP				X
3	UP	UP	UP			X	X
4	UP	UP	UP	X		X	
5	UP	UP	UP		X	X	
6	UP	UP	UP	X			X
7	UP	UP	UP		X		X
8	UP	DOWN	UP			X	
9	UP	DOWN	UP				X
10	UP	DOWN	UP			X	X
11	UP	DOWN	UP	X		X	
12	UP	DOWN	UP		X	X	
13	UP	DOWN	UP	X			X
14	UP	DOWN	UP		X		X
15	DOWN	UP	UP			X	
16	DOWN	UP	UP				X
17	DOWN	UP	UP			X	X
18	DOWN	UP	UP	X		X	
19	DOWN	UP	UP		X	X	
20	DOWN	UP	UP	X			X
21	DOWN	UP	UP		X		X
22	UP	UP	DOWN			X	
23	UP	UP	DOWN				X
24	UP	UP	DOWN			X	X
25	UP	UP	UP		X		
26	UP	UP	UP	X			
27	UP	UP	UP	X	X		
28	UP	DOWN	UP		X		
29	UP	DOWN	UP	X			
30	UP	DOWN	UP	X	X		
31	DOWN	UP	UP		X		
32	DOWN	UP	UP	X			
33	DOWN	UP	UP	X	X		
34	UP	UP	DOWN		X		
35	UP	UP	DOWN	X			
36	UP	UP	DOWN	X	X		
37	UP	UP	DOWN	X		X	
38	UP	UP	DOWN		X	X	
39	UP	UP	DOWN	X			X
40	UP	UP	DOWN	X		X	
41	UP	DOWN	DOWN		X		
42	UP	DOWN	DOWN	X			
43	UP	DOWN	DOWN	X	X		
44	DOWN	UP	DOWN			X	
45	DOWN	UP	DOWN				X
46	DOWN	UP	DOWN			X	X

NOTE: Pump numbers refer to Figure IX-2 where they are given as I, II III, and IV.

X. SUMMARY AND CONCLUSIONS

The existing river intake of NSP's Sherco Electric Power Generating Plant had to be equipped with Johnson Screens and two additional pumps to provide additional cooling make-up water for Unit No. 3, currently under construction. A 1:6 scale undistorted model of the Sherco River (cooling) water intake was built at the St. Anthony Falls Hydraulic Laboratory, University of Minnesota and used for three main purposes:

(a) To test the hydraulic performance of several elements of the design,

(b) to develop new design features, and

(c) to serve as a documentation tool for the training of 90 plant operators in 6 separate training sessions (Fig. X-1).

The sediment backwash (silt sluicing) system designed by Black and Veatch to periodically remove sand and silt around the screens was found to be very effective. It is recommended that it be operated at 7500 gpm per manifold, which is one-half the design flow rate and for periods no longer than 10 minutes.

The air backwash system to remove debris deposits from the screen surface was found to be very effective with leaves being the typical debris expected in the river.

A warm water discharge manifold for ice control was designed and tested with very good results.

Flow conditions in the pump sump were extensively tested. Structural modifications consisting of floor attached wedges and an anti-vortex grating were tested and recommended. With these additions, the pump sump will function satisfactorily for all possible combinations of gate openings and pumps in operation. The most suitable conditions have been identified (ranked).

Fig. X-1. Plant operators observing model performance.

XI. ACKNOWLEDGEMENTS

This study was conducted for Northern States Power Company, Mr. A. E. Johnson, Project Manager, and Donna L. Stephenson, Don Anderson, Bruce LaMar, staff members of NSP in charge of various aspects of the project. Close cooperation with Black and Veatch, design engineers for the project, was essential. Mr. Craig Johnson was the representative of that firm.

XII. REFERENCES

Durgin, W. W. and F. A. Anderson, "Davis Pumped Storage Project Hydraulic Model Studies; Intake Model Upper Storage Reservoir," Alden Research Laboratories, Worcester Polytechnique Institute, Holden, Massachusetts, October 1972.

Lee, Hsiao-Lieu and William W. Durgin, "The performance of crossed-vane swirl meters," ASME Symposium on Vortex Flows, Chicago, Illinois, 1980.

Williams, G. P., "Frazil Ice Dynamics, a review of its properties, with a selected biography," Engineering Journal, Vol. 42, No. 11, Nov. 1959, pp. 55-60.

APPENDIX A

Prototype and Model Sediment Characteristics

ANALYSIS OF SHERCO SAND SAMPLE

(by Terry Zien)

This sand is composed of 95% quartz grains and 5% heavy mineral grains. These heavy minerals include pyrite (iron sulfide), magnetite (magnetic iron sulfide), chalcopyrite (non-copper sulfide) and hornblende. The sand is very well sorted, medium sand size (.25 - .50 mm). The roundness of the grains varies, with 33% very well rounded, 33% subangular, and 33% very angular. 95% of the grains are equant to mildly subequant, being nearly the same length in all three dimensions (spheres or cubes). Five percent of the grains are elongate.

Zones of glacial sand and gravel outwash parallel the valley of the Elk, Mississippi, and St. Francis Rivers. In the central and eastern parts of Sherburne County, dune sands occur as a veneer over many of the morainic ridges and knolls. This indicates the area had substantial sediment transport by wind, but this situation has stabilized since dune formation.

The surficial geology in and around Becker, Minnesota, is sandy prairie, especially between Becker and the Mississippi River. The Elk River, which parallels the Mississippi from the northwest to the southeast corner of Sherburne County, drains most of the area. It flows into the Mississippi River at the town of Elk River, southeast of Becker. The tract of land between the Elk and Mississippi River is a sandy prairie, the surface of which is covered with glacio-fluvatile sediments.

The surficial geology of Benton County, northwest of Becker along the Mississippi River, is similar to the glacial sandy plain of Sherburne County. Thus, the most probable source for the sand in the Mississippi River at the Sherco intakes is this sandy prairie. This area will continue to be the dominant sediment source for the Mississippi River at Sherco, at least until another glacial advance or catastrophic erosion occurs, neither of which is very probable.

Bibliography

Thiel, G. A., 1947, The Geology and Underground Waters of Northeastern Minnesota, Minnesota Geological Survey Bulletin 32, The University of Minnesota Press, Minneapolis.

Blatt, H., 1982, Sedimentary Petrology, W. H. Freeman and Company, San Francisco.

SEDIMENT CHARACTERISTICS

	Fall Velocity in cm/s (ft/s) at Temp. (°C)		
	0°	10°	20°
Prototype			
d_{50} = .33 mm	3.2(.11)	3.8(.13)	4.5(.15)
d_{80} = .7 mm	8.5(.28)	10.0(.33)	11.5(.38)
Model			
d_{50} = .23 mm	1.9(.06)	2.4(.08)	2.8(.09)
d_{80} = .36 mm	3.6(.12)	4.4(.14)	5.0(.16)
Ratios - V_m/V_p			
d_{50}	.59	.63	.62
d_{80}	.42	.44	.43

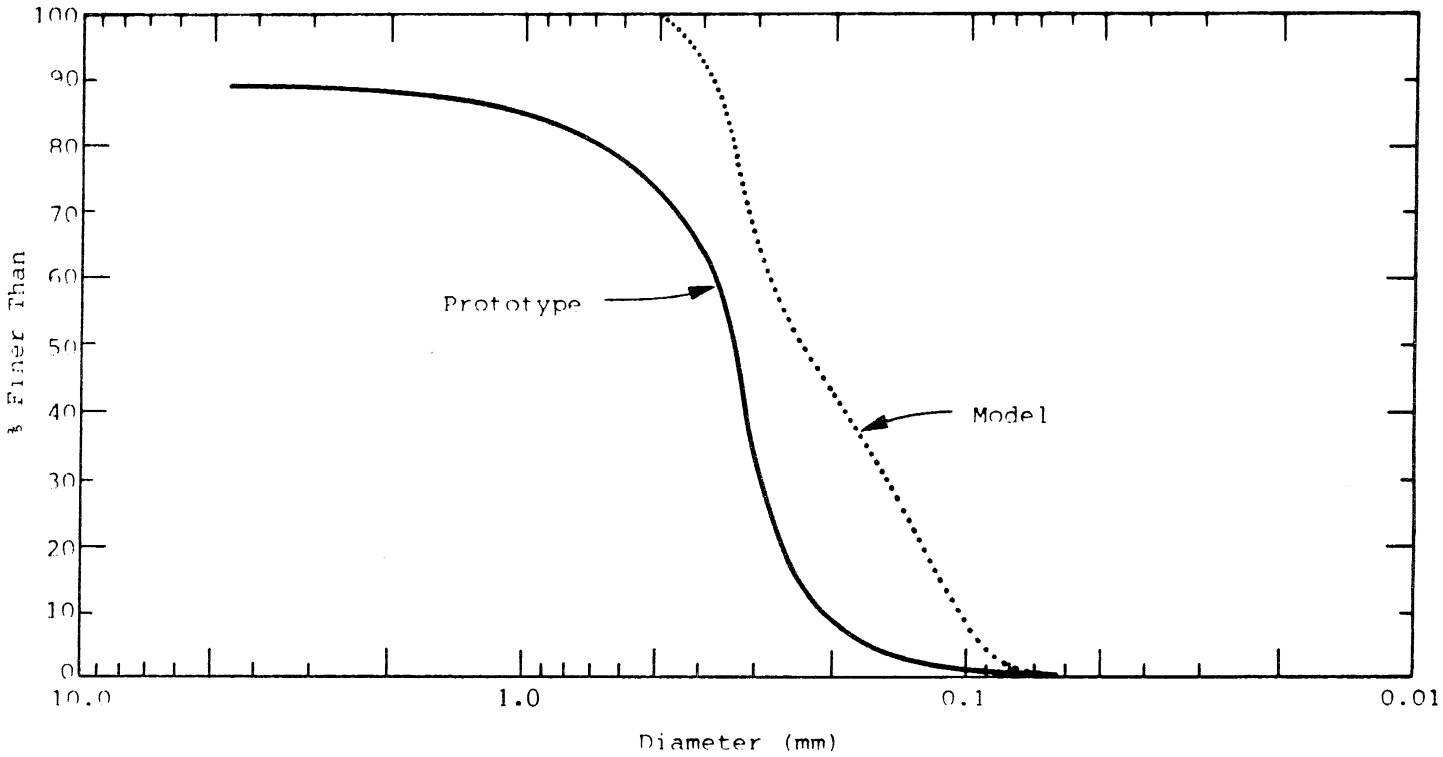

Fig. A. Sherco sediment sample analyses.

APPENDIX B

Design of the Air Blowout Model

TANK PRESSURES

Prototype

gage pressure 100 psi

Model

gage pressure 16.7 psi

TANK VOLUME

Prototype

130 ft^3

Air outlet depth of submergence 919-909 = 10'

Absolute back pressure

$$= 14.3 + \frac{10(62.4)}{144}$$

$$= 14.3 + 4.3 = 18.6 \text{ psi}$$

At that pressure, tank volume will expand to

$$\frac{100 + 14.3}{18.6} \times 130 = 799 \text{ ft}^3$$

Of this volume, 130 ft^3 will be left behind in the tank after the blow-out process, ignoring volume in pipe system (about 10 ft^3).

Volume of air discharged

$$799 - 130 = 669 \text{ ft}^3$$

Model

Scaled at 1:6, this gives 3.10 ft^3 of uncompressed air blown out in the model.

To obtain required model tank volume, the above calculation has to be done in reverse.

Model tank pressure is 16.7 psi gage or

$$14.3 + 16.7 = 31.0 \text{ psi absolute}$$

Discharge pressure in the model will be

$$\frac{10'}{6} \times \frac{62.4}{144} = 0.722 \text{ psi gage or } 15.0 \text{ psia}$$

Model tank volume required is obtained by compressing 3.10 ft^3 + 1 tank volume from 15.0 psia to 31.0 psia (14.3 + 16.7 psi).

$$(3.10 + V_T)\frac{15.0}{31.0} = V_T$$

$$V_T(1 - 0.483) = .48(3.10)$$

$$V_T = 2.90 \text{ ft}^3$$

AIR DISCHARGE VELOCITY AND PIPE FRICTION

Prototype

Entrance losses, non-projecting, loss coefficient = 0.5

local losses, 5 elbows @ .3 loss coefficient = 1.5

1 Tee, loss coefficient = 1.0

2 x 10 orifices, 1/4" dia (model)

$A = 0.049 \text{ in}^2/\text{orifice}$

Contraction Coefficient $C_c = 0.6$

$A_{total} = (20)(.6)(.049) = .59 \text{ in}^2$ (model)

$A_{total} = 21.24 \text{ in}^2 = .147 \text{ ft}^2$ (prototype)

compared to 6" pipe = 0.196 ft^2

$$V_{orifice} = \frac{.196}{.147} V_{pipe} = 1.34\ V_{pipe}$$

Exit loss coeff. in terms of pipe velocity = 1.79

Friction:

Rough pipe f = .019

$(f)(\frac{L}{D}) = (0.019)(\frac{33}{.5})$ = 1.25

Loss coefficients, Total = 6.04

Pipe velocity

$$6.04\ V_p^2 = \frac{2\Delta p}{\rho}$$

Initial velocity

$$\Delta p = 100 \text{ psi} - 4.3 = 95.7 \text{ psi}$$

$$\rho_{\text{standard air}} = 0.02378 \text{ slugs/ft}^3 \text{ (@ 14.69 psia)}$$

$$\rho_{\text{compr. air}} = \frac{100 + 14.3}{14.69}(.002378)$$

$$= 0.0185 \text{ slugs/ft}^3$$

$$V_p^2 = [\frac{2}{6.04}][\frac{(95.7)(144)}{.0815}] = 246{,}660 \text{ ft}^2/\text{s}^2$$

$$V_p = 496 \text{ fps}$$

Initial air flow rate

$$V_p A_p = 97.5 \text{ ft}^3/\text{s}$$

Model

Entrance losses, not projecting = 0.50

Local losses, 5 Elbows @ .75 = 3.75

1 Tee = 1.00

Model orifice placement

Numbers for each half of screen

ten 1/4" dia holes in two equal lines, five on each side of the pipe spaced 2" apart.

$A_{\text{total w. contr.}} = .59 \text{ in}^2$

compared to $1\frac{1}{4}$" pipe = 1.23 in^2

$V_{\text{orifices}} = \frac{1.23}{.59} \quad V_{\text{pipe}} = 2.08$

Exit loss coeff. in terms of pipe velocity head = 4.32

Friction

$$f = .033$$

$$(f)(\frac{L}{D}) = (.033)(\frac{5.5}{.64}) = \quad = 1.75$$

Added losses due to nozzles at tank exit

4 nozzles, 3/8" dia.

$$A_{\text{nozzles}} = .36 \text{ in}^2$$

$$A_{\text{pipe}} = 1.23 \text{ in}^2$$

$$V_{\text{nozzles}} = 3.42 V_{\text{pipe}}$$

change in entrance loss coeff.

$$= \frac{-0.5 V_p^2 + 0.5 V_n^2}{V_p^2}$$

$$= .5[(\frac{V_n}{V_p})^2 - 1] \quad = 5.35$$

added expansion loss coeff.

$$= \frac{(V_n - V_p)^2}{V_p^2} = (2.42)^2 = 5.85$$

Loss coefficients, Total = 22.50

Pipe velocity

Target value is 202 ft/s.

Initial p = 16.7 - .7 = 16.0 psig which is also 1/6 of 95.7 psig.

ρ_{air} at 16.7 psig

$$= \frac{(0.002378)(14.3 + 16.7)}{14.67} = .00503 \text{ slugs/ft}^3$$

$$V_p = \sqrt{\frac{2\Delta p}{\rho(22.5)}} = \sqrt{\frac{(2)(16.0)(144)}{(.00503)22.5}} = 202 \text{ ft/s}$$

Check of scale ratio:

$$\frac{V_{p \text{ prototype}}}{V_{p \text{ model}}} = \frac{496}{202} = 2.46 \cong \sqrt{6}$$

APPENDIX C

Vortex Classification

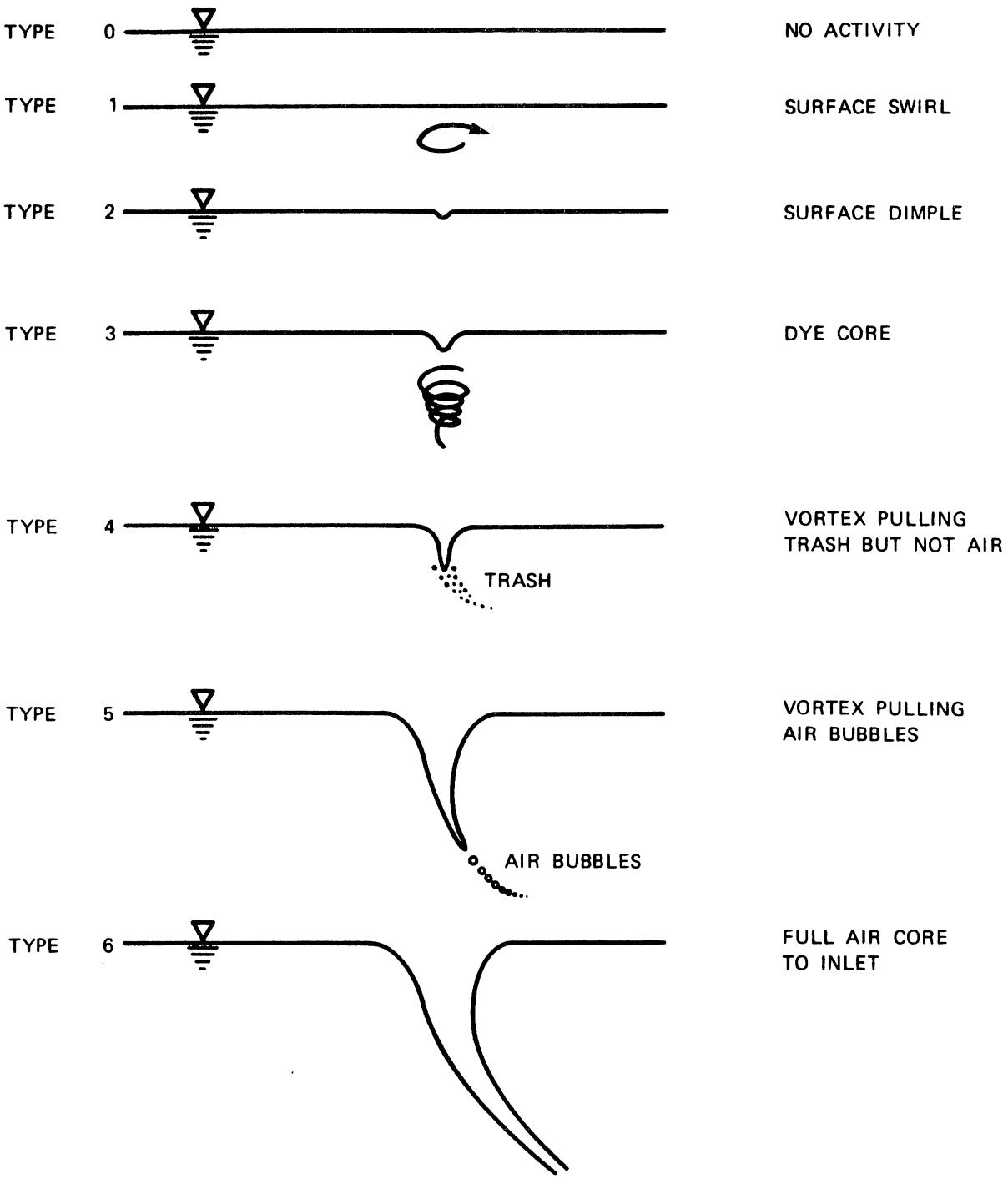

Fig. C-1. Surface vortex classification scheme. [Durgin et al., 1972].

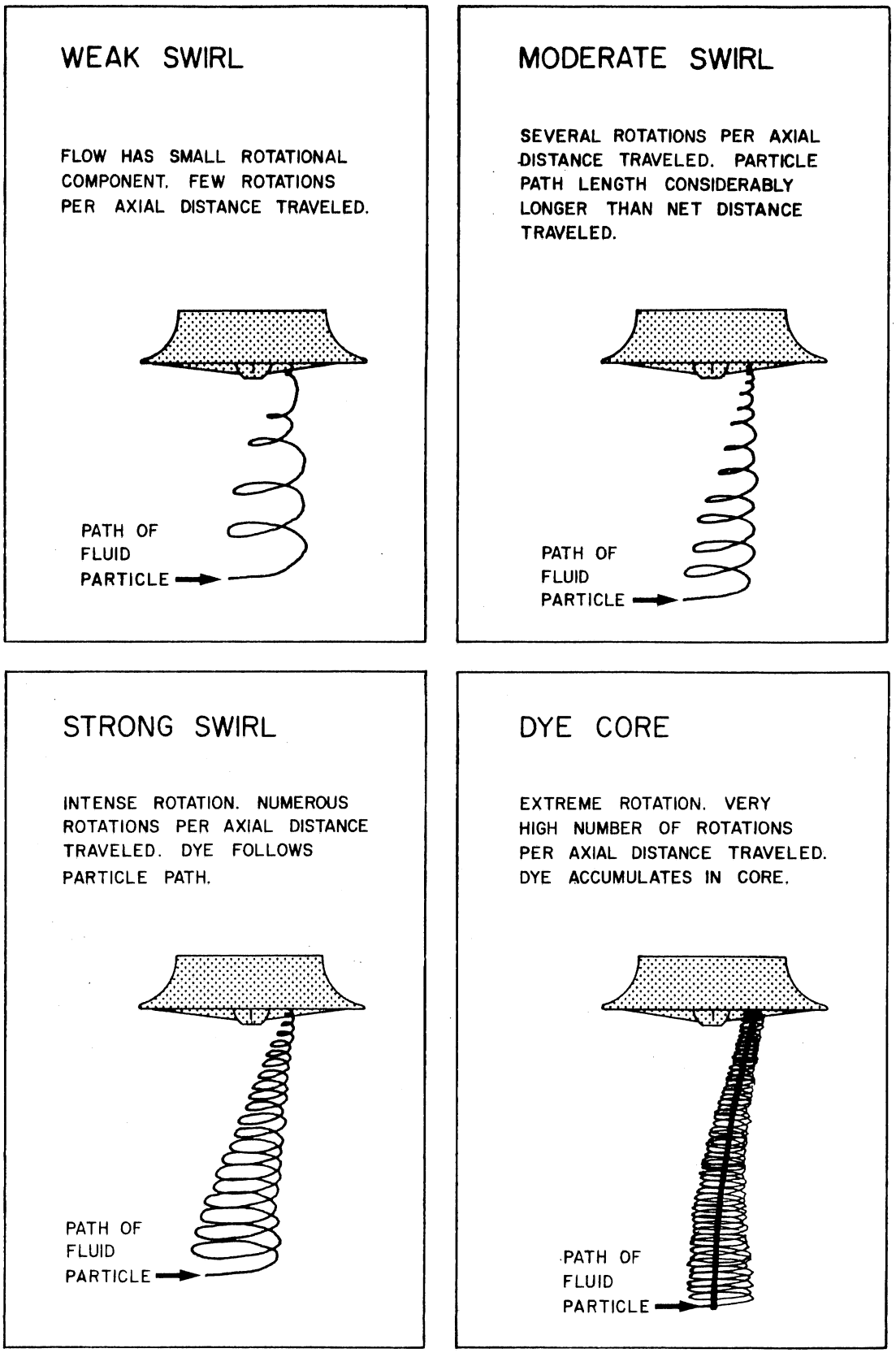

Fig. C-2. Submerged vortex classification scheme.

APPENDIX D

Samples of Pump Column Velocity Records

FLOW CONFIGURATION 1

COLUMN 4

QUADRANT 1

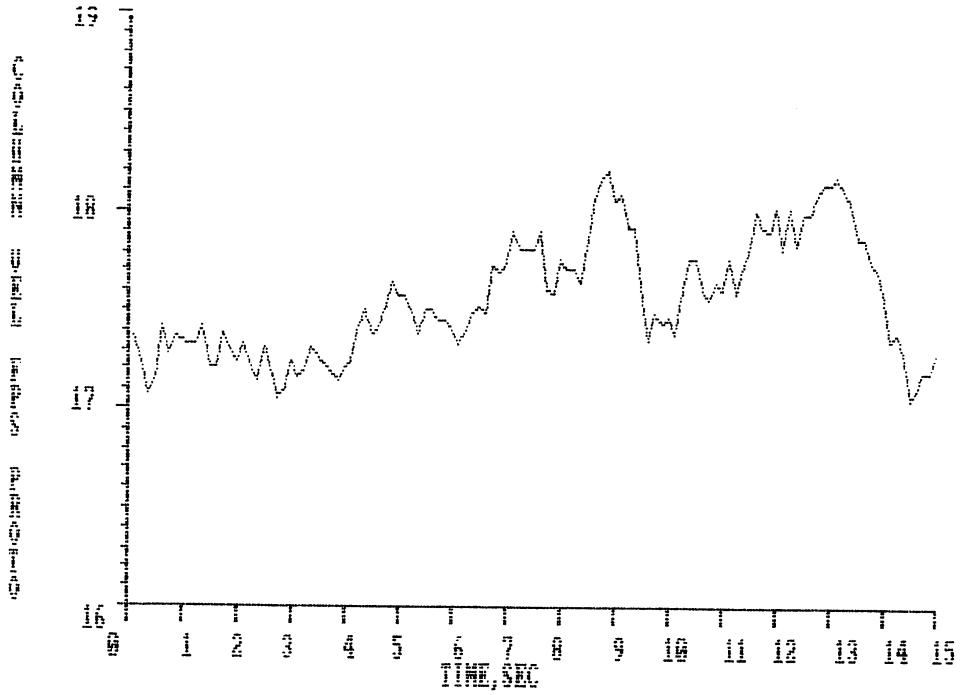

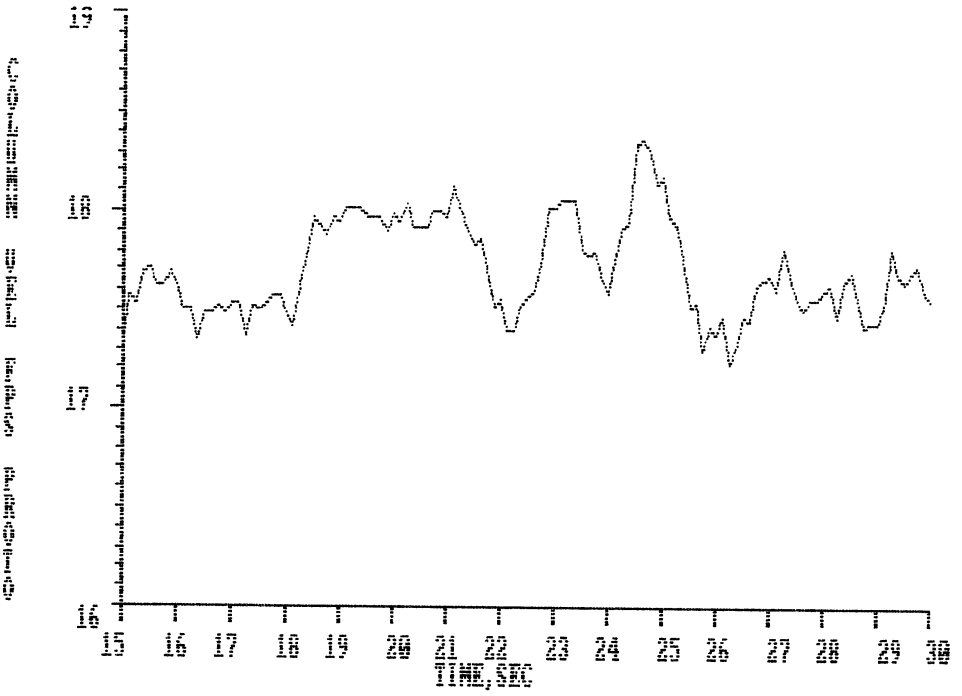

(Cont'd)

FLOW CONFIGURATION 1

COLUMN 4

QUADRANT 1

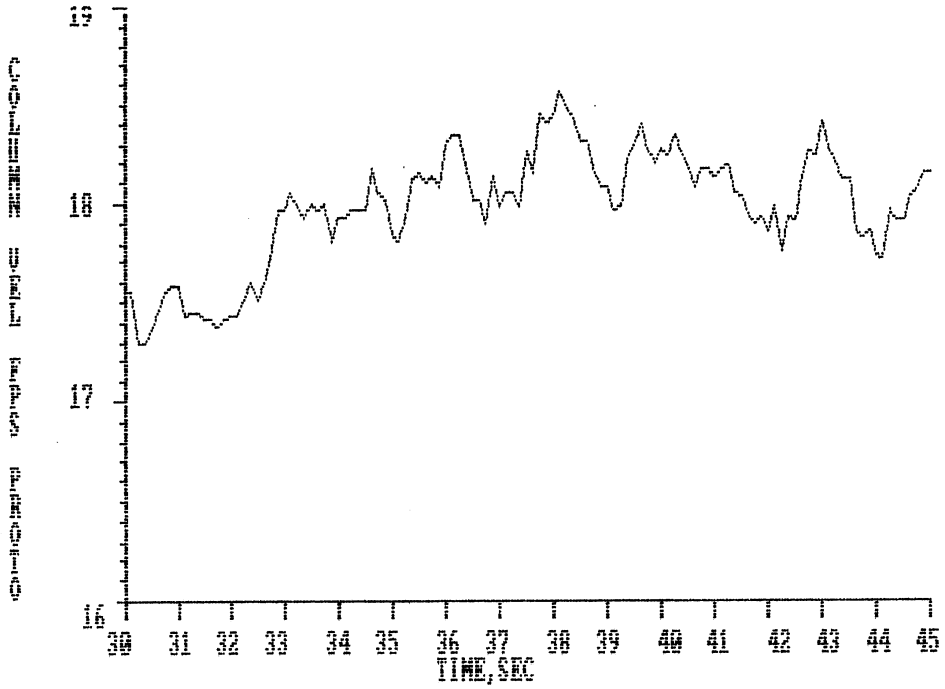

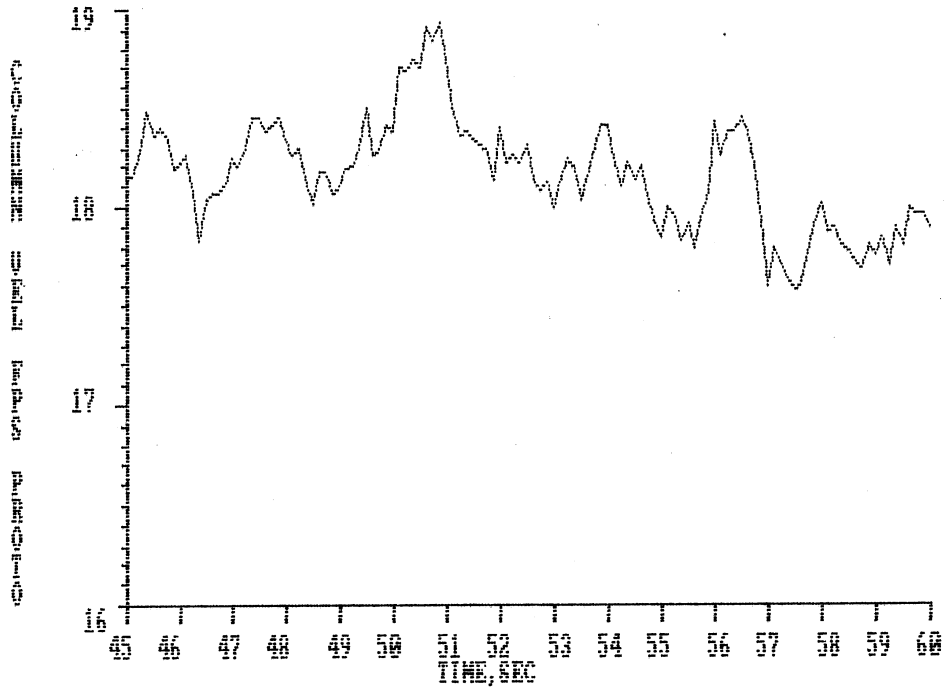

FLOW CONFIGURATION 1

COLUMN 4

QUADRANT 2

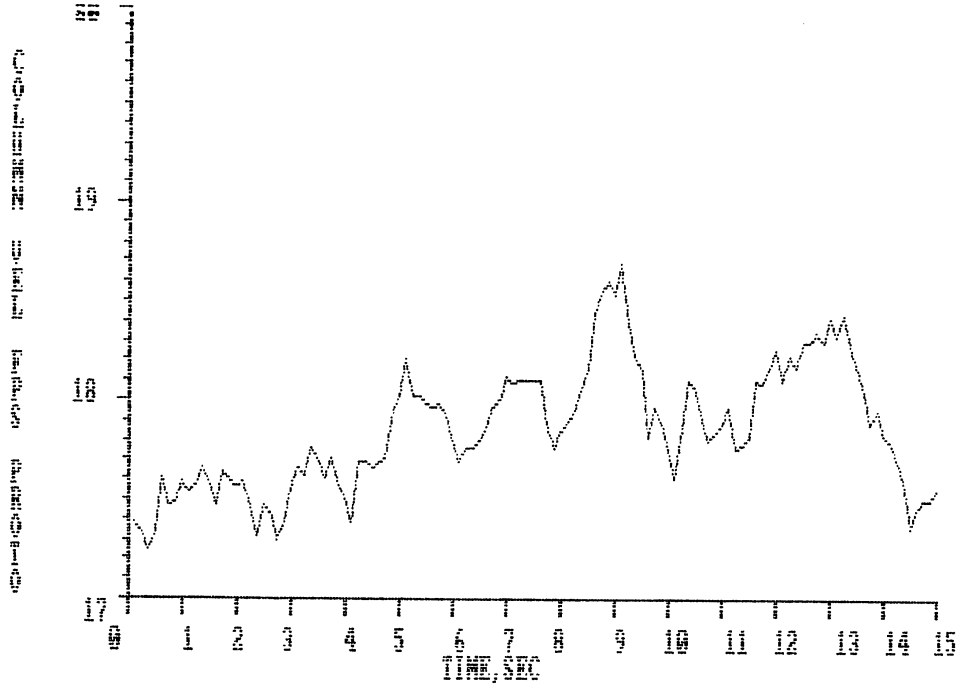

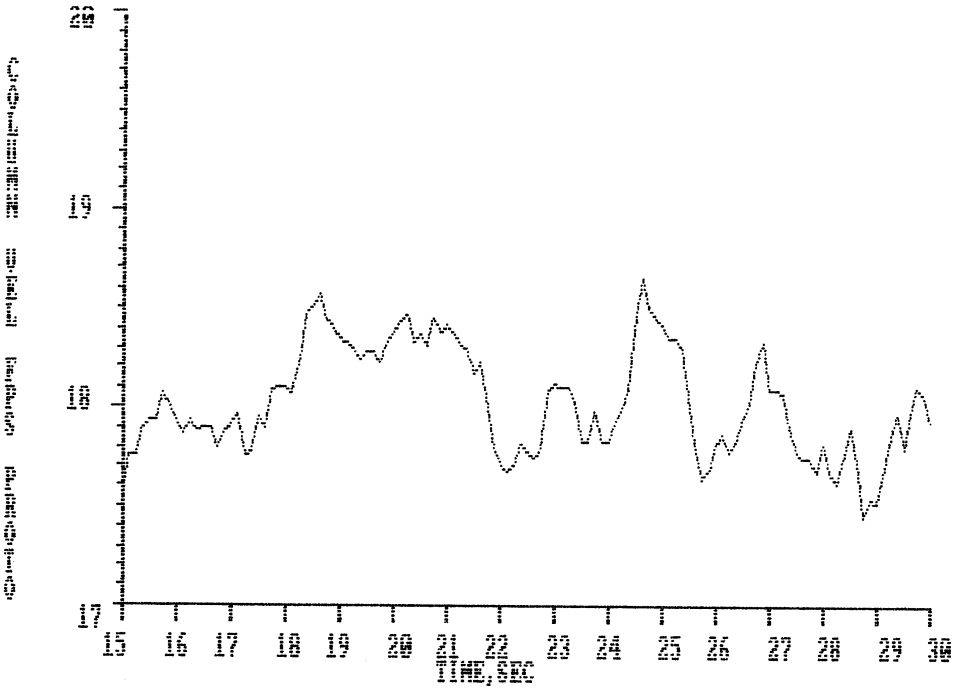

(Cont'd)

FLOW CONFIGURATION 1

COLUMN 4

QUADRANT 2

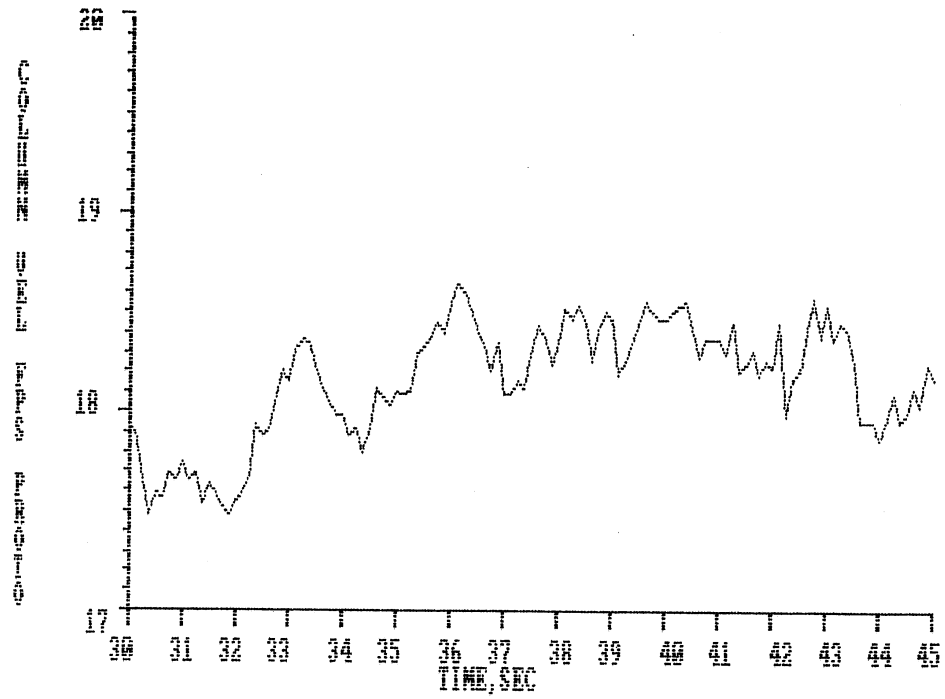

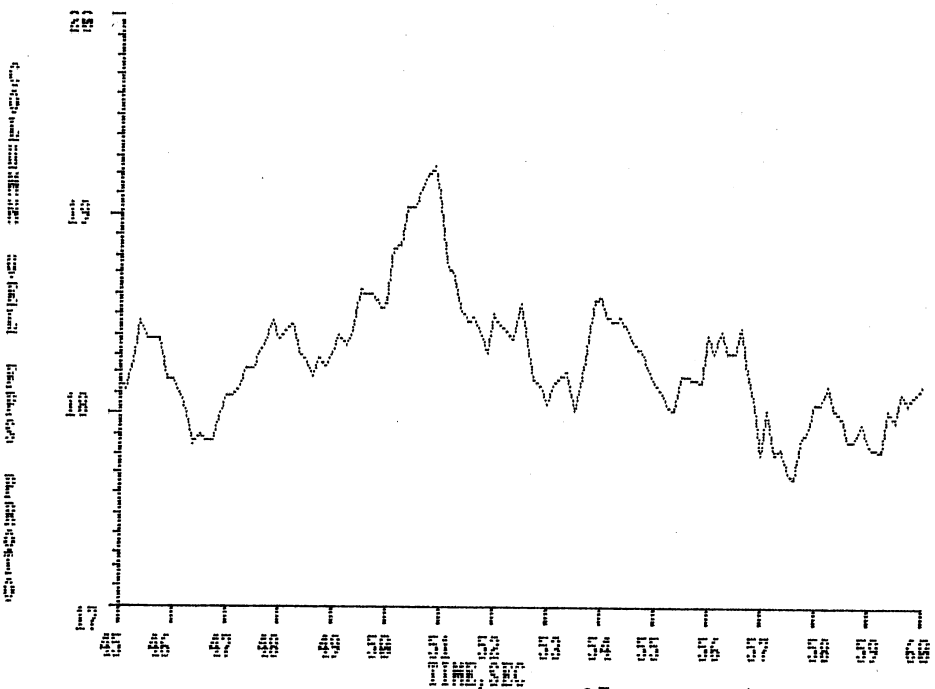

FLOW CONFIGURATION 1

COLUMN 4

QUADRANT 3

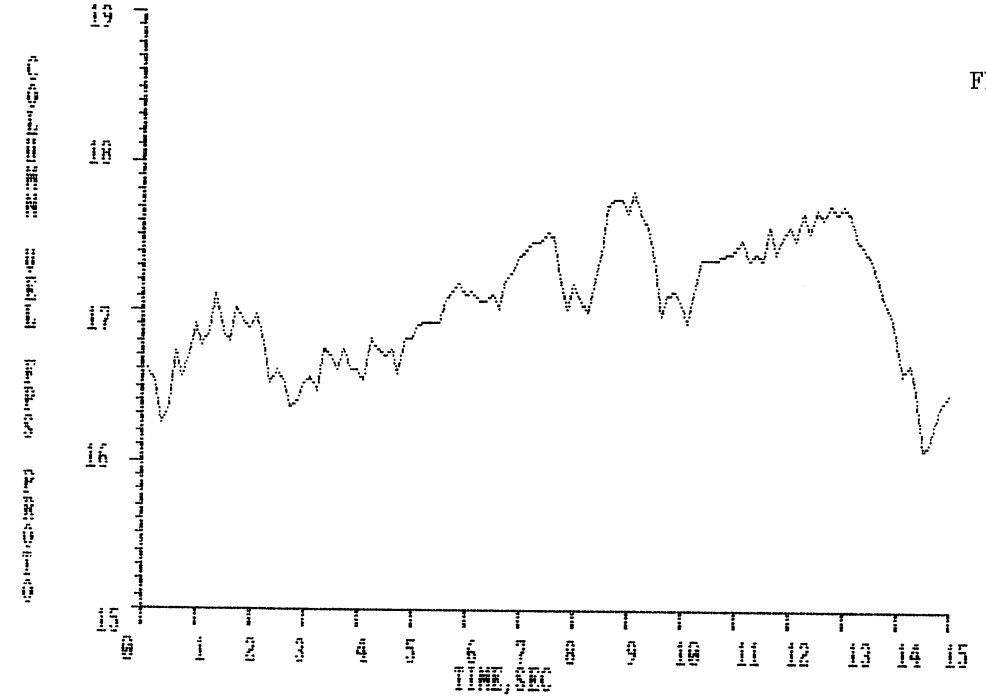

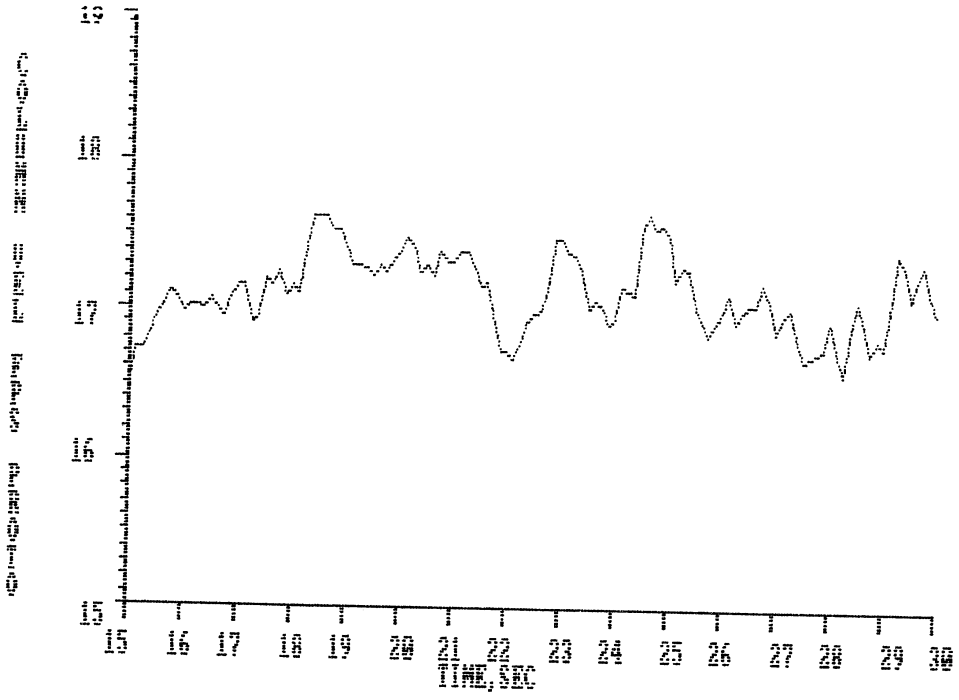

(Cont'd)

FLOW CONFIGURATION 1

COLUMN 4

QUADRANT 3

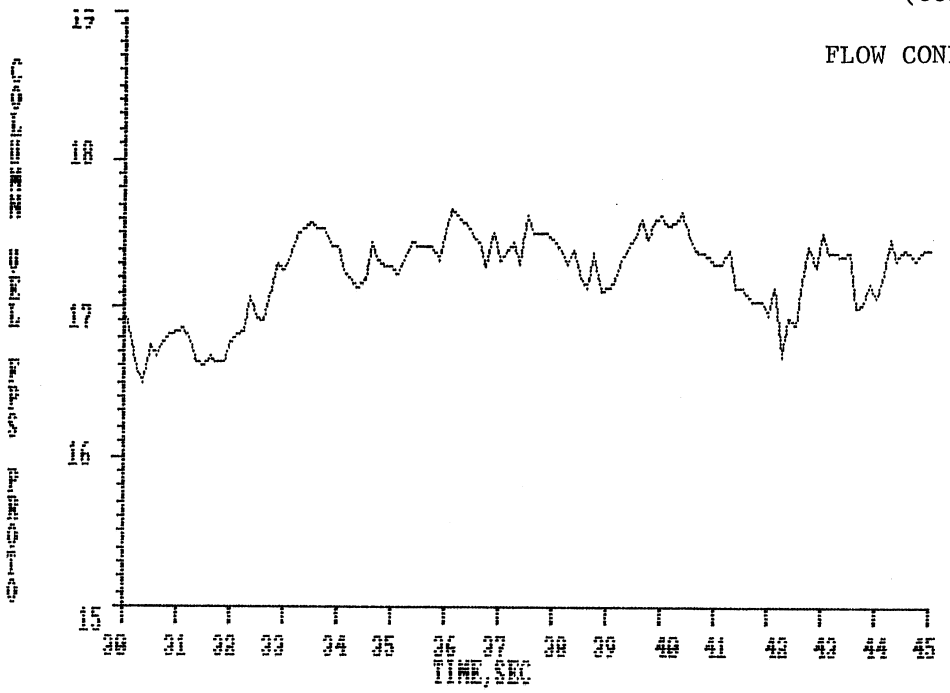

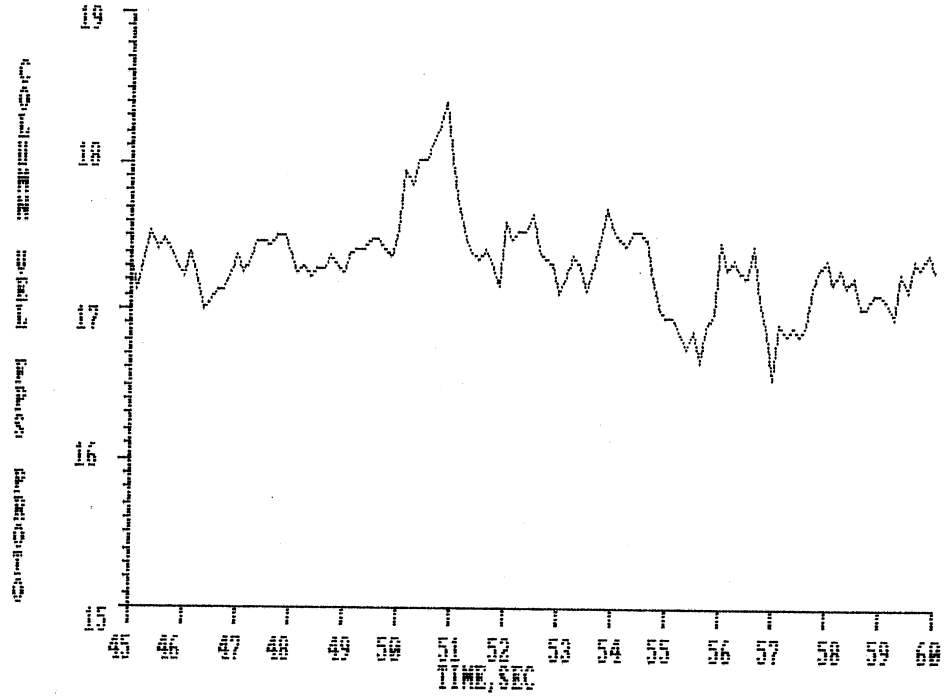

FLOW CONFIGURATION 1

COLUMN 4

QUADRANT 4

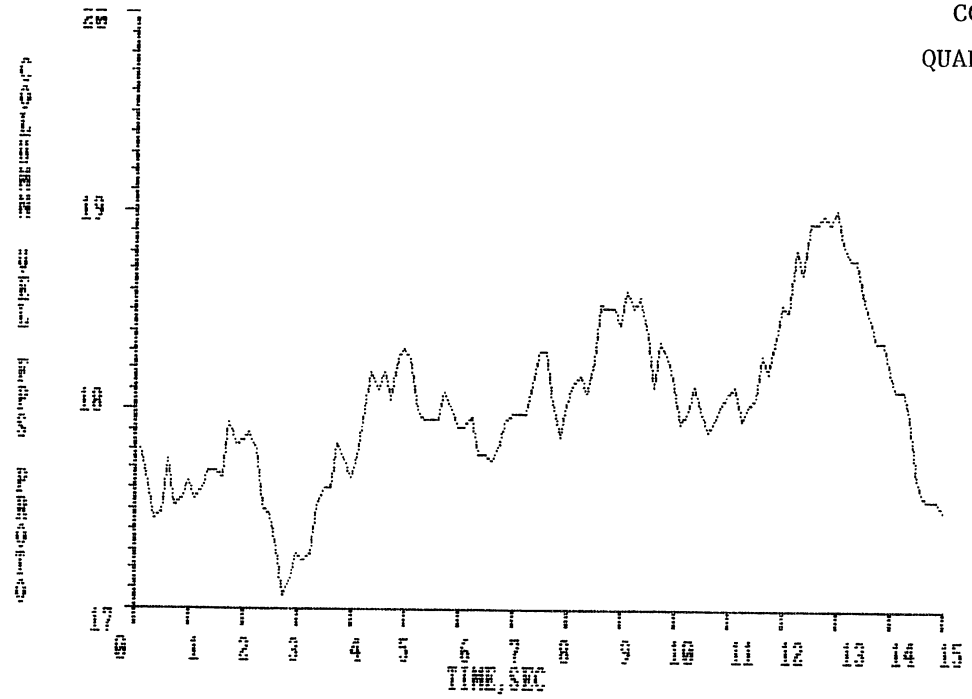

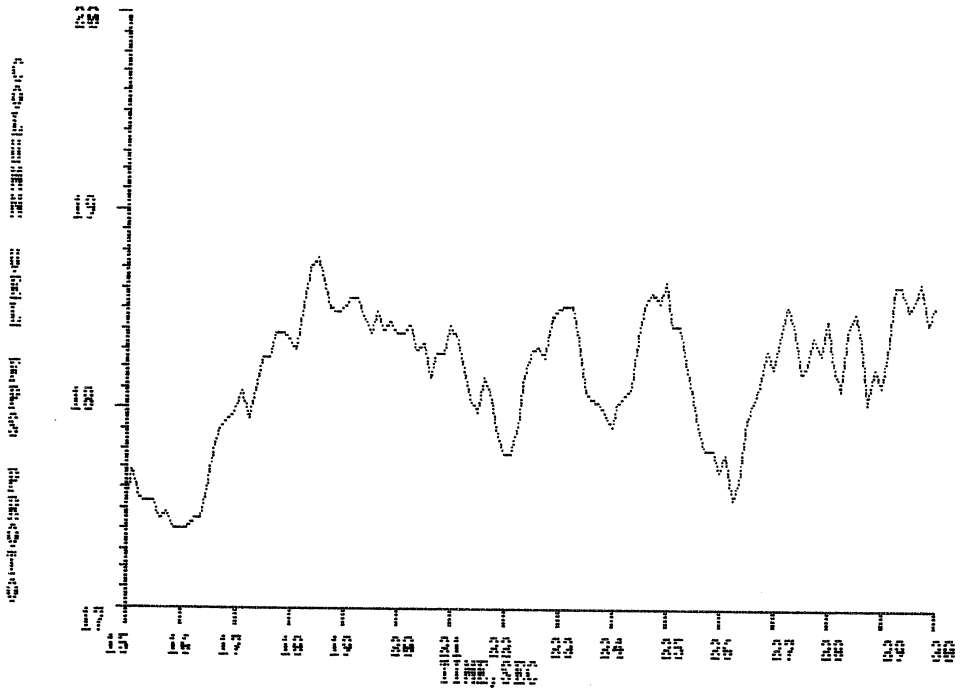

(Cont'd)

FLOW CONFIGURATION 1

COLUMN 4

QUADRANT 4